

**DEVELOPMENT OF LOW TEMPERATURE COMBUSTION MODES TO
REDUCE OVERALL EMISSIONS FROM A MEDIUM-DUTY, FOUR
CYLINDER DIESEL ENGINE**

A Thesis

by

JONATHAN ROBERT BREEN

Submitted to the Office of Graduate Studies of
Texas A&M University
in partial fulfillment of the requirements for the degree of

MASTER OF SCIENCE

August 2010

Major Subject: Mechanical Engineering

**DEVELOPMENT OF LOW TEMPERATURE COMBUSTION MODES TO
REDUCE OVERALL EMISSIONS FROM A MEDIUM-DUTY, FOUR
CYLINDER DIESEL ENGINE**

A Thesis

by

JONATHAN ROBERT BREEN

Submitted to the Office of Graduate Studies of
Texas A&M University
in partial fulfillment of the requirements for the degree of

MASTER OF SCIENCE

Approved by:

Chair of Committee,	Jerald A. Caton
Committee Members,	Timothy J. Jacobs
	Sergio C. Capareda
Head of Department,	Dennis L. O'Neal

August 2010

Major Subject: Mechanical Engineering

ABSTRACT

Development of Low Temperature Combustion Modes to Reduce Overall Emissions
from a Medium-Duty, Four Cylinder Diesel Engine. (August 2010)

Jonathan Robert Breen, B.S., Texas A&M University

Chair of Advisory Committee: Dr. Jerald A. Caton

Low temperature combustion (LTC) is an appealing new method of combustion that promises low nitric oxides and soot emissions while maintaining or improving on engine performance. The three main points of this study were to develop and validate an engine model in GT-Power capable of implementing LTC, to study parametrically exhaust gas recirculation (EGR) and injection timing effects on performance and emissions, and to investigate methods to decrease pressure rise rates during LTC operation. The model was validated at nine different operating points, 3 speeds and 3 loads, while the parametric studies were conducted on 6 of the 9 operating points, 3 speeds and 2 loads.

The model consists of sections that include: cylinders, ports, intake and exhaust manifolds, EGR system, and turbocharger. For this model, GT-Power calculates the combustion using a multi-zone, quasi-dimensional model and a knock-induced combustion model. The main difference between them is that the multi-zone model is directly injected while the knock model is port injected. A variety of sub models calculate the fluid flow and heat transfer.

A parametric study varying the EGR and the injection timing to determine the optimal combination was conducted using the multi-zone model while a parametric study that just varies EGR is carried out using the knock model. The first parametric study showed that the optimal EGR and injection timing combination for the low loads occurred at high levels of EGR (60%) and advanced injection timings (30 to 40 crank angle degrees before top dead center). The optimal EGR and injection timing combination for the high loads occurred at low levels of EGR (30% to 40%) and retarded injection timings (7.5 to 5 crank angle degrees before top dead center). The knock model determined that the ideal EGR ratio for homogeneous charge compression ignition (HCCI) operation varied from 30% to 45%, depending on the operating condition. Three methods were investigated as possible ways to reduce pressure rise rates during LTC operation. The only feasible method was the multiple injection strategy which provided dramatically reduced pressure rise rates across all EGR levels and injection timings.

ACKNOWLEDGEMENTS

I would like to offer my sincerest gratitude to Dr. Jerald Caton, my committee chair, for the opportunity to conduct this research and for his guidance throughout this process. I would also like to thank my committee members, Dr. Jacobs and Dr. Capareda, for their support of my research. My deepest appreciation goes to the Houston Area Research Center for their financial support and commitment to this research project.

I must thank both of my parents who have given me the most amazing love and support even when I definitely did not deserve it. Lastly, my profoundest love goes to my beautiful wife whose unwavering patience and love have made me who I am today.

NOMENCLATURE

BMEP	Brake Mean Effective Pressure
bTDC	before Top Dead Center
CA	Crank Angle in Degrees
CFD	Computational Fluid Dynamics
CO	Carbon Monoxide
EGR	Exhaust Gas Recirculation
HC	Hydrocarbons
HCCI	Homogeneous Charge Compression Ignition
IMEP	Indicated Mean Effective Pressure
ISFC	Indicated Specific Fuel Consumption
LTC	Low Temperature Combustion
NO _x	Nitrogen Oxides
rpm	Revolutions per Minute

TABLE OF CONTENTS

	Page
ABSTRACT	iii
ACKNOWLEDGEMENTS	v
NOMENCLATURE	vi
TABLE OF CONTENTS	vii
LIST OF FIGURES	ix
LIST OF TABLES	xiii
1. INTRODUCTION	1
2. OBJECTIVES	3
3. LITERATURE REVIEW	4
3.1 Experimental implementation of LTC engine systems.....	4
3.1.1 The effects of multiple injections and fuel properties on LTC...	
3.1.2 Methods to decrease pressure rise rates during LTC	6
3.2 Modeling LTC and HCCI engine operation	7
3.2.1 Overall LTC and HCCI engine modeling	7
3.2.2 Combustion modeling for LTC engines	7
3.2.3 NOx and soot emissions modeling for LTC engines	9
4. MODEL AND CALCULATIONS	10
4.1 Model development	10
4.2 General model calculations	11
4.2.1 Fluid flow models	11
4.2.2 Heat transfer models	13
4.2.3 Combustion models.....	14
4.2.4 Emissions models.....	18
4.3 Equations for the performance characteristics	20
5. RESULTS AND DISCUSSION	21

	Page
5.1 Engine inputs.....	21
5.2 Model validation.....	22
5.3 EGR and injection timing parametric studies	30
5.3.1 Injection profiles for the operating points	30
5.3.2 Performance characteristics for each operating point	35
5.3.3 Emissions values for each operating point	45
5.3.4 Optimal EGR and injection timing combinations.....	56
5.4 Knock-induced combustion parametric studies	60
5.5 Combustion noise and possible reduction methods.....	65
5.5.1 Ability of high EGR to reduce pressure rise rates	65
5.5.2 Ability of highly cooled EGR to reduce pressure rise rates	68
5.5.3 Ability of multiple injections to reduce pressure rise rates	69
6. CONCLUSIONS AND RECOMMENDATIONS	71
6.1 Conclusions	72
6.2 Recommendations	73
REFERENCES	74
APPENDIX A: VALIDATION DATA FOR THE HIGH LOAD CASES	76
APPENDIX B: MULTI-ZONE MODEL RAW DATA.....	79
APPENDIX C: HCCI MODEL RAW DATA	93
APPENDIX D: DIESEL FUEL PROPERTIES	96
VITA	97

LIST OF FIGURES

	Page
Figure 1 Separated fluid regions for in-cylinder flow.....	12
Figure 2 Axial and radial combustion zones for the multi-zone model.....	14
Figure 3 Example of zonal distribution throughout an injection.....	15
Figure 4 Pressure vs. CA comparison for 1400 rpm / low load	23
Figure 5 Heat release rate vs. CA comparison for 1400 rpm / low load.....	23
Figure 6 Pressure vs. CA comparison for 1400 rpm / mid load	24
Figure 7 Heat release rate vs. CA comparison for 1400 rpm / mid load.....	25
Figure 8 Pressure vs. CA comparison for 1900 rpm / low load	26
Figure 9 Heat release rate vs. CA comparison for 1900 rpm / low load.....	26
Figure 10 Pressure vs. CA comparison for 1900 rpm / mid load	26
Figure 11 Heat release rate vs. CA comparison for 1900 rpm / mid load.....	27
Figure 12 Pressure vs. CA comparison for 2400 rpm / low load.....	28
Figure 13 Heat release rate vs. CA comparison for 2400 rpm / low load.....	28
Figure 14 Pressure vs. CA comparison for 2400 rpm / mid load	29
Figure 15 Heat release rate vs. CA comparison for 2400 rpm / mid load.....	29
Figure 16 Multi-injection profile for 1400 rpm / low load operating condition..	31
Figure 17 Single injection profile for 1400 rpm / low load operating condition.	31
Figure 18 Injection profile for 1400 rpm / mid load operating condition	32
Figure 19 Injection profile for 1900 rpm / low load operating condition	33

	Page
Figure 20 Injection profile for 1900 rpm / mid load operating condition	33
Figure 21 Injection profile for 2400 rpm / low load operating condition	34
Figure 22 Injection profile for 2400 rpm / mid load operating condition	34
Figure 23 ISFC for multi-injection 1400 rpm / low load condition.....	36
Figure 24 Ind. eff. for multi-injection 1400 rpm / low load condition	36
Figure 25 Max pressure for multi-injection 1400 rpm / low load condition.....	36
Figure 26 ISFC for single injection 1400 rpm / low load condition.....	37
Figure 27 Ind. eff. for single injection 1400 rpm / low load condition.....	37
Figure 28 Max pressure for single injection 1400 rpm / low load condition	38
Figure 29 ISFC for 1400 rpm / mid load condition	39
Figure 30 Ind. eff. for 1400 rpm / mid load condition	39
Figure 31 Max pressure for 1400 rpm / mid load condition.....	39
Figure 32 ISFC for 1900 rpm / low load condition	40
Figure 33 Ind. eff. for 1900 rpm / low load condition	40
Figure 34 Max pressure for 1900 rpm / low load condition.....	41
Figure 35 ISFC for 1900 rpm / mid load condition	41
Figure 36 Ind. eff. for 1900 rpm / mid load condition	42
Figure 37 Max pressure for 1900 rpm / mid load condition.....	42
Figure 38 ISFC for 2400 rpm / low load condition	43
Figure 39 Ind. eff. for 2400 rpm / low load condition	43
Figure 40 Max pressure for 2400 rpm / low load condition.....	44

	Page
Figure 41 ISFC for 2400 rpm / mid load condition	44
Figure 42 Ind. eff. for 2400 rpm / mid load condition	45
Figure 43 Max pressure for 2400 rpm / mid load condition.....	45
Figure 44 NOx for multi-injection 1400 rpm / low load condition	46
Figure 45 HC for multi-injection 1400 rpm / low load condition	47
Figure 46 CO for multi-injection 1400 rpm / low load condition	47
Figure 47 NOx for single injection 1400 rpm / low load condition.....	48
Figure 48 HC for single injection 1400 rpm / low load condition.....	48
Figure 49 CO for single injection 1400 rpm / low load condition.....	48
Figure 50 NOx for 1400 rpm / mid load condition.....	49
Figure 51 HC for 1400 rpm / mid load condition.....	50
Figure 52 CO for 1400 rpm / mid load condition	50
Figure 53 NOx for 1900 rpm / low load condition	51
Figure 54 HC for 1900 rpm / low load condition	51
Figure 55 CO for 1900 rpm / low load condition	52
Figure 56 NOx for 1900 rpm / mid load condition.....	53
Figure 57 HC for 1900 rpm / mid load condition	53
Figure 58 CO for 1900 rpm / mid load condition	53
Figure 59 NOx for 2400 rpm / low load condition	54
Figure 60 HC for 2400 rpm / low load condition	54
Figure 61 CO for 2400 rpm / low load condition	55

	Page
Figure 62 NOx for 2400 rpm / mid load condition.....	55
Figure 63 HC for 2400 rpm / mid load condition	56
Figure 64 CO for 2400 rpm / mid load condition	56
Figure 65 ISFC for six operating conditions using HCCI model	61
Figure 66 Ind. eff. for six operating conditions using HCCI model	61
Figure 67 Max pressure for six operating conditions using HCCI model	62
Figure 68 NOx for six operating conditions using HCCI model.....	63
Figure 69 HC for six operating conditions using HCCI model.....	63
Figure 70 CO for six operating conditions using HCCI model.....	64
Figure 71 Pressure rise rates for 1400 rpm / mid load condition.....	66
Figure 72 Pressure rise rates for 1900 rpm / low load condition.....	66
Figure 73 Pressure rise rates for 1900 rpm / mid load condition.....	66
Figure 74 Pressure rise rates for 2400 rpm / low load condition.....	67
Figure 75 Pressure rise rates for 2400 rpm / mid load condition.....	67
Figure 76 Pressure rise rates vs. intake temperature for 3 conditions.....	68
Figure 77 Pressure rise rate for multi-injection 1400 rpm / low load condition .	70
Figure 78 Pressure rise rate for single injection 1400 rpm / low load condition.	70

LIST OF TABLES

	Page
Table 1 General characteristics of the test engine system.....	21
Table 2 EGR ratio (%) for different speed / load combinations.....	22
Table 3 SOI (degrees) timing for different speed / load combinations.....	22
Table 4 First set of conventional engine results	57
Table 5 Second set of conventional engine results	57
Table 6 Criteria for selection of optimal EGR and injection timings [16]	57
Table 7 Optimal EGR and injection timing combination for 1400 rpm cases	58
Table 8 Optimal EGR and injection timing combination for 1900 rpm cases	58
Table 9 Optimal EGR and injection timing combination for 2400 rpm cases	59

1. INTRODUCTION

The importance of diesel engines in today's society is seen through their widespread usage in the areas of transportation and power generation. This engine system is used more commonly in the ground transportation, the maritime transportation, and the base-load power generation industries over the spark-ignition (i.e. gasoline) engine due to its improved fuel efficiency. The diesel engine is also known as the compression-ignition engine due to the method by which the fuel is ignited inside the cylinder. Air inside the cylinder is compressed to high pressures resulting in a high temperature environment into which the fuel is directly injected. This fuel then ignites and the subsequent combustion provides the energy required to drive the piston. The major drawback to this type of engine comes in the form of high levels of nitric oxides (NO_x) and soot emissions. Due to the widespread usage of this type of engine, efforts are being made to improve the performance and emissions levels through variations in combustion types and temperatures.

The formation of NO_x inside a diesel engine is heavily dependent on the temperatures that are reached in the cylinder. This is due to the fact that the Zeldovich mechanism dominates the formation of NO_x from free radicals inside the exhaust gases immediately post combustion. The Zeldovich mechanism predicts that NO_x formation occurs exponentially higher at combustion temperatures higher than 1800 K [1]. This leads to the development of low temperature combustion (LTC) operating modes that

This thesis follows the style of the SAE International Journal of Engines.

help to decrease the inherent NO_x production inside the cylinder. These modes are nominally accomplished through the use of high levels of EGR, which suppresses combustion temperatures. Soot is formed predominately through the development of soot precursors in pockets of fuel rich areas inside the cylinder [1]. The formation of these precursors is highly dependent on the fuel rich pockets and is therefore combated through the elimination of these pockets by forming an overall lean mixture inside the cylinder. The formation of this lean mixture is accomplished through increased levels of mixing in the cylinder prior to the start of ignition. This mixing is done through high swirl ratios and long ignition delay times resulting in part from decreased overall in-cylinder temperatures.

LTC and specifically HCCI operating modes provide all of the necessary combustion attributes required to decrease the NO_x and soot levels in diesel engines. The development and implementation of these combustion modes comes with problems of their own, such as increases in hydrocarbon (HC) and carbon monoxide (CO) emissions and increases in overall engine noise due to large pressure rise rates. The use of these combustion modes in diesel engines over the next few decades will be absolutely vital to meet ever increasing governmental emissions regulations.

2. OBJECTIVES

The overall objective of this thesis study is to use an engine simulation model to develop ideal conditions for low temperature combustion in a diesel engine and to use the model at those conditions to analyze performance and emissions characteristics. The process by which this objective will be attained is threefold.

The first step is to develop and validate the model using the GT-Power modeling software. This involves the setup of the model in a way that accurately represents the laboratory test engine. The EGR and turbocharger systems along with their respective intercoolers are included with the cylinders, ports, and manifolds in correct configurations. The model is then developed until the pressure and heat release rate diagrams accurately reflect the experimental engine data.

The second step is conducting parametric studies using multiple combustion models to determine the optimal EGR and injection timing configurations that stay within 10% of the lab engine's performance and provide at least 70% better NO_x emissions. The parametric studies done to determine the optimal EGR and injection timing combinations are performed using the multi-zone, quasi-dimensional combustion model while the knock-induced combustion model is used for ideal EGR analysis.

The third step consist of investigating potential methods of decreasing pressure rise rates, which are a major limiting factor in LTC operation. This step requires the analysis of three different methods to lower the pressure rise rates inside the cylinder. The completion of these steps will provide accurate LTC operation data.

3. LITERATURE REVIEW

Low temperature combustion (LTC) engine systems are a very current topic of research inside the automotive industry. This novel combustion mode is heavily present in current literature due to its probable application in next generation diesel engines. Industry and academic research centers are experimentally implementing this combustion concept in modified and production level laboratory engines and mathematically modeling this concept accurately to develop an overall understanding. The publication dates contained within this review range from 2005 to 2008; therefore, these documents contain current and novel research in this area.

3.1 Experimental implementation of LTC engine systems

3.1.1 The effects of multiple injections and fuel properties on LTC

The experiments conducted in [2] and [3] used a 4 cylinder, 4 stroke Ford DuraTorq “Puma” engine setup to implement LTC with controlled EGR. These experiments determined the major factors associated with thermal and fuel efficiency during LTC engine operation. It was determined that the fuel and thermal efficiency was highly determined by the combustion phasing inside the cylinder and that the implementation of a multiple injection strategy was key to achieving the maximum attainable efficiency [2, 3]. The idea that multiple injection strategies have the ability to combat the problems associated with LTC engine modes is supported by the experiments in [4, 5, 6]. One of the major problems with LTC operation involves an increase in HC and CO emissions as NO_x and soot decrease. The study in [4] consists of implementing

single and double pilot injections along with the main injection to try and combat this problem. This experiment was conducted at 1750 rpm and 3 bar brake mean effective pressure (BMEP) and the results show that the single injection is better in the area of HC, CO, and soot but is worse in the area of engine noise. The single pilot injection is slightly better in HC emissions and engine noise but worse in all other areas. The double pilot injection was much worse in all areas except engine noise. This was contended with during the experiment by implementing a separation of approximately 8 CA degrees with the single pilot injection which provided improvements in all areas over the single injection except in soot production [4]. The experiment in [5] showed performance and emissions improvements by implementing a multiple pulsed injection strategy that provided 5 pulse injections of progressively increased quantity to provide increased mixing and distribution throughout the cylinder. In this case the injections began at 87 CA degrees bTDC and used an increased injection pressure to provide a more homogeneous mixture and improve HCCI implementation. Sun et al. [6] showed that the start of injection (SOI) for HCCI implementation must be selected carefully when using single and multiple injections to avoid spray-wall impingement caused by too early injections and non-homogeneity caused by too late injections. It was also shown that the HC and CO emissions come from lean, over-mixed regions with low temperatures just as NO_x and soot come from rich, non-homogeneous areas with high temperatures. Fuel properties can also have an effect on the emissions from LTC engines. Some experiments [7] show that decreasing the cetane number increases the ignition delay and subsequently improves the mixing inside the cylinder. This reduces

the particulate emissions. The experiment also displayed better efficiencies at higher loads when using fuel with a decreased cetane number [7].

3.1.2 Methods to decrease pressure rise rates during LTC

Another problem associated with LTC and specifically HCCI operation is the high engine noise resulting from large pressure rise rates during the sudden combustion of a fully premixed cylinder charge. Different methods for controlling the pressure rise rates have been presented and include using multiple injection strategies, highly cooled EGR, and high levels of EGR. The experiment in study [4] already showed that the implementation of one or more pilot injections with up to 10 CA degrees separation from the main injection have the ability to decrease the overall engine noise. This is likely due to the spreading out of combustion events inside the cylinder from one large sudden heat release to multiple smaller heat releases. One study [8] shows the possibility of using highly cooled EGR to decrease the pressure rise rate. This occurs because the decreased EGR temperature leads to a decreased intake manifold temperature which causes the initiation of the combustion event to be slightly delayed while the total event is prolonged. A slight drop in maximum cylinder pressure is also seen which all together presents a decreased pressure rise rate while not affecting engine performance. Another study [9] shows the possibility of high levels of EGR leading to decreased pressure rise rates. These pressure rise rate drops coincide with drops in peak cylinder pressure associated with the EGR level. The drawbacks to this method are that at high levels of EGR combustion efficiency decreases rapidly which leads to poor engine performance.

3.2 Modeling LTC and HCCI engine operation

3.2.1 Overall LTC and HCCI engine modeling

In many cases [2, 3, 5, 6] engine modeling is used to supplement experimental results to be able to more easily gather large scale data without having to set up experimental systems which require much more time. These models are developed and validated by comparing results produced by the model to experimental results using the same input parameters. There are generally three different levels of engine combustion modeling zero-dimensional, multi-zone quasi-dimensional, and multi-dimensional with CFD and combustion chemistry included.

3.2.2 Combustion modeling for LTC engines

Studies [2, 3, 9] show examples of zero-dimensional combustion and engine cycle simulations. In zero-dimensional modeling, a single zone in-cylinder temperature model is used even though the temperature in the cylinder varies throughout. This simplifies the calculation to one temperature calculation per transient event. Using the zero-dimensional model to calculate in-cylinder changes of state for HCCI systems requires the assumption of a homogenous reactor [9]. This system calculates mass and heat flows in and out of the system along with surface states along the surface of the cylinder leading to a fully developed transient energy balance equation. The systems heat transfer is calculated using the Woschni model [9].

The multi-dimensional model with computational fluid dynamics (CFD) and combustion chemistry included is by far the most accurate and complicated combustion analysis. The studies in [5, 6] coupled CFD code with chemical calculations to

numerically model multi-dimension engine simulations. The CFD code used was KIVA-3V combined with the RNG k- ϵ turbulence model. The Linearized Instability Sheet Atomization (LISA) and the Taylor Analogy Breakup (TAB) models were used for analyzing droplet breakup processes at low pressures while the Kelvin-Helmholtz and the Rayleigh-Taylor hybrid model was used to calculate the droplet breakup at high pressures [5, 6]. Along with this code was included to predict droplet vaporization, droplet collision, and droplet-wall interactions along with a polar interpolation method to calculate the momentum transfer between the liquid and gas phases [6]. The diesel fuel chemistry was calculated using a 30 species n-heptane chemistry mechanism in conjunction with the CFD code [6]. The major drawback to calculating this highly accurate engine cycle simulation is the massive amount of time and computer power required to run even one cycle of simulations.

This is the reason that multi-zone, quasi-dimensional combustion and engine calculations are much more common. The multi-zone model is fairly accurate while requiring only limited computer calculation time. The study in [10] shows that the multi-zone combustion model can be used to predict heat release rate, thermal efficiency, indicated mean effective pressure (IMEP), and emissions with much higher accuracy than a single-zone model. This study's results show that more combustion zones in the colder in-cylinder regions can help improve emissions prediction, that the Woschni model is the most effective at heat transfer prediction, and that the mass exchange model has a huge impact on CO prediction [10].

3.2.3 NO_x and soot emissions modeling for LTC engines

The development of accurate NO_x and soot prediction models is absolutely necessary to the correct modeling of LTC operation in diesel engines. The model developed in [11] adds hydrogen cyanide (HCN) and the CH radical to the ERC's reduced 12-step NO_x mechanism. This mechanism more accurately predicts the observable increase in NO_x associated with increases in engine load that is not seen with the current reduced NO_x mechanism. This new NO_x mechanism improves the ERC 2-step soot model by introducing the CH radical as a soot precursor along with the other precursors [11]. This model has application as an addition to the current CHEMKIN code for improved emission prediction in LTC engines. The model in [12] has a more active soot prediction method that analyzes soot precursor development inside the diesel jet 0.5 ms after the end of evaporation. This model only predicts soot from precursors and does not include soot combustion that occurs in the jet boundary [11].

4. MODEL AND CALCULATIONS

4.1 Model development

A model was developed to determine the optimal EGR and injection timing combinations for LTC conditions to occur in the experimental engine at three different engine speeds and two different load levels. This model was also used to determine engine performance data, emissions data, and to investigate possible ways to decrease engine noise during LTC operation. To accomplish this task, the model was designed in GT-Power as a 4 cylinder, direct injection diesel engine just like the one available in the laboratory. The GT-Power model has an EGR system that redirects a certain percentage of the exhaust through an intercooler and combines it with the intake air flow stream. The model also includes the exit state for the compressor and the intake state for the turbine developed from SAE maps [13]. Another model was designed that uses a very similar setup but has port injection and the combustion is calculated using the Knock-induced combustion model instead of the multi-zone, quasi-dimensional model associated with the direct injection model. For these two models, GT-Power calculates all thermodynamic states and system attributes through a variety of other models and objects. These models were developed through assumptions and calculations with corrections based on experimental data. The calculations are from known equations developed through countless years of diesel engine research and are implemented in the models. The details and the equations that make these up are shown in the multiple sections below.

4.2 General model calculations

The general models below provide the necessary equations and calculations needed to understand the results of the EGR and injection timing parametric studies.

4.2.1 Fluid flow models

GT-Power models fluid flow using the conservation of mass and energy along with one-dimensional Navier-Stokes equations. This model discretizes each fluid flow into multiple sections with scalar quantities, such as pressure and temperature, defined for each section and vector quantities, such as mass flow rate and velocity, defined at each boundary. The conservation of mass and energy along with the Navier-Stokes equations used for these calculations are shown below [14].

$$\begin{aligned}
 \text{Continuity: } \quad \frac{dm}{dt} &= \sum_{\text{boundaries}} \dot{m} \\
 \text{Energy: } \quad \frac{d(me)}{dt} &= p \frac{dV}{dt} + \sum_{\text{boundaries}} (\dot{m}H) - hA_s (T_{\text{fluid}} - T_{\text{wall}}) \quad \text{(explicit solver)} \\
 \text{Enthalpy: } \quad \frac{d(\rho HV)}{dt} &= \sum_{\text{boundaries}} (\dot{m}H) + V \frac{dp}{dt} - hA_s (T_{\text{fluid}} - T_{\text{wall}}) \quad \text{(implicit solver)} \\
 \text{Momentum: } \quad \frac{d\dot{m}}{dt} &= \frac{dpA + \sum_{\text{boundaries}} (\dot{m}u) - 4C_f \frac{\rho u |u|}{2} \frac{dxA}{D} - C_p \left(\frac{1}{2} \rho u |u| \right) A}{dx}
 \end{aligned}$$

Specific conditions are set up to model the flow of fluid inside the cylinder and this is conducted by the GT-Power reference object EngCylFlow. This model breaks up the cylinder into 4 different regions including the head region, the squish region, the

center region, and the piston region. This fluid model also includes equations for the calculation of swirl and tumble. Figure 1 shows the different fluid regions and the equations for swirl and tumble are below it [14].

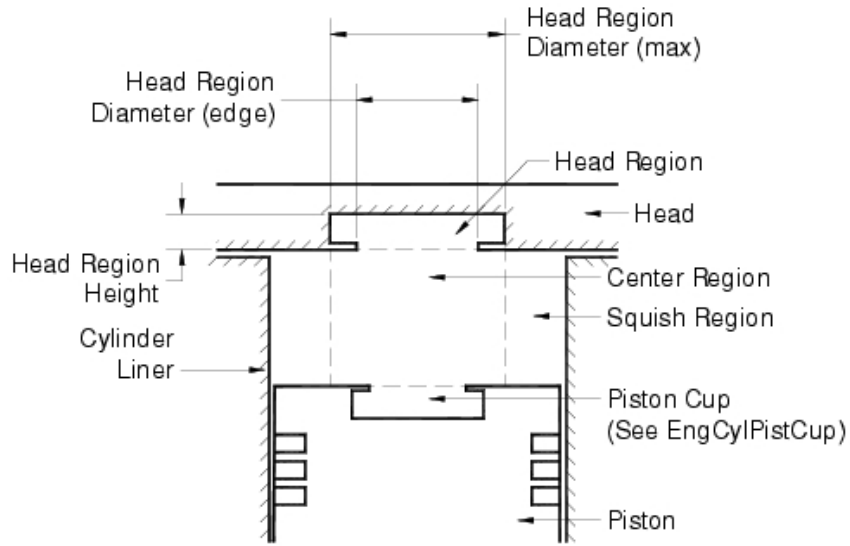


Figure 1 Separated fluid regions for in-cylinder flow

$$\text{Swirl Coefficient} = \frac{T_s}{\dot{m} * U_{is} * .5 * D}$$

$$\text{Tumble Coefficient} = \frac{T_t}{\dot{m} * U_{is} * .5 * D}$$

$$U_{is} = \sqrt{RT_o} \left\{ \frac{2\gamma}{\gamma - 1} \left[1 - P_r^{\frac{\gamma-1}{\gamma}} \right] \right\}^{\frac{1}{2}}$$

This model uses the cylinder geometry, piston motion and the flow rate of the entering and exiting gases in conjunction with the swirl and tumble coefficients of those

gases to calculate the radial, axial, and swirl velocities at each time step [13]. From this an accurate picture of flow inside the cylinder takes shape and is used with the injection and combustion models to determine the complete cylinder picture for each cycle.

4.2.2 Heat transfer models

The in-cylinder heat transfer was developed and is currently modeled through a correlation that allows for the accurate prediction of the heat transfer throughout the cylinder. The Woschni correlation was developed to accurately form a convective heat transfer coefficient while taking into account the increase in gas velocity during combustion. The Hohenberg correlation was designed directly from the Woschni correlation and has been shown to more accurately predict convective heat transfer coefficients for direct injection diesel engines [15].

Original Woschni Correlation

$$h_{\text{Woschni}} = B^{-0.2} \cdot p^{0.8} \cdot T^{-0.53} \cdot \left(C_1 \bar{S}_p + C_2 \frac{V_d T_r}{p_r V_r} (p - p_{\text{mot}}) \right)^{0.8}$$

$$C_1 = 2.28 + 0.308 \frac{\pi B w_p}{\bar{S}_p}, \quad C_2 = 0.00324$$

Hohenberg Correlation

$$h_{\text{Hohenberg}} = 130 \cdot V^{0.6} \cdot p^{0.8} \cdot T^{-0.4} \cdot (\bar{S}_p + 1.4)^{0.8}$$

The intercoolers, both EGR and compressor, are basically modeled as simple heat exchangers between the hot gases and the ambient air. This makes sense because the cooling system used on an automobile has the hot gases pass through a series of

tubes which are cooled by outside air passing over them while the automobile is driven. In GT-Power, the intercoolers are modeled semi-predictively as air passing over a multiple pipe outlet. The equation governing the cooling is the basic heat exchanger equation which is shown below [14].

$$T_{out} = T_{in} - \varepsilon(T_{in} - T_{amb})$$

4.2.3 Combustion models

The direct injection model uses a multi-zone, quasi-dimensional combustion model to accurately calculate the combustion of the diesel injection as it enters the cylinder. GT-Power uses the object EngCylCombDIJet to define this combustion model within the overall model. The diesel fuel from the injection spray is split into up to 500 different zones, 5 radial zones and up to 495 axial zones, which are each split up into 3 different sub-zones made up of unburned liquid fuel, unburned air/fuel mix, and burned combustion gasses. The unburned sections and the burned sections have different temperatures. The distribution of zones is shown in Figure 2 and zonal distribution from an actual model is shown in Figure 3 [14].

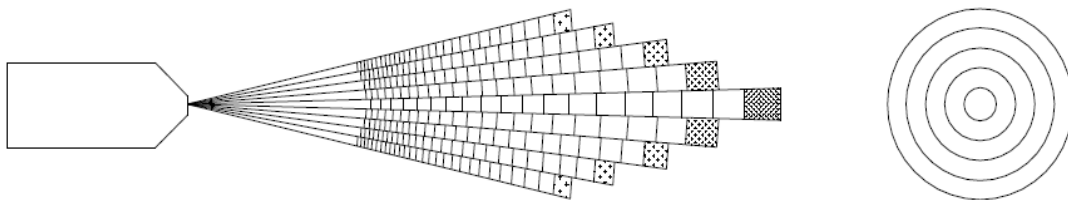


Figure 2 Axial and radial combustion zones for the multi-zone model

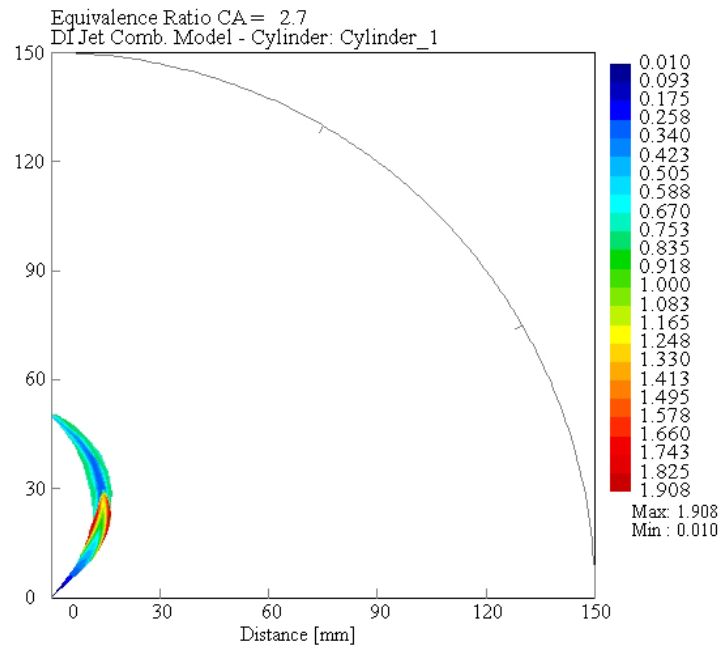


Figure 3 Example of zonal distribution throughout an injection

When the diesel jet is first injected into the cylinder it is entirely liquid fuel but as it passes into the cylinder it pulls in air that is alongside the outer edges and entrains it into each of the zones. This entrainment of air into the zones causes drag on the injection which leads to the more centralized radial zones being injected farther into the cylinder than the outer zones because they entrain air much slower than the outer zones. Once the air enters the zone it combines with the evaporated diesel fuel to form the air/fuel sub-zone while the remaining liquid fuel forms another sub-zone. Temperature, pressure, and air-fuel ratio are calculated for each zone at each time step and when the temperature and pressure get high enough along with the correct air-fuel ratio the zone goes through combustion. This moves the combusted gases into the third sub-zone of burned gasses and allows for calculation of burn rate, or combustion rate. The NO_x and

soot emissions are calculated inside the burned gasses sub-zone using the temperature and air-fuel ratio at that time. Many sub-models are included in this multi-zone, quasi-dimensional combustion model such as the injection model, the fuel spray breakup and penetration model, the droplet breakup model for radial zones, the air entrainment model, and the droplet evaporation model [13]. The ignition delay is the time between the start of injection and the beginning of combustion and is important to the development of LTC. A long ignition delay is important in LTC engines because it allows for good mixing inside the cylinder leading to a homogeneous charge and overall very lean combustion which helps decrease temperatures. The ignition delay sub-model for the multi-zone model is shown below [13].

$$\begin{cases} \tau = \frac{Ai \times 10^{-6}}{\phi(3-\phi)^2} P^{Bi} \exp\left(\frac{C_i}{T}\right) & \text{for } \phi < 3.0 \\ \tau = \infty & \text{for } \phi > 3.0 \end{cases}$$

The other model used in this study to calculate the combustion of the fuel/air mixture inside the cylinder is the knock-induced combustion model. This is modeled inside the overall system using port injection and simulating in-cylinder combustion using a knocking mechanism. The overall combustion model is a two-zone model, unlike the multi-zone model used in the other case, which has an unburned zone and a burned zone. All the gases initial start in the unburned zone inside the cylinder then at each time step a portion of the fuel-air mixture is passed into the burned zone according

to the burn rate. This burn rate follows the Wiebe model and is non-predictive. At the end of each time step, the burned zone is used in a lumped form to calculate emissions based on temperature and fuel/air mixture. The energy equations for the unburned and the burned zones and the apparent heat release rate equation are shown below [14].

Unburned Zone:

$$\frac{d(m_u e_u)}{dt} = -p \frac{dV_u}{dt} - Q_u - \left(\frac{dm_f}{dt} h_f + \frac{dm_a}{dt} h_a \right) + \frac{dm_{f,i}}{dt} h_{f,i}$$

Burned Zone:

$$\frac{d(m_b e_b)}{dt} = -p \frac{dV_b}{dt} - Q_b + \left(\frac{dm_f}{dt} h_f + \frac{dm_a}{dt} h_a \right)$$

$$AHRR = \frac{\left(-p \frac{dV_{tot}}{dt} - Q_{tot} - \frac{d(m_{tot} e_{tot,s})}{dt} \right)}{m_{f,tot} * LHV_i}$$

This overall two-zone combustion model is combined with the knock sub-model defined by the GT-Power object, EngCylKnock. The calculation of knock is based on the Douaud and Eyzat formula and knock occurs inside the cylinder when the induction time integral is equal to 1. The knock index is also calculated using this model. The equations for both are shown below [14].

$$\tau = 5.72e6 P \left(\frac{ON}{100} \right)^{3.402} p^{-1.7} \exp \left(\frac{3800}{AT_u} \right)$$

$$T = \int_{NVC}^{t_{kn}} \frac{I}{\tau} dt$$

$$KI = 10000 * A * km * \left(\frac{V_{IDC}}{V_I} \right) e^{-T_s/T_a} * \max[0, (1 - (1 - \phi)^2)] * T_{avg}$$

4.2.4 Emissions models

Emissions simulations from these models are very important to the development of the optimal EGR and injection timing combinations that are the focus of this study. GT-Power models the NO_x emissions using the extended Zeldovich method which includes three oxidation reactions and their respective reaction rates. These reactions and reaction rates are shown below [14].

N₂ oxydation rate equation: $O + N_2 = NO + N$ (1)

N oxidation rate equation: $N + O_2 = NO + O$ (2)

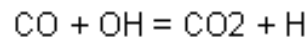
OH reduction rate equation: $N + OH = NO + H$ (3)

$$k1 = F_1 * 7.60 * 10^{10} * e^{-38000 * A_1 / T_b}$$

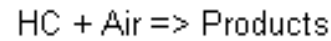
$$k2 = F_2 * 6.40 * 10^6 * T_b * e^{-3150 * A_2 / T_b}$$

$$k3 = F_3 * 4.10 * 10^{10}$$

GT-Power also has the ability to model the formation of both CO and HC emissions inside the engine. These two emissions values are very important to LTC and HCCI operation. This is due to the fact that as more lean charges and lower combustion temperatures are developed to reduce the NO_x and soot they have an opposite effect on the formation of CO and HC. The CO and HC formation equations are respectively shown on the subsequent page [14].

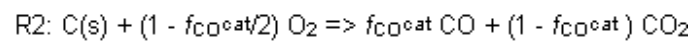
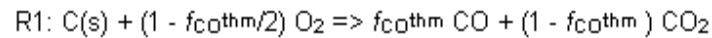


$$k_1 = A * 6.76 * 10^7 * e^{\frac{T}{B * 1102}}$$



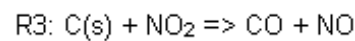
$$k_1 = A \cdot 1 * 10^{12} \cdot [\text{HC}][\text{O}_2] * e^{-19000 * B/T}$$

GT-Power also calculates soot formation using a complicated series of equations but the actual soot formation numbers are often inaccurate. These equations are meant to be used to formulate and discuss trends within parametric studies. The equations are shown below [14].

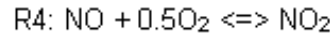


$$\dot{r}_{\text{soot}} = -(K_{\text{thm}} + K_{\text{cat}}) S_p \rho_w Y_{\text{O}_2} \frac{M_c}{M_{\text{O}_2}}$$

$$K_{\text{thm}} = A_T T e^{-\left(\frac{E_T}{T}\right)} \quad \text{and} \quad K_{\text{cat}} = A_C T e^{-\left(\frac{E_C}{T}\right)}$$



$$\dot{r}_3 = A_3 \exp\left(\frac{-E_3}{T}\right) Y_{\text{NO}_2}$$



$$\dot{r}_4 = A_4 \exp\left(\frac{-E_4}{T}\right) \left(c_{NO} c_{O_2}^{0.5} - \frac{c_{NO_2}}{K_{eq}(T)} \right)$$

4.3 Equations for the performance characteristics

Important factors in determining whether or not an EGR and injection timing combination is ideal for a certain engine operating condition are the engine performance characteristics. These characteristics are most readily noticeable through 3 different given values the indicated mean effective pressure (IMEP), indicated specific fuel consumption (ISFC), and the indicated efficiency. The GT-Power model calculates these values using the equations shown below [14].

$$imepc = \frac{\oint P dV}{V_{disp}}$$

$$isfcc = \left[\frac{fuel_{tot}}{V_{disp} \bullet imepc} \right] \bullet 0.036$$

$$ieffc = \left[\frac{V_{disp} \bullet imepc}{fuel_{nrg}} \right] \bullet 10^7$$

$$fuel_{nrg} = (LHV_f) \oint \dot{m}_{f,i,gas} dt + (LHV_f - HVP_f) \oint \dot{m}_{f,i,liq} dt$$

5. RESULTS AND DISCUSSION

The model developed above was combined with general engine inputs and then calibrated to accurately reflect the laboratory engine. The main focus of this study was to conduct parametric studies on both the EGR ratio and injection timings for general operating conditions to develop optimized LTC operating modes. EGR ratio and injection timing were chosen as parameters because both have the ability to greatly affect LTC operation and implementation. The secondary focus of this study was to analyze and investigate possible methods to reduced combustion noise associated with in-cylinder pressure rise rates.

5.1 Engine inputs

The engine system used for these experiments was a 4.5 liter, 4 cylinder inline John Deere diesel engine running on common diesel fuel. The fuel characteristics are shown in Appendix D. The general engine specifics are noted in Table 1.

Table 1 General characteristics of the test engine system

Engine Type	4-Cylinder, 4-Stroke John Deere
Fuel Type	Diesel
Displacement [L]	4.5
Bore [mm]	106
Stroke [mm]	127
Connection Rod Length [mm]	200
TDC Clearance Height [mm]	1.3
Compression Ratio	16.6:1
Valve System	4 valves per cylinder, OHV, Roller Lifter
Injection System	Common rail direct injection system
EGR System	High pressure, cooled EGR
Turbocharging System	Air cooled compressor and variable geometry turbine

5.2 Model validation

The model was effectively validated using preliminary experimental data from the laboratory engine. The validation was conducted for 9 different operation cases, 3 speed and 3 load conditions. The cases were given at speeds of 1400 rpm, 1900 rpm, and 2400 rpm with loads at 68 N-m, 204 N-m, and 408 N-m for each speed. These loads will be referred to as low, mid, and high loads respectively. Each of these speed and load combinations had general EGR ratios and SOI values associated with them. These values are shown in Table 2 – Table 3.

Table 2 EGR ratio (%) for different speed / load combinations

Load (N-m)	Speed (rpm)		
	1400	1900	2400
68	-17.4	-17	-24
204	-5	-5	-12.2
408	-3	-7	-13

Table 3 SOI (degrees) timing for different speed / load combinations

Load (N-m)	Speed (rpm)		
	1400	1900	2400
68	0	0	0
204	0	0	0
408	18.2	18.3	20.9

The model's validation consisted of a series of pressure and heat release rate comparisons between the experimental data and the model data. These graphs are shown in Figure 4 – Figure 5.

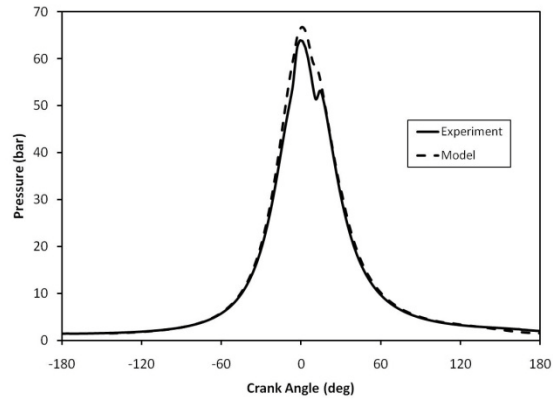


Figure 4 Pressure vs. CA comparison for 1400 rpm / low load

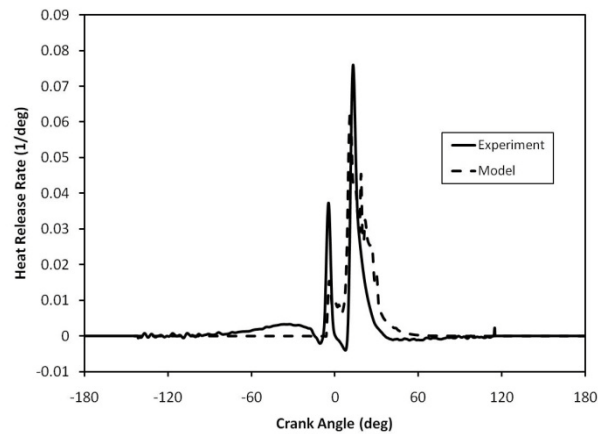


Figure 5 Heat release rate vs. CA comparison for 1400 rpm / low load

Figure 4 shows that there is a fairly good pressure comparison between the model results and the experimental data at 1400 rpm / low load. The model has a slightly higher peak pressure and is smoother than the experimental results, but this is to be

expected. The heat release rates for the model and the experiment at 1400 rpm / low load is shown in Figure 5. The model matches the second peak closely but does release heat longer starting at about 20 CA degrees. The model also does not show a high enough heat release rate at the first peak corresponding to the pilot injection's ignition. These discrepancies are due to differences in the amount of fuel injected during the pilot injection and the main injection between the experiment and the model. This leads to different amounts of combustion resulting from the pilot and the main injections which shows in the shorter model heat release rate after the pilot injection and the longer heat release rate after the main injection.

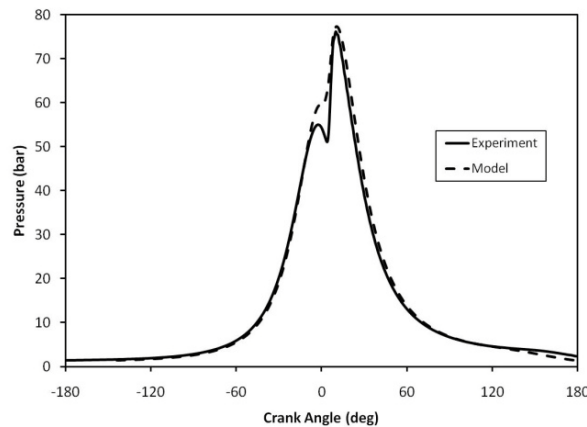


Figure 6 Pressure vs. CA comparison for 1400 rpm / mid load

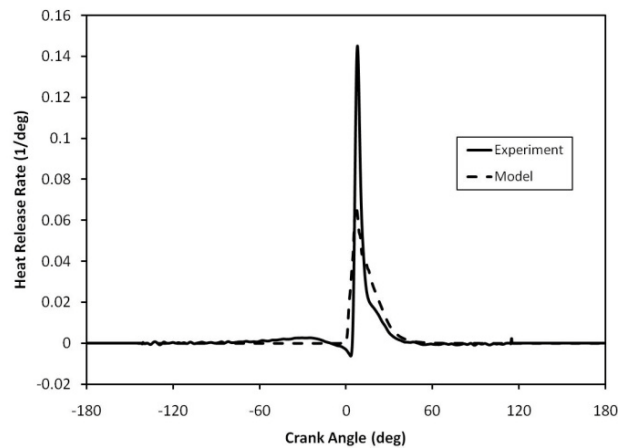


Figure 7 Heat release rate vs. CA comparison for 1400 rpm / mid load

Figure 6 shows the pressure comparison for the mid load level at 1400 rpm and this is very similar to the 1400 rpm / low load pressure comparisons. This figure shows model results that have higher peak levels and are smoother than the experiment. On the other hand, the heat release rate comparison shown in Figure 7 has the model result differing significantly from the experiment. This is also likely the result of estimates of the injection pressures in the model since only the injection voltage signal, not the exact injection pressures, are known.

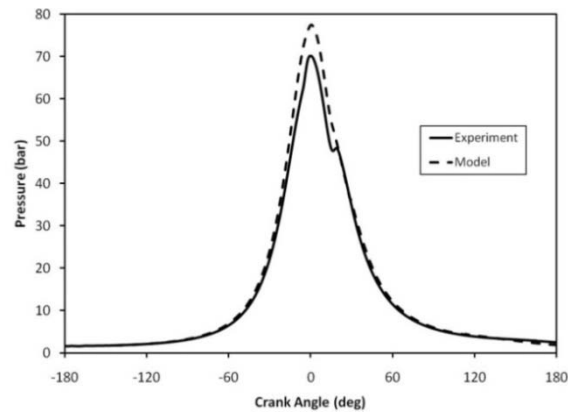


Figure 8 Pressure vs. CA comparison for 1900 rpm / low load

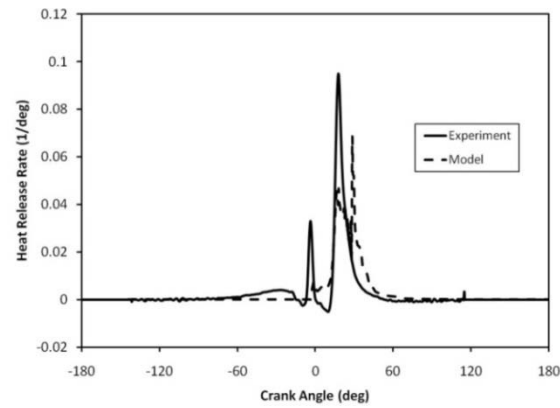


Figure 9 Heat release rate vs. CA comparison for 1900 rpm / low load

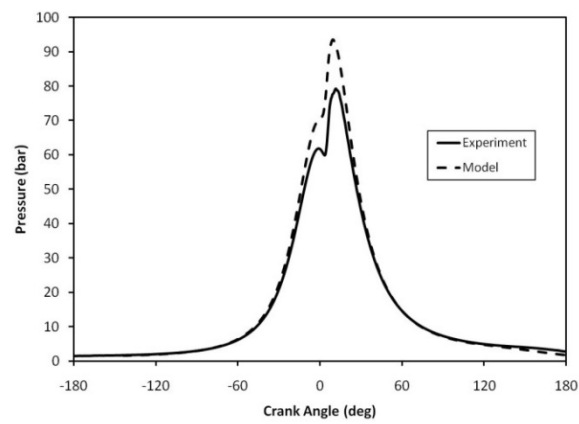


Figure 10 Pressure vs. CA comparison for 1900 rpm / mid load

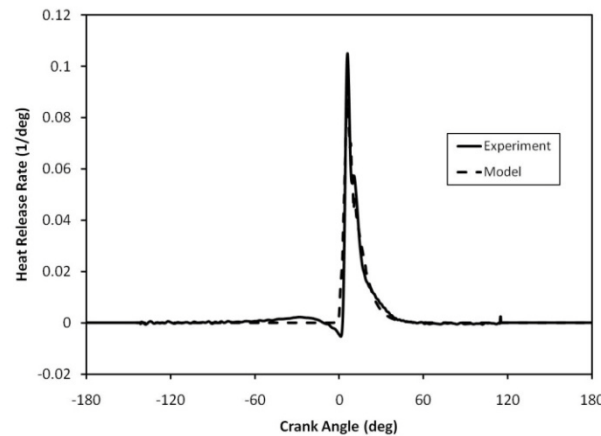


Figure 11 Heat release rate vs. CA comparison for 1900 rpm / mid load

Figure 8 – Figure 11 show the pressure and heat release rate comparisons for the 1900 rpm / low load and the 1900 rpm / mid load conditions. The pressure comparison graphs both show slightly increased peak pressure values in the model over the experimental engine. This pressure difference is similar to the pressure differences located in the 1400 rpm / low load and the 1400 rpm / mid load conditions. The most likely cause of the discrepancy is slight differences in the actual amount of fuel injected in the experimental engine compared to the estimated fuel injected in the model. This is the direct result of estimated injection pressure values. The heat release rate comparison for the 1900 rpm / low load condition shows that the model is more erratic and slightly longer than the experiment. This is due to differences in combustion rate in the model compared to the experiment. Due to the longer heat release in the model, it will release nearly the same amount of heat as the experiment which is shown by the nearly matching pressure comparisons. The heat release rate for the 1900 rpm / mid load condition is almost exactly the same between the model and the experiment which

indicates very similar cylinder conditions. The discrepancies in this system are well within tolerable limits for engine modeling.

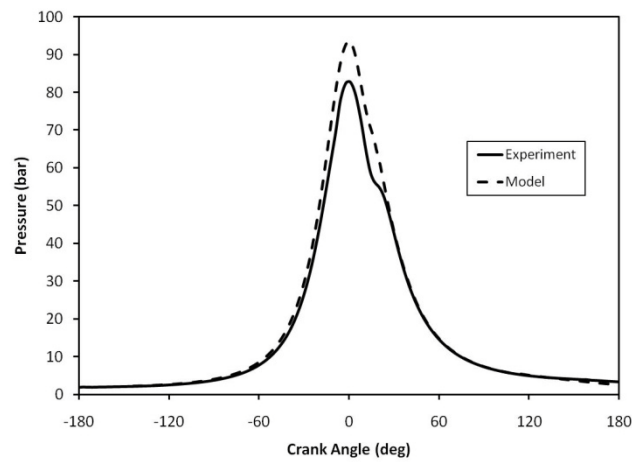


Figure 12 Pressure vs. CA comparison for 2400 rpm / low load

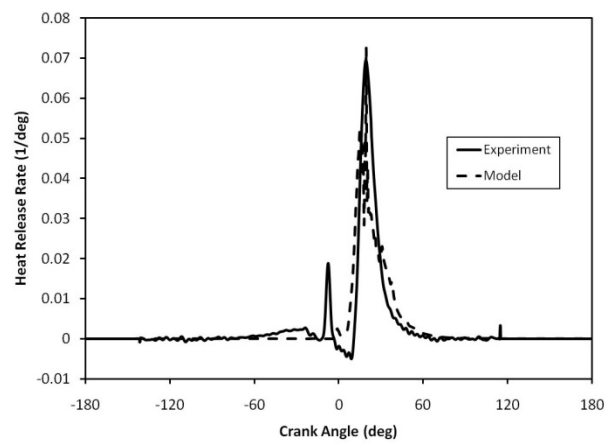


Figure 13 Heat release rate vs. CA comparison for 2400 rpm / low load

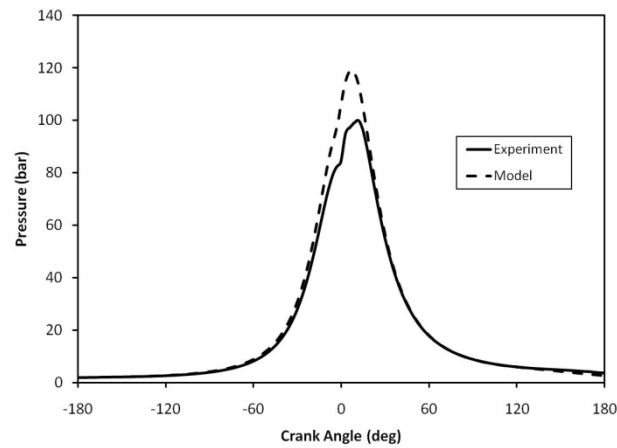


Figure 14 Pressure vs. CA comparison for 2400 rpm / mid load

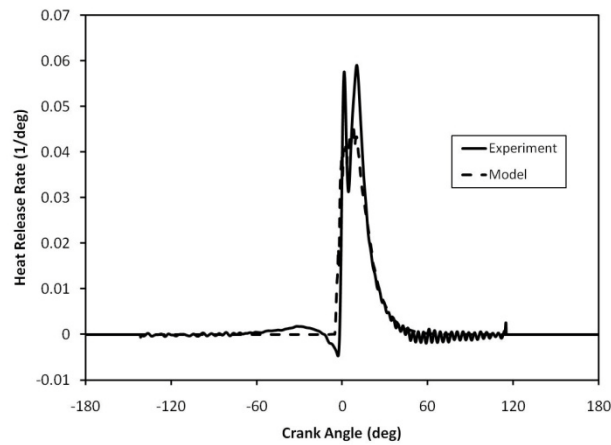


Figure 15 Heat release rate vs. CA comparison for 2400 rpm / mid load

The pressure comparisons, shown in Figure 12 and Figure 14, are similar to the pressure comparisons for the 1400 rpm and the 1900 rpm cases. The heat release rate comparisons, shown in Figure 13 and Figure 15, both show good comparisons between the model and the experiment except for the lack of accurate pilot injection modeling shown in the 2400 rpm / low load case. This pilot injection discrepancy is similar to the

1400 rpm / low load and the 1900 rpm / low load cases. As with the 1400 rpm and 1900 rpm cases, this validation shows that the engine model accurately predicts the experimental engine within acceptable tolerances.

The validation data for the all the engine speeds at the high load level is available in Appendix A. This data shows reference validation at these cases but the engine model breaks down when attempting to develop low temperature combustion using high EGR levels; therefore, parametric studies were not conducted for this load.

5.3 EGR and injection timing parametric studies

Parametric studies were conducted for the operating points at 1400 rpm, 1900 rpm, and 2400 rpm with low and mid load levels. These parametric studies were developed to determine the effects of varying the EGR ratio and the injection timing on LTC operation. The parametric studies consisted of varying the EGR ratio from 30% to 60% in increments of 10% while varying the injection timing from 40 CA degrees bTDC to 5 CA degrees bTDC in 2.5 CA degree increments.

5.3.1 Injection profiles for the operating points

The injection profiles developed for each operating point were constructed from injector voltage signals in the experimental engine. These injection profiles are shown in figures on pages 31 – 36.

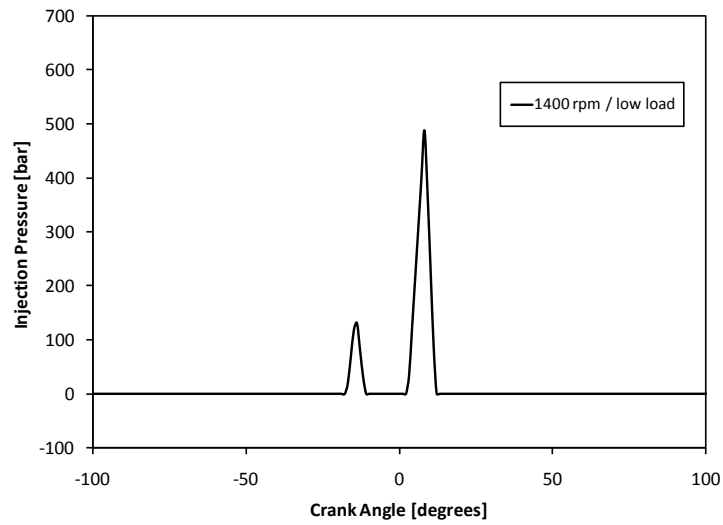


Figure 16 Multi-injection profile for 1400 rpm / low load operating condition

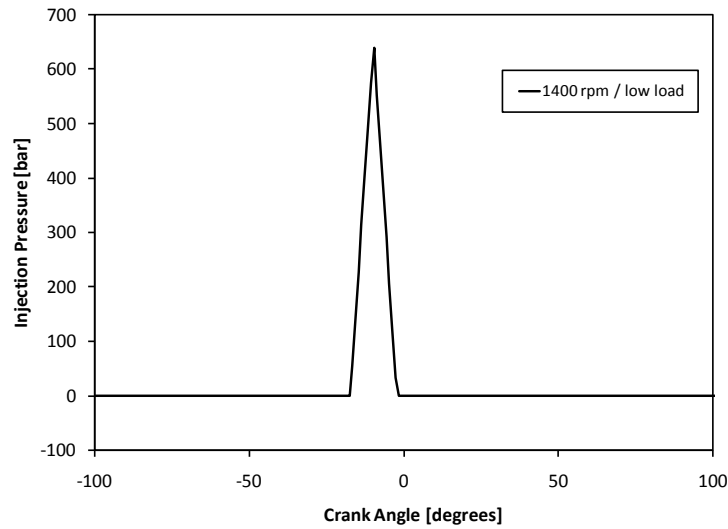


Figure 17 Single injection profile for 1400 rpm / low load operating condition

Two different injection profiles were developed for the 1400 rpm / low load condition. The multi-injection profile, shown in Figure 16, was developed from the experimental engine while the single injection profile, shown in Figure 17, was

developed as a comparison to the multi-injection profile. The single injection profile was designed to inject the same amount of fuel as the multi-injection profile. Figure 18 shows the injection profile for the 1400 rpm / mid load case. This injection profile is a single injection profile developed from the experimental engine. This profile has a maximum injection pressure of around 800 bar compared to the single injection profile for 1400 rpm / low load which has a maximum injection pressure of around 650 bar. This difference leads to increased amounts of fuel injected in the mid load condition which is necessary to account for the increased load.

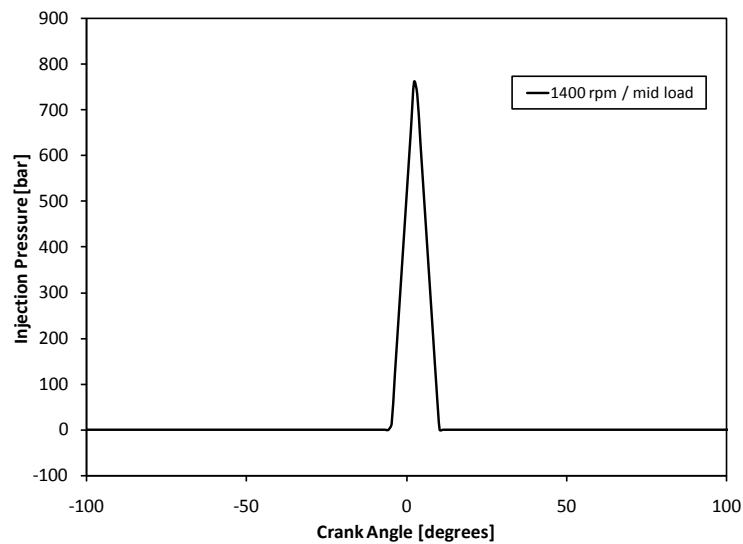


Figure 18 Injection profile for 1400 rpm / mid load operating condition

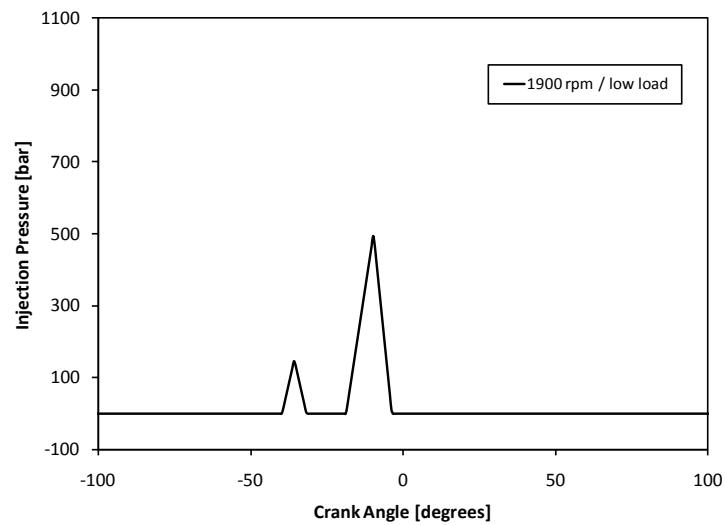


Figure 19 Injection profile for 1900 rpm / low load operating condition

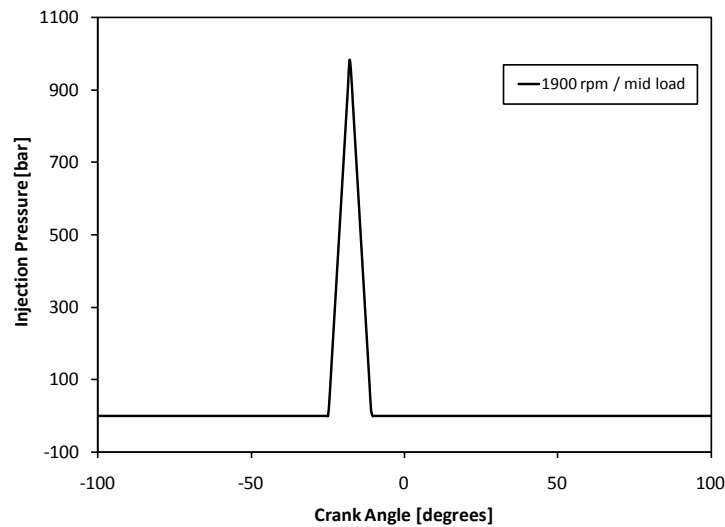


Figure 20 Injection profile for 1900 rpm / mid load operating condition

Figure 19 and Figure 20 show the injection profiles for the 1900 rpm / low load and the 1900 rpm / mid load conditions. The profile in Figure 19 is similar to the 1400

rpm / low load injection profile developed from the experimental engine. The 1900 rpm / low load injection profile shows longer injection durations than the 1400 rpm / low load injection profile due to the higher engine speed. The 1900 rpm / mid load injection profile has a higher injection pressure and slightly longer injection duration than the 1400 rpm / mid load injection profile also due to the increase in engine speed.

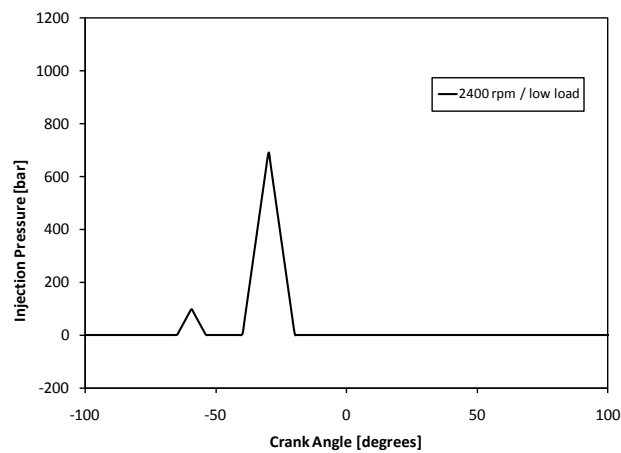


Figure 21 Injection profile for 2400 rpm / low load operating condition

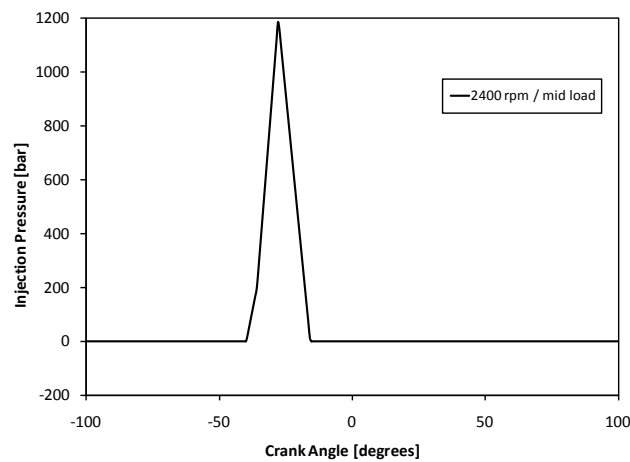


Figure 22 Injection profile for 2400 rpm / mid load operating condition

The 2400 rpm / low load and 2400 rpm / mid load injection profiles, shown in Figure 21 and Figure 22 respectively, are very similar to their 1400 rpm and 1900 rpm counterparts. The only differences are an increase in pressure for both cases over the 1400 rpm and 1900 rpm cases during the main injections to account for the increase in engine speed. Also the pilot injection in the 2400 rpm / low load case was slightly decreased in comparison to the other engine speed cases.

5.3.2 Performance characteristics for each operating point

The EGR and injection timing parametric studies were evaluated using multiple performance characteristics. These performance characteristics were the ISFC, the indicated efficiency, and the maximum pressure. Figure 23 – Figure 25 show the trends for ISFC, indicated efficiency, and maximum pressure for each of the four EGR parametric cases as they vary with injection timing at the 1400 rpm / low load operating condition. All of the cases vary in a similar fashion, which includes a decrease in ISFC and an increase in indicated efficiency as the injection timing recedes from TDC. This displays that earlier injection timings lead to an increase in engine performance for these four cases. This is corresponded by an increase in max cylinder pressure with earlier injection timings because a higher cylinder pressure leads to more available work per stroke. Net work out is the area under the P-V curve over the whole engine cycle. These graphs show that the most efficient case is at the earliest injection time and the highest level of EGR. The actual optimal EGR and injection timing combination for this condition may not be at this peak efficiency level due to other limiting factors like NO_x, HC, and CO emissions.

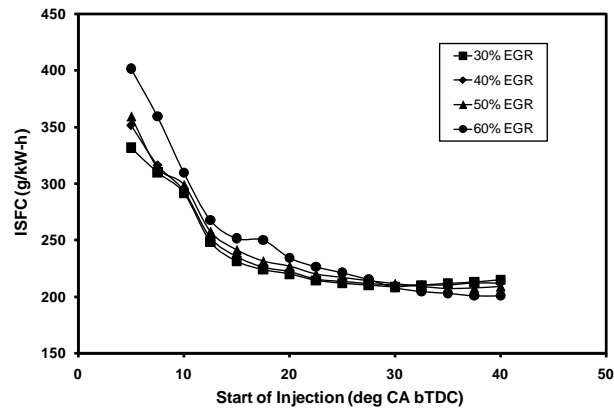


Figure 23 ISFC for multi-injection 1400 rpm / low load condition

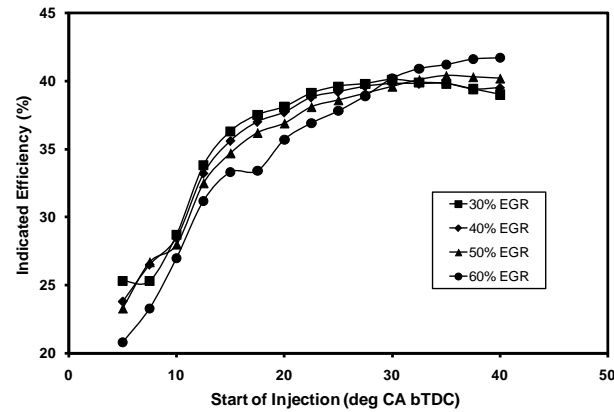


Figure 24 Ind. eff. for multi-injection 1400 rpm / low load condition

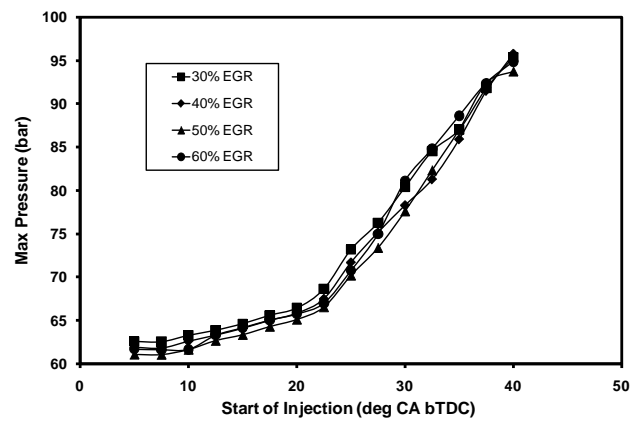


Figure 25 Max pressure for multi-injection 1400 rpm / low load condition

Figure 26 – Figure 28 show the parametric study results for the single injection 1400 rpm / low load condition. These figures show a general trend of increasing engine performance as the EGR level is increased and as the injection timing is receded from away from TDC. This trend is displayed by the decrease in ISFC, the increase in indicated efficiency and the increase in maximum pressure as EGR is increased and injection timing is advanced. The best performing case is at the highest EGR and most advanced injection timing but might not be the optimal case due to emissions values.

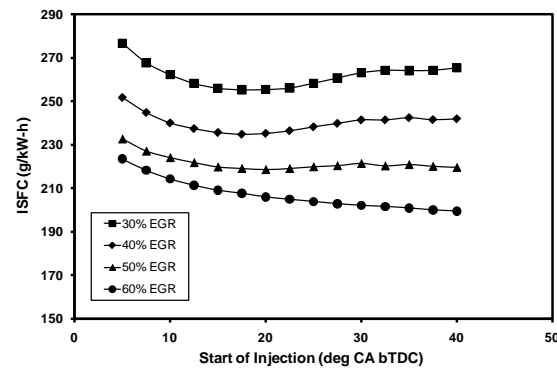


Figure 26 ISFC for single injection 1400 rpm / low load condition

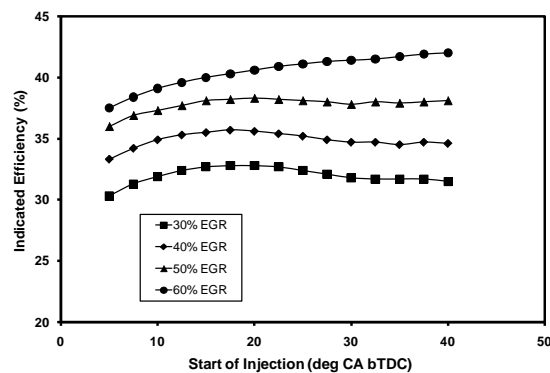


Figure 27 Ind. eff. for single injection 1400 rpm / low load condition

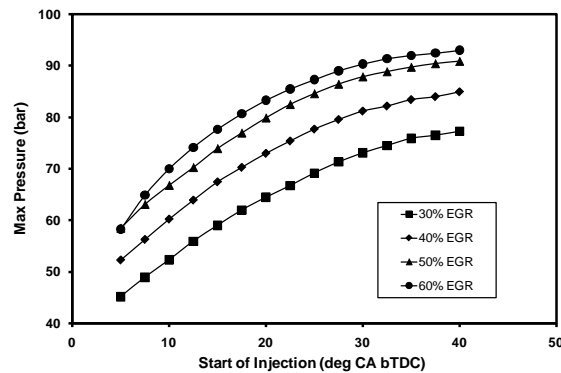


Figure 28 Max pressure for single injection 1400 rpm / low load condition

Figure 29 – Figure 31 display the ISFC, the indicated efficiency, and the maximum pressure for the 1400 rpm / mid load condition. This condition was only developed up to 50% EGR instead of 60% EGR because the built-in GT-Power EGR controller was unable to provide a 60% EGR ratio at this level. The EGR controller would have to be redesigned in GT-Power or completely replaced to allow for 60% EGR in this case. The 1400 rpm / mid load condition displays different types of trends than the 1400 rpm / low load conditions. These trends show better engine performance in all cases as the injection timing nears TDC with more dramatic shifts in the 30% and 40% EGR cases when compared to the 50% EGR case. This trend is opposite ones seen at 1400 rpm / low load conditions which show better engine performance at heavily advanced engine timings. The maximum pressure trend is the same as the one at the 1400 rpm / low load conditions implying that other factors than maximum pressure influenced the engine's performance.

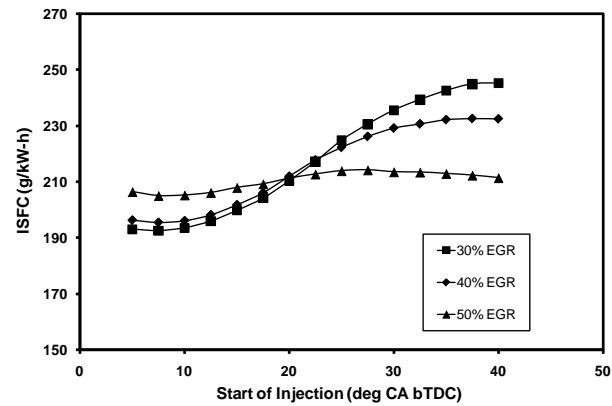


Figure 29 ISFC for 1400 rpm / mid load condition

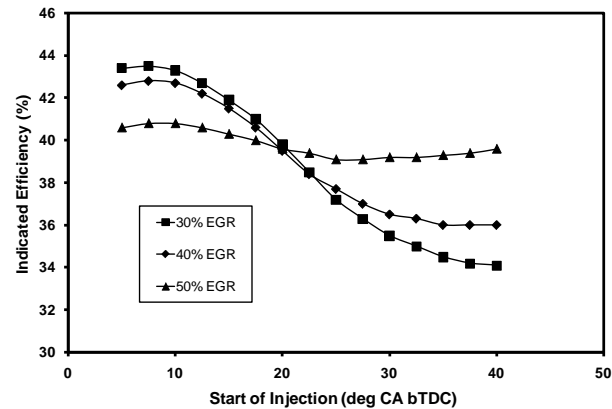


Figure 30 Ind. eff. for 1400 rpm / mid load condition

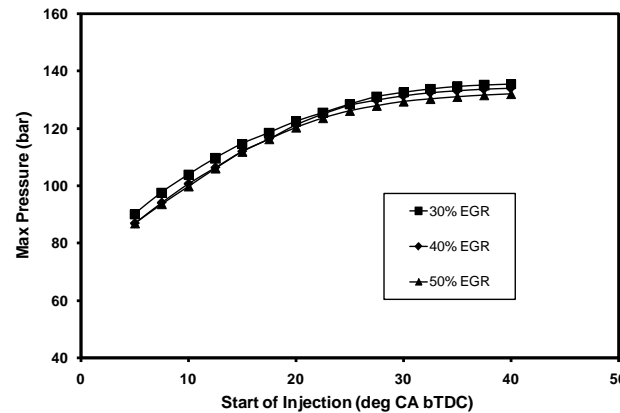


Figure 31 Max pressure for 1400 rpm / mid load condition

Figure 32 – Figure 34 show the engine performance data collected from the EGR and injection timing parametric study for the 1900 rpm / low load condition. This condition displays trends similar to the multi-injection 1400 rpm / low load case with good engine performance occurring at advanced injection timings and very little difference between the changes in EGR level. The optimal EGR and injection timing combination may not be at the most advanced injection timing due to other factors.

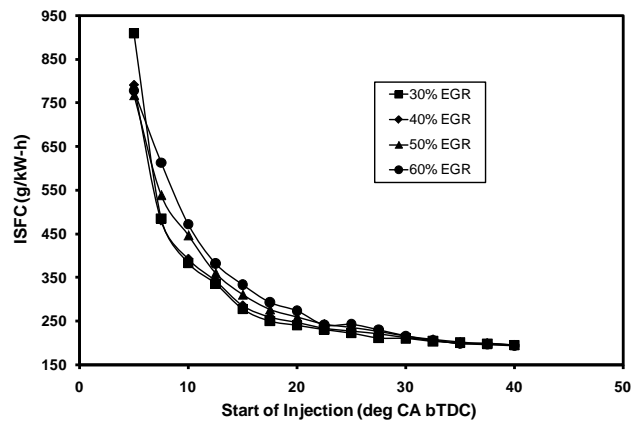


Figure 32 ISFC for 1900 rpm / low load condition

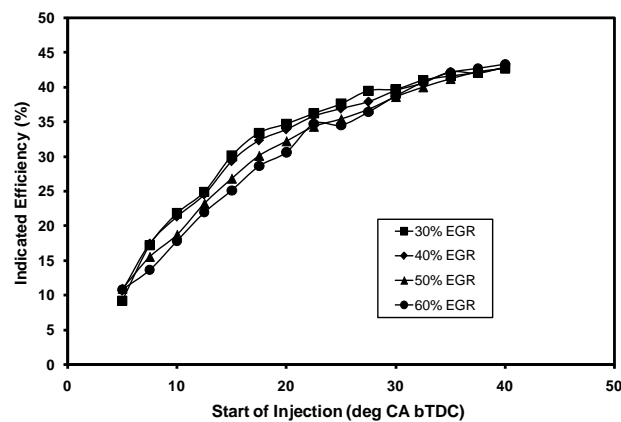


Figure 33 Ind. eff. for 1900 rpm / low load condition

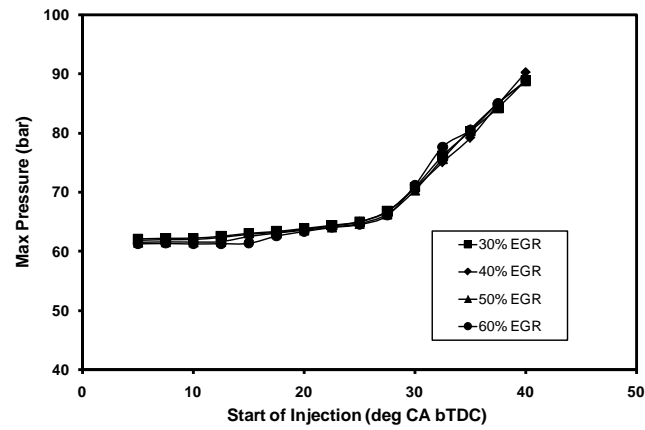


Figure 34 Max pressure for 1900 rpm / low load condition

The engine performance data, shown in Figure 35 – Figure 37, is for the 1900 rpm / mid load operating condition. These graphs show trends that are similar to the 1400 rpm / mid load operating condition but are much more exaggerated.

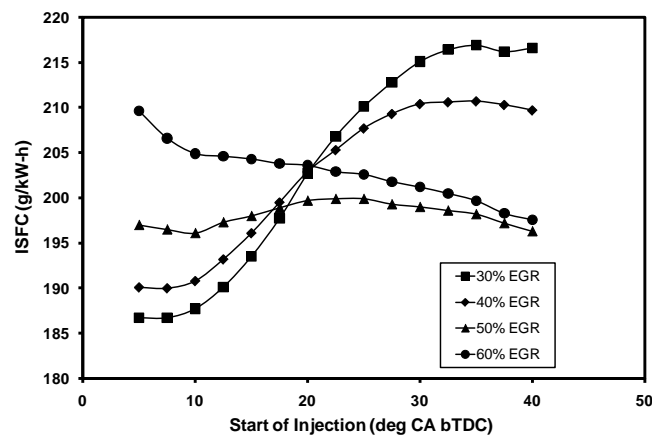


Figure 35 ISFC for 1900 rpm / mid load condition

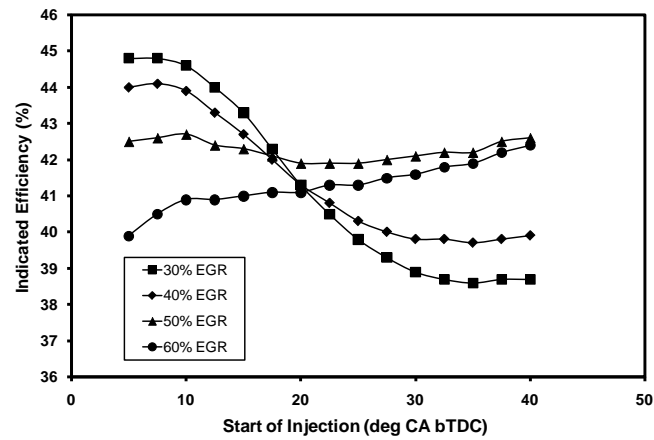


Figure 36 Ind. eff. for 1900 rpm / mid load condition

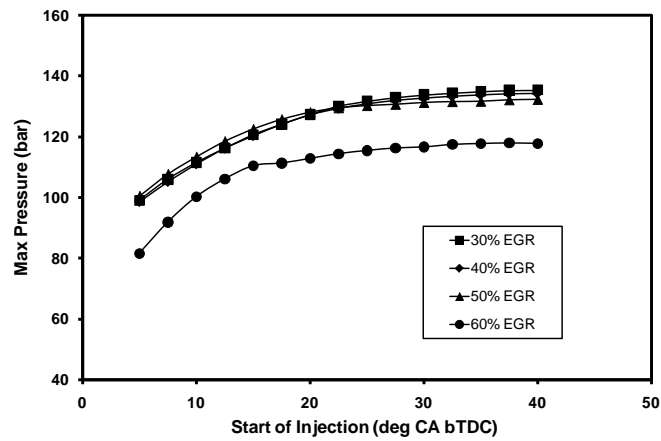


Figure 37 Max pressure for 1900 rpm / mid load condition

Figure 38 – Figure 40 display the general engine performance trends associated with the 2400 rpm / low load operating condition. This engine condition also shows better engine performance at the advanced engine timings which is similar to the 1400 rpm / low load and 1900 rpm / low load conditions. The general trends are not as

consistent or smooth as the trends for the lower engine speed conditions due to the decrease in flow and combustion calculation accuracy.

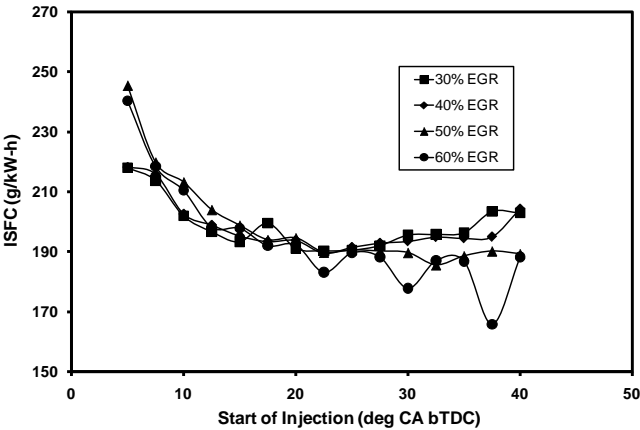


Figure 38 ISFC for 2400 rpm / low load condition

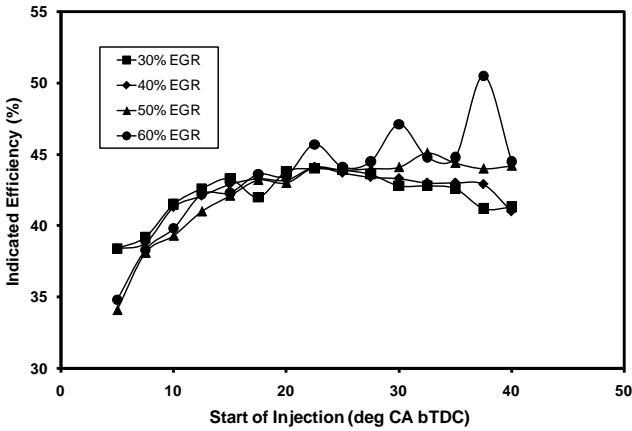


Figure 39 Ind. eff. for 2400 rpm / low load condition

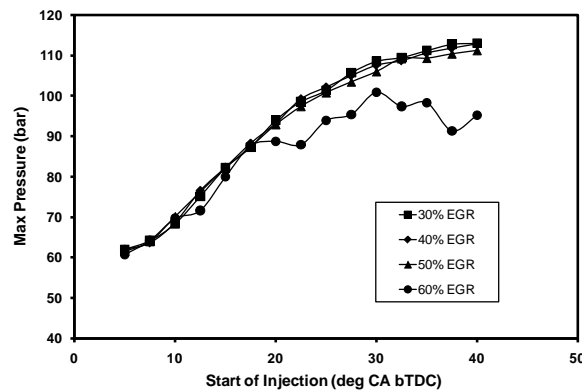


Figure 40 Max pressure for 2400 rpm / low load condition

The ISFC, indicated efficiency, and maximum pressure data for the 2400 rpm / mid load operating condition is shown in Figure 41 – Figure 43. These figures exhibit increasing engine performance as the injection timings are advanced for the 30%, 40%, and 50% EGR ratios. The engine's performance is dramatically worse for the 60% EGR ratio showing a heavy breakdown of combustion efficiency due to the high level of EGR present in the cylinder at this high speed and high load condition.

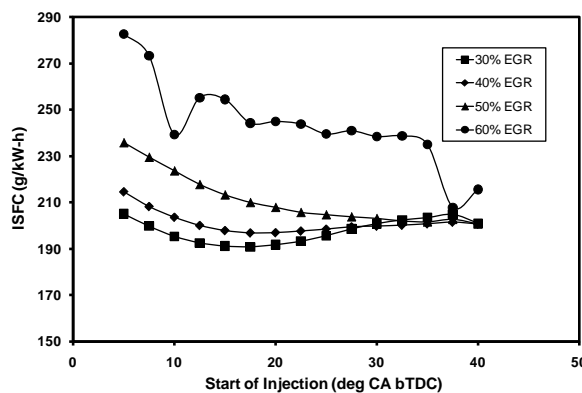


Figure 41 ISFC for 2400 rpm / mid load condition

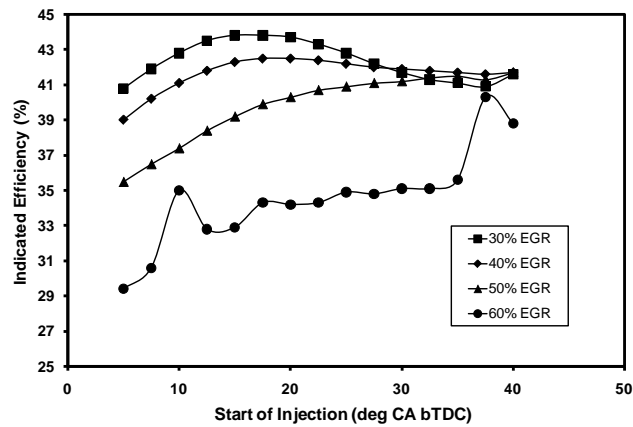


Figure 42 Ind. eff. for 2400 rpm / mid load condition

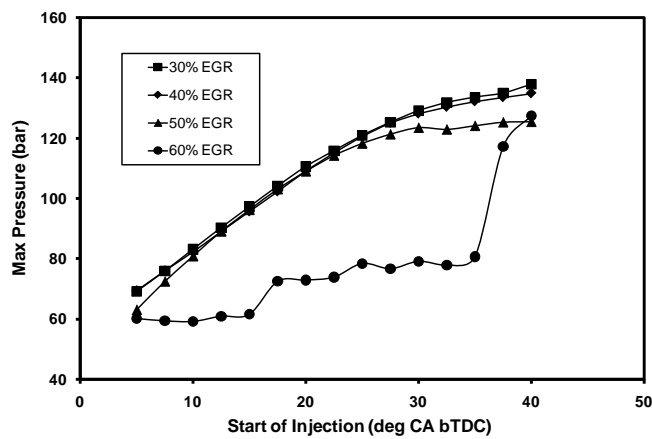


Figure 43 Max pressure for 2400 rpm / mid load condition

5.3.3 Emissions values for each operating point

The major purpose of this model is to develop a low temperature combustion operating mode that decreases engine emissions without sacrificing engine performance. Crucial to the selection of optimal EGR and injection timing combinations for all operating conditions are the emissions levels produced at each of these combinations.

Figure 44 – Figure 46 show the emissions values for the multi-injection 1400 rpm / low load condition. In these figures the NO_x emissions show an opposing trend to the HC and CO emissions which is common in LTC operation. The NO_x emissions in this case show decreases with both increases in EGR ratio and retarding of injection timing toward TDC. The HC and CO emissions show increases with decreases in EGR ratio and retarding of injection timing toward TDC which is the opposite of the NO_x emissions and to be expected.

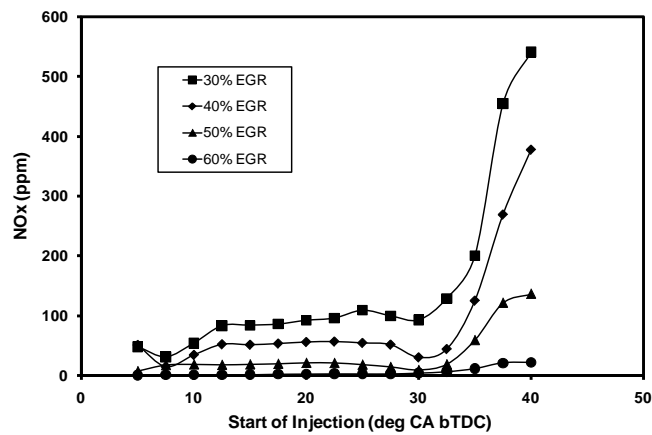


Figure 44 NO_x for multi-injection 1400 rpm / low load condition

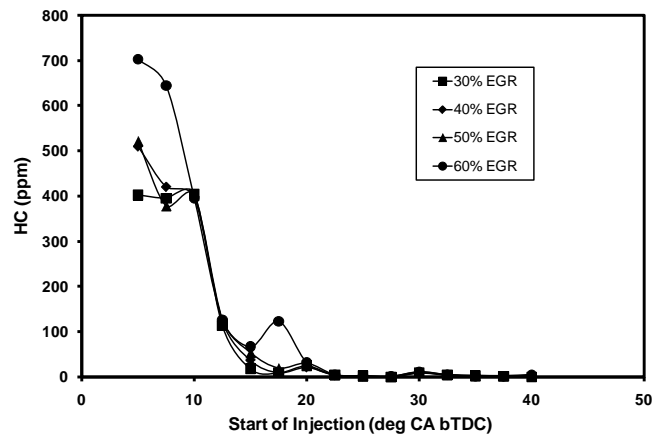


Figure 45 HC for multi-injection 1400 rpm / low load condition

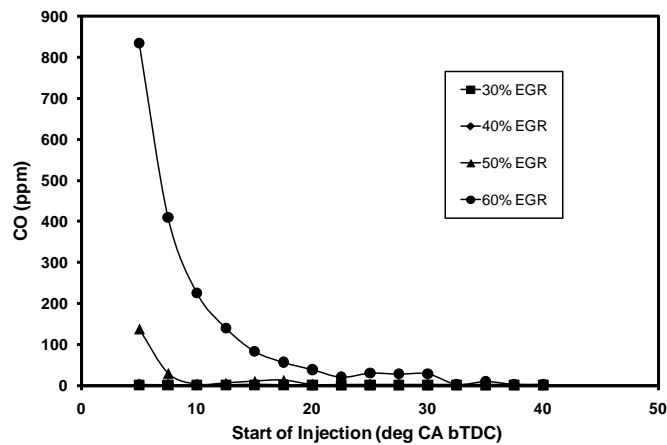


Figure 46 CO for multi-injection 1400 rpm / low load condition

Figure 47 – Figure 49 show the emissions values for the single injection 1400 rpm / low load operating condition. This condition shows overall higher and more erratic emissions values than the multi-injection 1400 rpm / low load condition. That being said, this condition also shows the same trends that the multi-injection condition displays.

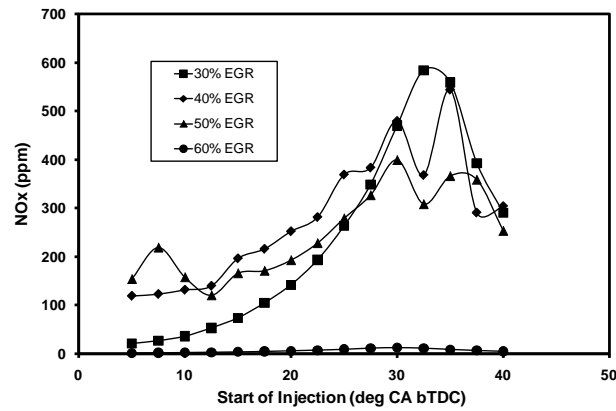


Figure 47 NOx for single injection 1400 rpm / low load condition

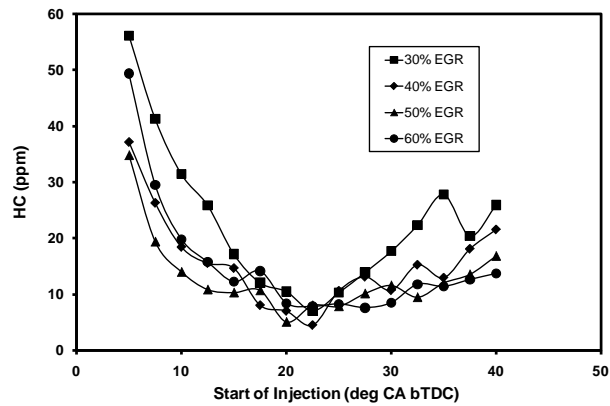


Figure 48 HC for single injection 1400 rpm / low load condition

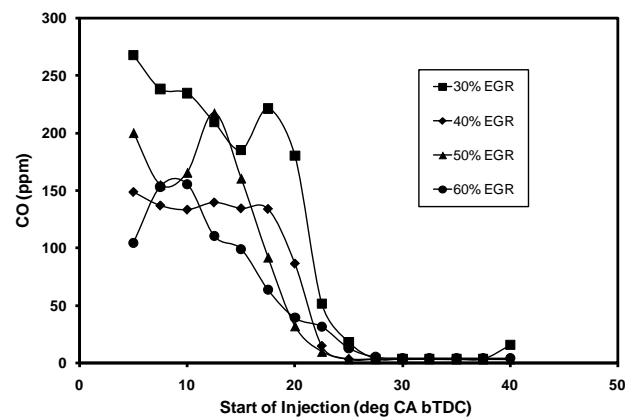


Figure 49 CO for single injection 1400 rpm / low load condition

The 1400 rpm / mid load operating condition's emissions values are displayed in Figure 50 – Figure 52. As mentioned before, this operating condition was developed only through 50% EGR instead of 60% EGR due to a breakdown in the models ability to achieve 60% EGR. This condition shows lower NO_x values with increases in EGR and injection timings near TDC. The highest NO_x appears to peak around 27.5 CA degrees bTDC for both the 30% and 40% EGR ratios with very little change in the 50% EGR ratio as the injection timing changed. The HC emissions were fairly erratic but followed the same general trend across all 3 EGR levels. This trend showed lower HC values as the EGR level decreased except near 10 and 20 CA degrees bTDC. The CO emissions were generally constant as the injection timing was varied but show a massive increase from 30% to 50% EGR. This causes CO emissions to be a heavily limiting factor in the optimal EGR and injection timing combination selection.

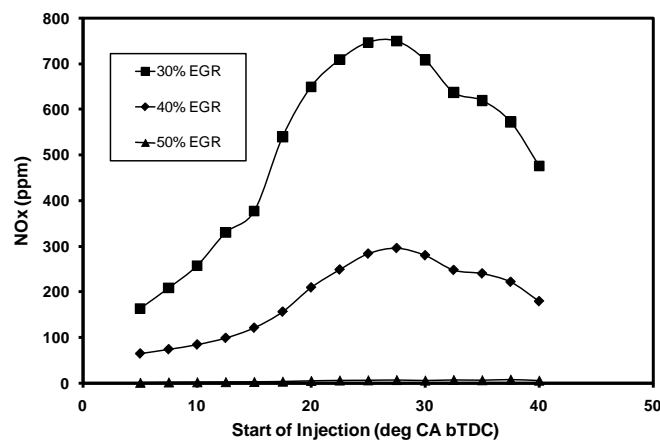


Figure 50 NO_x for 1400 rpm / mid load condition

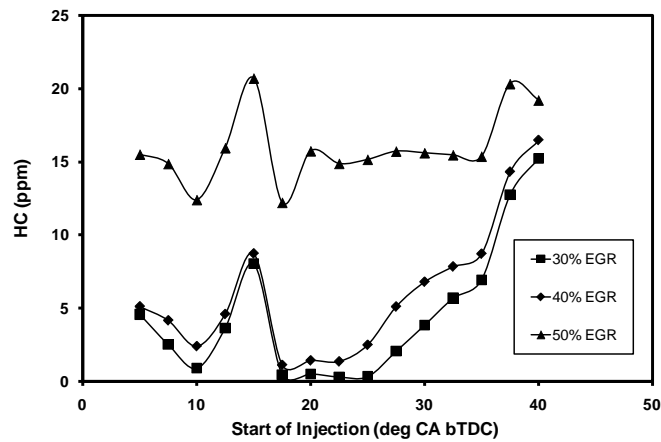


Figure 51 HC for 1400 rpm / mid load condition

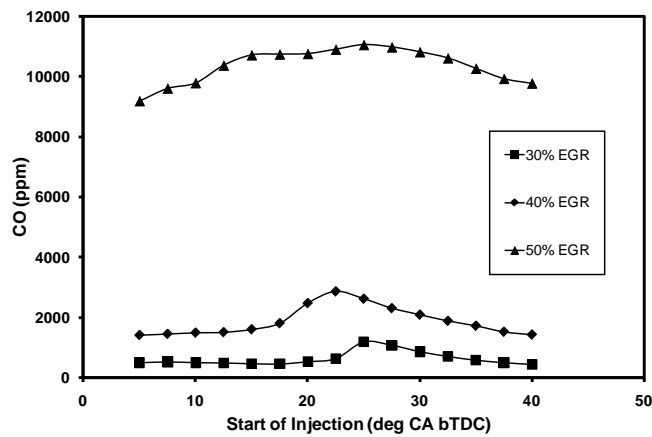


Figure 52 CO for 1400 rpm / mid load condition

The emissions values for the 1900 rpm / low load condition, shown in Figure 53 – Figure 55, display decreasing NO_x emissions and increasing HC and CO emissions as both the EGR ratio is increased and the injection timing is retarded toward TDC. The NO_x values are more erratic than in the 1400 rpm / low load conditions and the HC and

CO emissions show huge increases as the injection timings near TDC. This was a major limiting factor in the selection of an optimal EGR and injection timing combination.

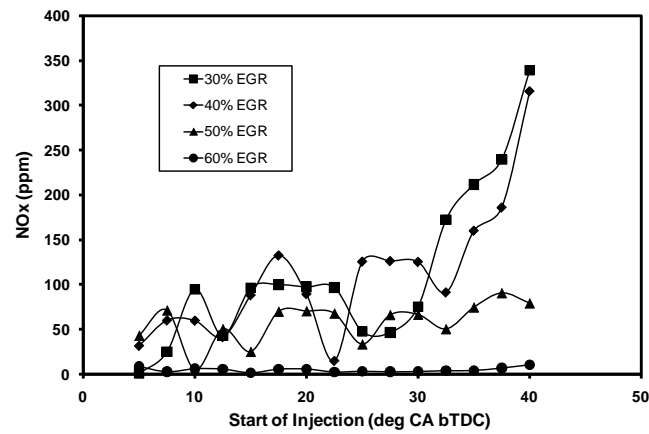


Figure 53 NOx for 1900 rpm / low load condition

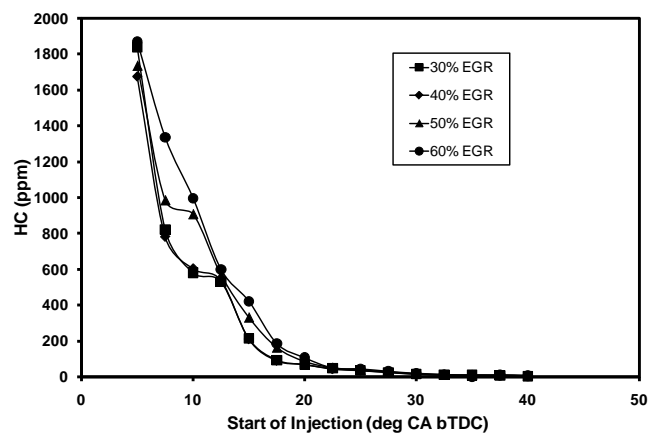


Figure 54 HC for 1900 rpm / low load condition

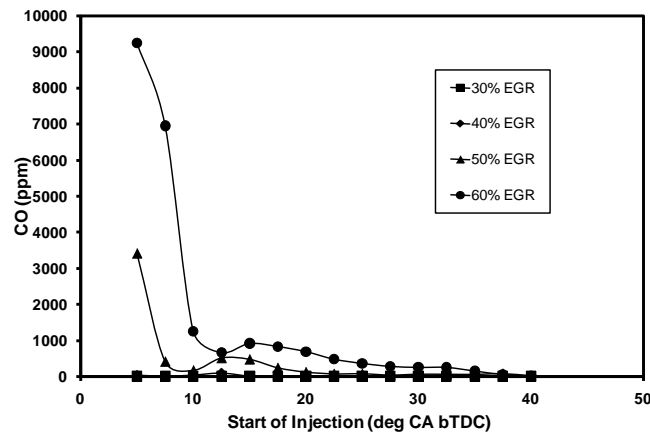


Figure 55 CO for 1900 rpm / low load condition

Figure 56 – Figure 58 display the emissions values for the 1900 rpm / mid load operating condition. This condition shows decreasing NO_x and increasing HC and CO emissions as the EGR ratio is increased. The NO_x emissions show only a small change as the injection timing varies for the 50% and 60% EGR ratios. At the lower EGR ratios, the NO_x emissions show a peak at 17.5 CA degrees bTDC and a general trend of increasing emissions as the injection timing is advanced. The HC emissions show an opposing trend with emissions decreasing as the injection timing is advanced. The CO emissions are fairly heavily dependent on EGR changes with massive increases as the EGR ratio is increased but shows very small changes as the injection timing is varied from 5 CA degrees bTDC to 40 CA degrees bTDC.

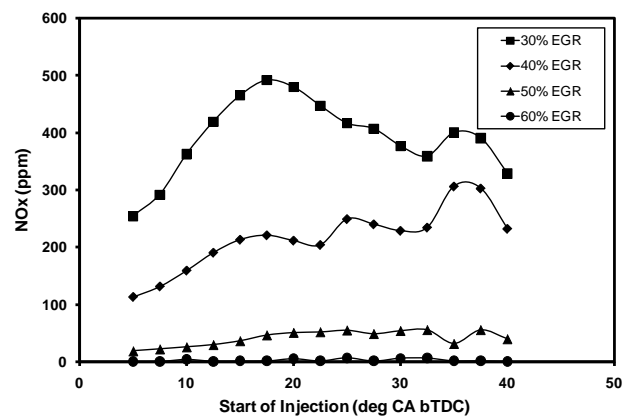


Figure 56 NOx for 1900 rpm / mid load condition

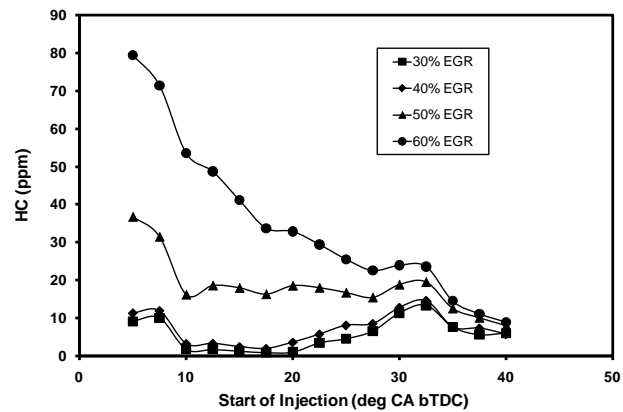


Figure 57 HC for 1900 rpm / mid load condition

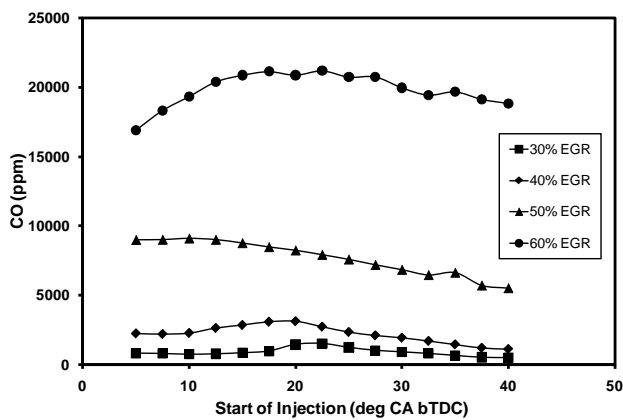


Figure 58 CO for 1900 rpm / mid load condition

The emissions values for the 2400 rpm / low load condition are shown in Figure 59 – Figure 61. The NO_x emissions for this case show decreases as the EGR ratio is increased and the data becomes more and more erratic as the EGR decreases. The emissions still show a general trend of decreasing values as the injection timing is retarded toward TDC. The HC and CO emissions show opposing trends with both the EGR and the injection timings and have only slight errata.

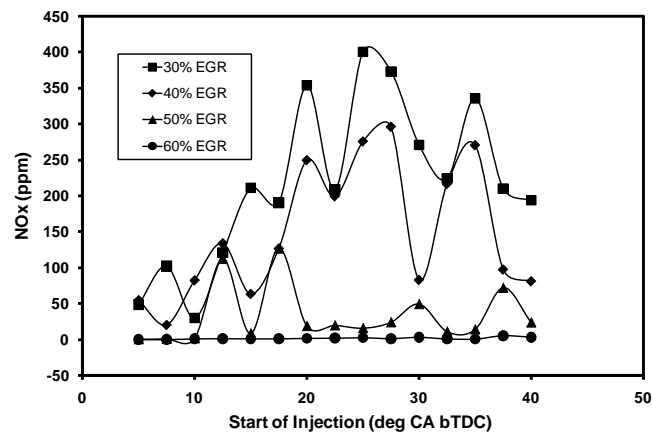


Figure 59 NO_x for 2400 rpm / low load condition

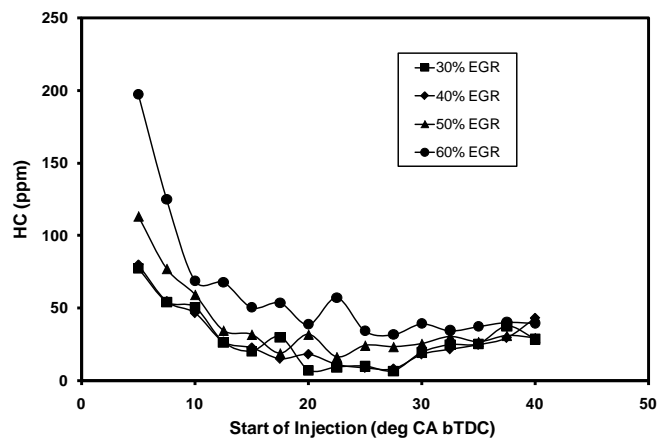


Figure 60 HC for 2400 rpm / low load condition

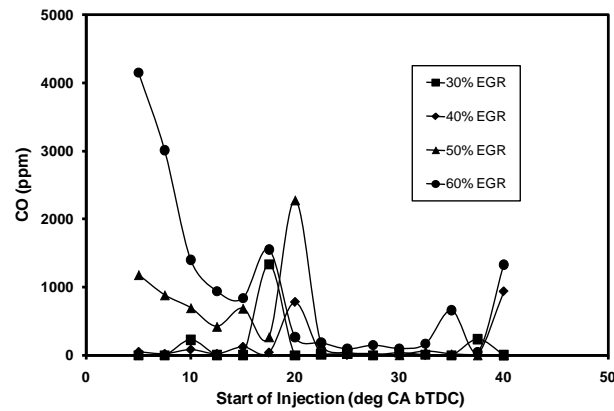


Figure 61 CO for 2400 rpm / low load condition

Figure 62 – Figure 64 display the emissions values for the 2400 rpm / mid load condition. This condition shows decreases in NO_x emissions and increases in HC and CO emissions as the EGR ratio is increased. The NO_x emissions also show decreases as the injection timing is retarded toward TDC. This is more extreme for the 30% EGR ratio than the other 3 ratios. The HC emissions display large increases as the injection timing nears TDC and the CO emissions are largely unaffected by injection timing.

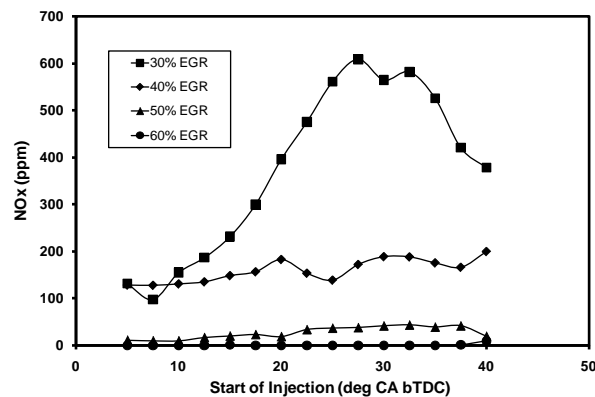


Figure 62 NO_x for 2400 rpm / mid load condition

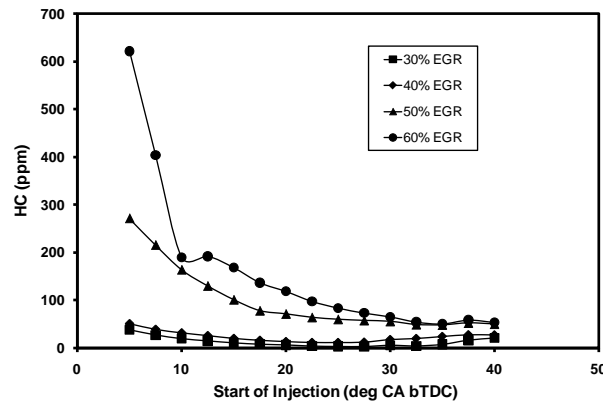


Figure 63 HC for 2400 rpm / mid load condition

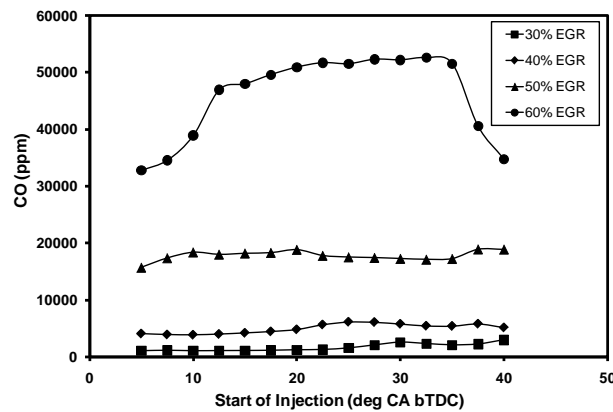


Figure 64 CO for 2400 rpm / mid load condition

5.3.4 Optimal EGR and injection timing combinations

The performance and emissions data from the parametric studies at each operating condition led to the development of optimal EGR and injection timing combinations. These selections were based on criteria developed by comparing the 6 operating condition parametric study runs to conventional diesel runs at those conditions. The conventional runs are shown in Table 4 – Table 5 while the criteria developed is shown in Table 6.

Table 4 First set of conventional engine results

	Conventional 1400 rpm / low load 0% EGR/17.4 CA degrees bTDC	Conventional 1400 rpm / mid load 0% EGR/5 CA degrees bTDC	Conventional 1900 rpm / low load 0% EGR/17 CA degrees bTDC
IMEP (bar)	3.53	8.19	3.54
ISFC (g/kW-h)	218.5	187.9	245.8
Indicated Efficiency (%)	38.3	44.5	34.1
Max. Pressure (bar)	66.76	77.39	77.52
dPmax/dCA (bar/degree)	2.004	4.488	2.411
Max. Temperature (K)	1217	1715	1148
NOx (ppm)	66.16	576.66	59.19
HC (ppm)	9.33	0.82	60.07
CO (ppm)	1.05	8.42	0.91
BSFC (g/kW-h)	420.8	241.7	578.1
Volumetric Efficiency (%)	112.1	113.1	133.2
A/F Ratio	60.69	30.64	63.82
Brake Efficiency (%)	19.9	34.6	14.5

Table 5 Second set of conventional engine results

	Conventional 1900 rpm / mid load 0% EGR/5 CA degrees bTDC	Conventional 2400 rpm / low load 0% EGR/24 CA degrees bTDC	Conventional 2400 rpm / mid load 0% EGR/12.2 CA degrees bTDC
IMEP (bar)	8.31	4.26	8.6
ISFC (g/kW-h)	180	247.3	186.6
Indicated Efficiency (%)	46.5	33.9	44.9
Max. Pressure (bar)	93.56	93.58	119.25
dPmax/dCA (bar/degree)	6.209	2.938	4.193
Max. Temperature (K)	1688	1153	1515
NOx (ppm)	763.22	81.91	466.18
HC (ppm)	0.41	64.74	1.32
CO (ppm)	1.52	0.84	1.07
BSFC (g/kW-h)	246.1	582.7	274.6
Volumetric Efficiency (%)	127.2	160.1	168.6
A/F Ratio	35.46	63.45	43.82
Brake Efficiency (%)	34	14.4	30.5

Table 6 Criteria for selection of optimal EGR and injection timings [16]

	1400 rpm	1900 rpm	2400 rpm
ISFC (g/kW-h)	Within 10% of conventional	Within 10% of conventional	Within 10% of conventional
dPmax/dCA (bar/degree)	< 10	< 30	< 30
NOx (ppm)	at least 70% less than conventional	at least 70% less than conventional	at least 70% less than conventional

The optimal EGR and injection timing combinations selected using these criteria for all of the rpm / load operating conditions are displayed in Table 7 – Table 9.

Table 7 Optimal EGR and injection timing combination for 1400 rpm cases

	Multi-Injection 1400 rpm / low load 60% EGR/32.5 CA degrees bTDC	Single Injection 1400 rpm / low load 60% EGR/5 CA degrees bTDC	1400 rpm / mid load 30% EGR/5 CA degrees bTDC
IMEP (bar)	3.77	3.48	7.98
ISFC (g/kW-h)	204.8	223.5	193
Indicated Efficiency (%)	40.9	37.5	43.4
Max. Pressure (bar)	84.81	58.27	90.18
dPmax/dCA (bar/degree)	9.932	8.993	11.291
Max. Temperature (K)	1381	1314	1724
NOx (ppm)	6.5	1.53	163.58
HC (ppm)	5.37	49.36	4.59
CO (ppm)	3.53	104.35	491.72
BSFC (g/kW-h)	417	413.1	256.9
Volumetric Efficiency (%)	46.4	42.3	76.3
A/F Ratio	25.11	22.71	20.67
Brake Efficiency (%)	20.1	20.3	32.6

Table 8 Optimal EGR and injection timing combination for 1900 rpm cases

	1900 rpm / low load 60% EGR/40 CA degrees bTDC	1900 rpm / mid load 40% EGR/7.5 CA degrees bTDC
IMEP (bar)	4.51	7.89
ISFC (g/kW-h)	193.4	190
Indicated Efficiency (%)	43.3	44.1
Max. Pressure (bar)	88.8	105.22
dPmax/dCA (bar/degree)	18.201	26.145
Max. Temperature (K)	1482	1793
NOx (ppm)	10.35	131.45
HC (ppm)	10.92	11.89
CO (ppm)	20.74	2204.57
BSFC (g/kW-h)	372.9	272.3
Volumetric Efficiency (%)	47.8	66.9
A/F Ratio	22.86	18.62
Brake Efficiency (%)	22.4	30.7

Table 9 Optimal EGR and injection timing combination for 2400 rpm cases

	2400 rpm / low load 60% EGR/37.5 CA degrees bTDC	2400 rpm / mid load 30% EGR/7.5 CA degrees bTDC
IMEP (bar)	6.54	8.05
ISFC (g/kW-h)	165.9	199.8
Indicated Efficiency (%)	50.5	41.9
Max. Pressure (bar)	91.38	75.92
dPmax/dCA (bar/degree)	28.257	7.814
Max. Temperature (K)	1825	1636
NOx (ppm)	5.43	97.87
HC (ppm)	40.2	27.32
CO (ppm)	48.61	1137.07
BSFC (g/kW-h)	306.2	277.5
Volumetric Efficiency (%)	45.4	74.5
A/F Ratio	17.17	19.34
Brake Efficiency (%)	27.3	30.2

The optimal EGR and injection timing combination for all 3 speeds at the low load condition have EGR ratios at the highest 60%. This provides at least a 70% reduction in NOx emissions compared to a conventional engine while maintaining performance within 10% of the conventional engine. All the speed levels at the low load condition show highly advanced injection timings around 30 to 40 CA degrees bTDC. All of these conditions have a pilot injection along with the main injection and the advanced injection timing allows for better mixing inside the cylinder. This mixing increases the amount of lean, homogeneous combustion occurring in the cylinder which drives down temperatures, NOx and soot emissions. These conditions do cause higher HC and CO emissions than normally seen in diesel engines but they are well within tolerable limits. The performance in these cases also does not seem to suffer as low ISFC and high indicated efficiencies are noticeable.

All the mid load cases and the single injection 1400 rpm / low load case all use single injection profiles. This leads to the optimal EGR and injection timing combinations for these cases being located at retarded injection timings near TDC and in all but the 1400 rpm / low load case being at low EGR levels. This leads to similar results as the low load conditions. This selection is due to the higher EGR cases for the mid load conditions showing massively off the charts CO emissions due to improper oxidation into CO₂. These oxidation problems are caused by the low combustion temperatures which do not allow the CO to CO₂ reaction to occur.

5.4 Knock-induced combustion parametric studies

Another set of parametric studies was conducted by developing LTC conditions using the knock-induced combustion model. From this point on the knock-induced combustion model will be known as the HCCI model. This model uses a port injection system as required by the two-zone combustion model that it employs. This model is used instead of the multi-zone, quasi-dimensional model used for the direct injection system. Since the injection was done through the intake port, the injection timing was not varied instead a common port injection SOI was used. This means that the only parameter varied in the parametric study was the EGR ratio, which was varied from 20% EGR to 50% EGR in increments of 5% EGR to provide sufficient data points for trend analysis. The performance characteristics for the 6 operating conditions using the HCCI model are shown in Figure 65 – Figure 67.

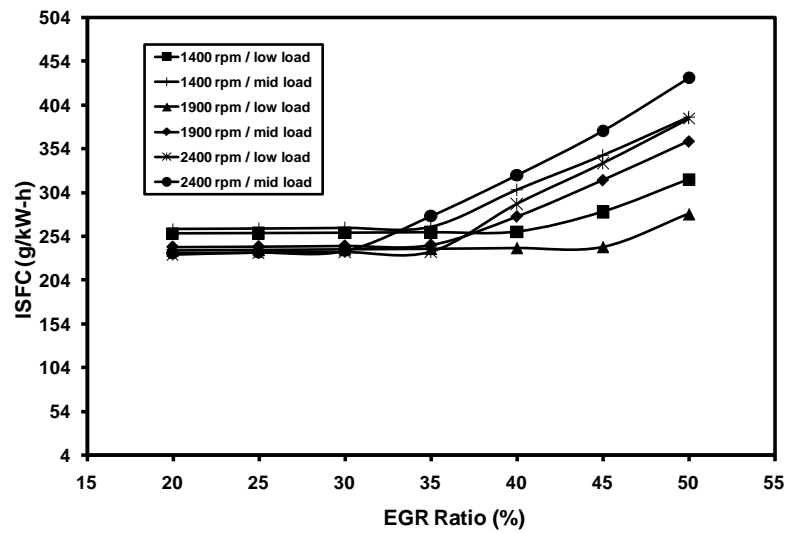


Figure 65 ISFC for six operating conditions using HCCI model

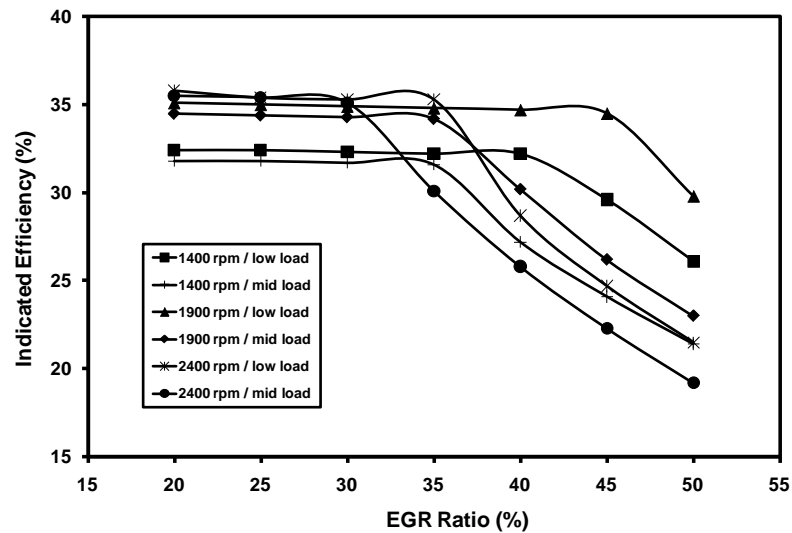


Figure 66 Ind. eff. for six operating conditions using HCCI model

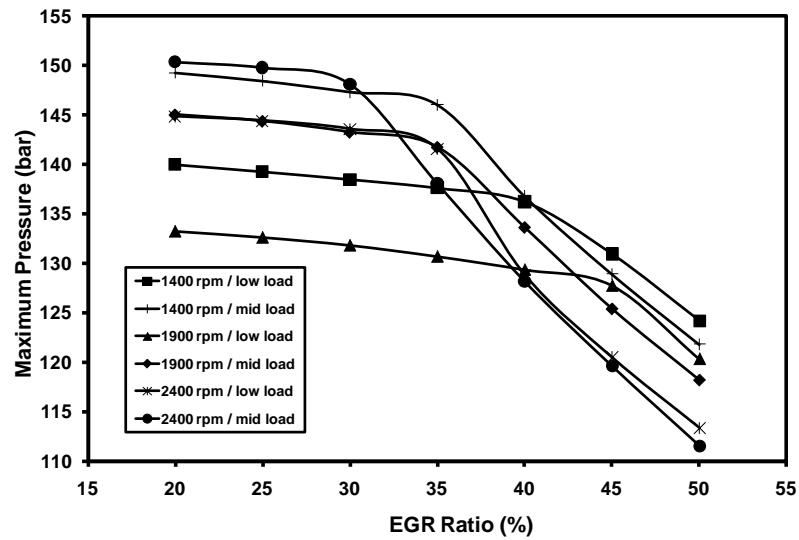


Figure 67 Max pressure for six operating conditions using HCCI model

The performance characteristics for the operating conditions using the HCCI model show a general decrease in performance as the EGR rate is increased across all levels. The higher engine speed and load conditions seem to reach this decrease in performance at lower EGR levels when compared to the lower engine speed and load conditions. These beginning declines start at 30% EGR for 2400 rpm / mid load condition and go all the way to 45% EGR for the 1900 rpm / low load condition. The other conditions begin their declines at 35% and 40% EGR. This means that the ideal operating EGR ratio for each condition will fall before these performance declines. The emissions characteristics of these conditions using the HCCI model are also important for determining the ideal EGR ratio and are shown in Figure 68 – Figure 70.

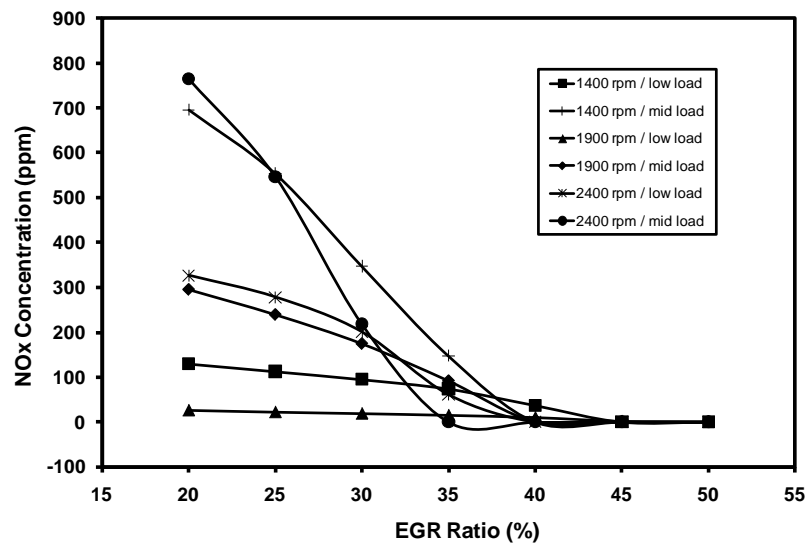


Figure 68 NOx for six operating conditions using HCCI model

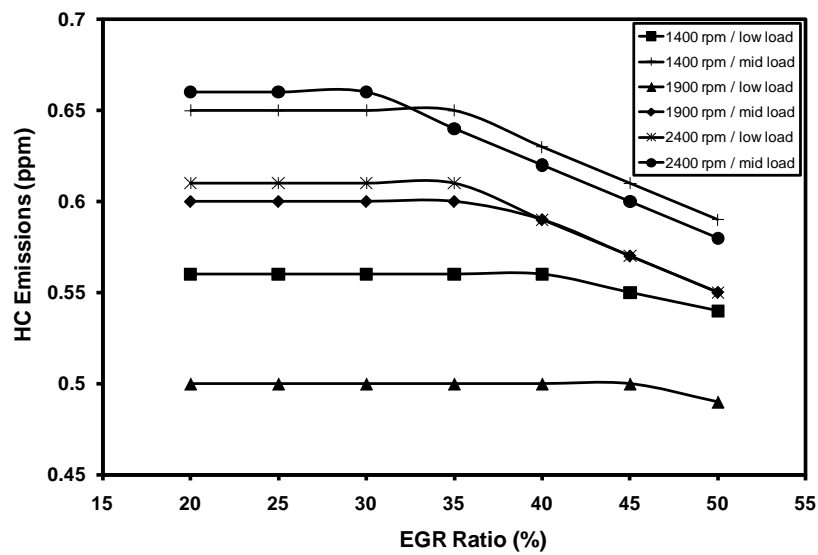


Figure 69 HC for six operating conditions using HCCI model

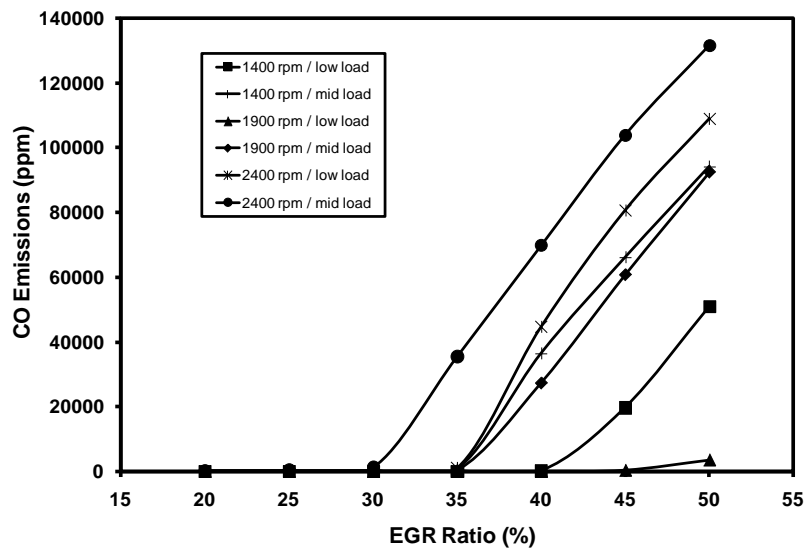


Figure 70 CO for six operating conditions using HCCI model

The emissions values for all 6 operating conditions using the HCCI model show similar trends to the performance data, except for the NO_x emissions values. The NO_x emissions show opposite trends to the performance data with the highest emissions occurring at low EGR levels and then tapering to near zero at the high EGR levels. The HC emissions levels actually change very little with respect to changing EGR levels in this model while the CO emissions show massive spikes at the same EGR levels that the performance data showed massive decreases. This implies that combustion efficiency breaks down at these EGR points as the performance level rapidly drops and the CO is unable to properly oxidize into CO₂. These graphs combined with the performance data show that the 1400 rpm / low load and the 1400 rpm / mid load conditions have ideal EGR points at 40% and 35% respectively. The 1900 rpm / low load and the 1900 rpm / mid load conditions have optimal EGR points at 45% and 35% respectively. Lastly, the

2400 rpm / low load and the 2400 rpm / mid load conditions have optimal EGR levels at 35% and 30% respectively.

5.5 Combustion noise and possible reduction methods

One of the major limiting factors in LTC and HCCI operation for diesel engines is the introduction of high levels of combustion noise pollution due to the increased pressure rise rates that occur during these types of operations. The pressure rise rates are by definition the quickness with which the pressure rises during the combustion event and is measured in bar/degrees. Conventional diesel engines generally produced excess noise pollution if the pressure rise rate is greater than 10 bar/degree [16]. LTC and HCCI engines are able to achieve much higher pressure rise rates due to the homogeneous charge developed inside the cylinder. This charge is thoroughly mixed to develop its homogeneity and is generally assumed to combust as one whole unit. This causes the entire injected fuel mass to release its heat all at once which creates a large pressure jump in a small amount of time. Some HCCI engines can support up to 30 bar/degree of pressure rise without creating massively excessive engine noise but it does cause undue wear and tear on the engine [16]. Methods are explored below to possibly decrease the pressure rise rates developed during the LTC parametric studies.

5.5.1 Ability of high EGR to reduce pressure rise rates

One developed study [9] hypothesized that high levels of EGR would cause significant decreases in in-cylinder pressure rise rates. Investigation of this method was done using data from the optimal EGR and injection timing parametric study. Figure 71 – Figure 75 show pressure rise rates for EGR and injection timing combinations.

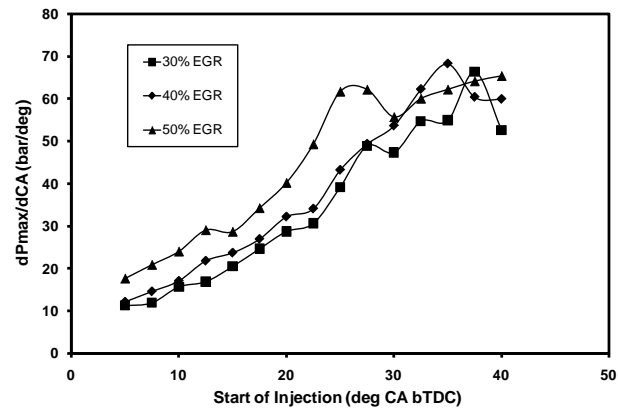


Figure 71 Pressure rise rates for 1400 rpm / mid load condition

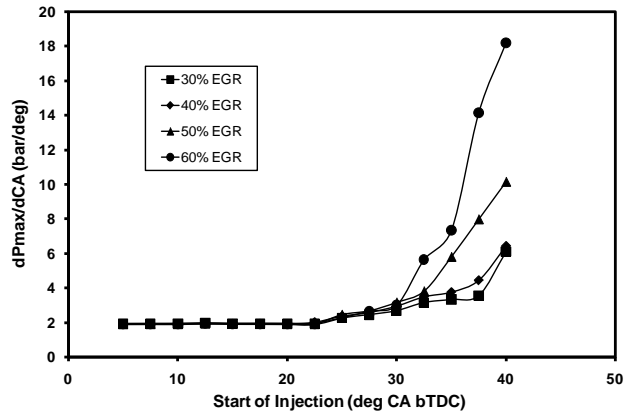


Figure 72 Pressure rise rates for 1900 rpm / low load condition

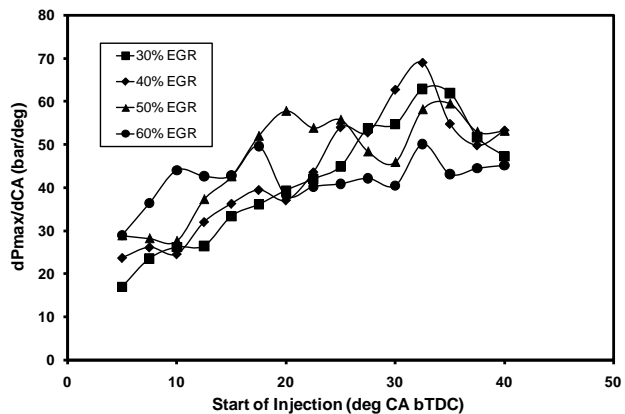


Figure 73 Pressure rise rates for 1900 rpm / mid load condition

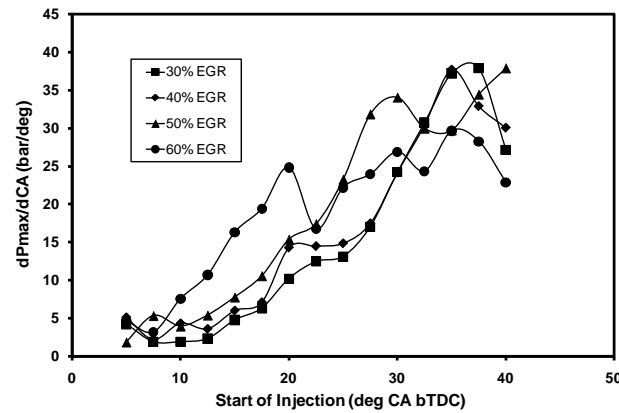


Figure 74 Pressure rise rates for 2400 rpm / low load condition

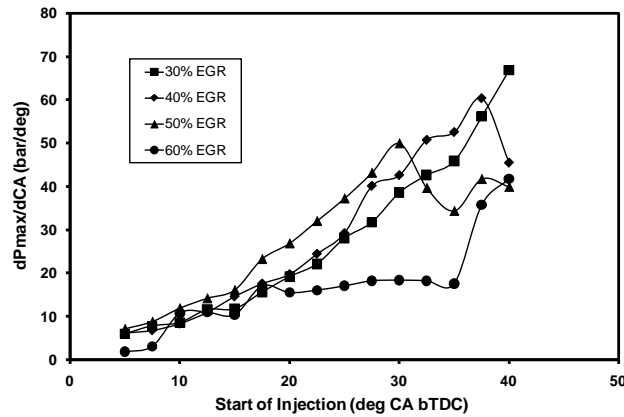


Figure 75 Pressure rise rates for 2400 rpm / mid load condition

At low speed conditions, such as 1400 rpm / mid load and 1900 rpm / low load, the higher levels of EGR generally show higher pressure rise rates than the lower levels of EGR. At the 1900 rpm / mid load and 2400 rpm / low load conditions the pressure rise rates are higher for the higher EGR levels at the retarded injection timings while a shift occurs at around 20 CA degrees bTDC for the 1900 rpm / mid load condition and around 30 CA degrees bTDC for the 2400 rpm / low load condition in which the higher

EGR levels produce lower pressure rise rates. At the high speed and mid load condition, 2400 rpm / mid load, the high EGR level produces the lowest pressure rise rate no matter what the injection timing is. These areas where the high EGR levels appear to decrease pressure rise rates are also areas where the combustion efficiency is beginning to break down; therefore, the most likely cause of these pressure rise rate drops is the overall degradation of the heat release occurring in the cylinder.

5.5.2 Ability of highly cooled EGR to reduce pressure rise rates

Another method of possibly decreasing pressure rise rates in LTC diesel engines that has been suggested is the use of highly cooled EGR inside the system [8]. A parametric study was conducted on the 3 operating conditions with the highest pressure rise rates to determine the effectiveness that this EGR cooling has on pressure rise rates in LTC operation. Figure 76 shows the pressure rise rates as a function of cooled intake temperature which was implemented by lowering the EGR coolant temperature.

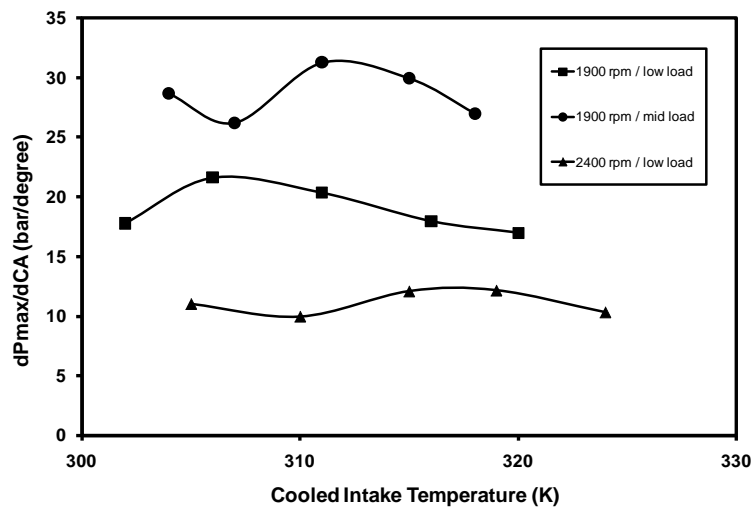


Figure 76 Pressure rise rates vs. intake temperature for 3 conditions

It appears that the cooled EGR has little to no effect on the overall pressure rise rates shown above. They vary slightly as the EGR is cooled but only rarely dip below the original pressure rise rate at around 320 K or 325 K. They sometimes even increase as the EGR is cooled. This is possibly caused by the cooled EGR allowing for more intake air to enter the cylinder which raises the air/fuel ratio and allows for a higher heat release. This increased heat release would offset any pressure rise rate gains by allowing the maximum in-cylinder pressure to increase. The cooler EGR could also allow for higher mixing due to increased ignition delay which would also increase the pressure rise rates by increasing the homogeneity of the mixture.

5.5.3 Ability of multiple injections to reduce pressure rise rates

The last method to decrease the overall pressure rise rates during LTC operation is to use a pilot injection along with the main injection to spread the heat release out and allow for a more even and smooth pressure increase. This method was investigated at the 1400 rpm / low load operating condition where a multiple injection profile and a single injection profile were developed. Figure 77 shows the pressure rise rates for the multi-injection system during the EGR and injection timing parametric study while Figure 78 shows the pressure rise rates for the single injection system during the EGR and injection timing parametric study.

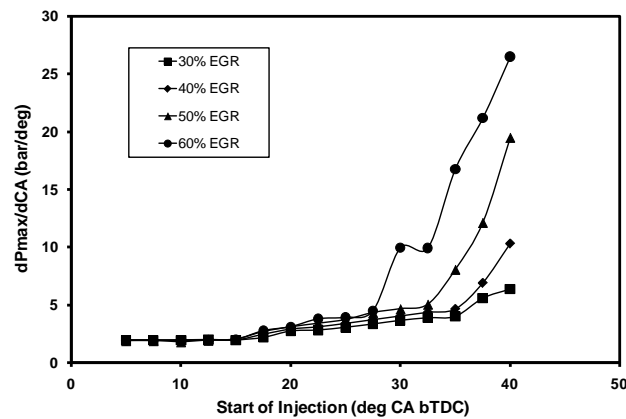


Figure 77 Pressure rise rate for multi-injection 1400 rpm / low load condition

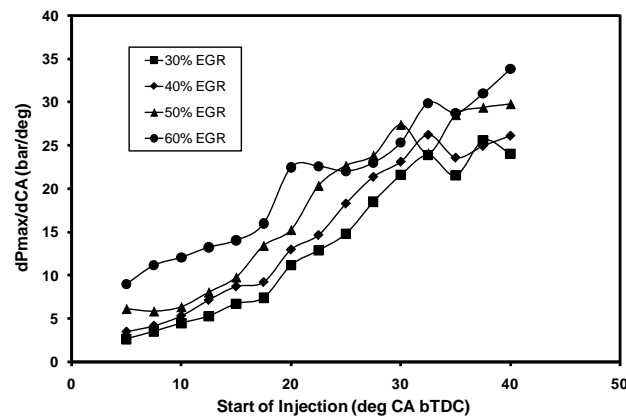


Figure 78 Pressure rise rate for single injection 1400 rpm / low load condition

These graphs show a dynamic difference in the pressure rise rates between the multiple injection and the single injection systems. The multiple injection system shows dramatically lower pressure rise rates across the entire range of EGR and injection timing combinations. This appears to be the best method for controlling in-cylinder pressure rise rates during LTC operation. The multiple injection system also provides better engine and emissions performance shown from the previous results.

6. CONCLUSIONS AND RECOMMENDATIONS

A general model was developed using GT-Power to accurately simulate a 4 cylinder, 4 stroke diesel engine operating at nine points: 1400 rpm / low load, 1400 rpm / mid load, 1400 rpm / high load, 1900 rpm / low load, 1900 rpm / mid load, 1900 rpm / high load, 2400 rpm / low load, 2400 rpm / mid load and 2400 rpm / high load. This model made use of two different combustion models to determine the effects that EGR and injection timing have on simulated results. These combustion models are the multi-zone, quasi-dimensional, direct injection model and the knock-induced, HCCI, port injection model. Using the multi-zone model a parametric study was conducted on six of the nine operating points to determine the correct EGR and injection timing combination that led to optimal LTC operation in the diesel engine. These optimal LTC operation points were evaluated using the performance characteristics: ISFC, indicated efficiency, and maximum pressure along with the emissions characteristics: NO_x, HC, and CO. The knock-induced model was used to determine the best EGR level to simulate HCCI operation and was evaluated using the same performance and emissions standards. Finally, using results from the EGR and injection timing parametric study, combustion noise from pressure rise rates was analyzed and investigations were conducted on three possible reduction methods: high EGR, highly cooled EGR, and multiple injection profiles. These simulations led to the conclusions discussed below.

6.1 Conclusions

1. This diesel engine model accurately predicted the LTC operation of the 4 stroke engine at the six operating points while using the multi-zone combustion model. The HCCI model correctly showed possible trends in performance and emissions for different EGR levels.
2. The optimal EGR and injection timing combination for the low load operating points fell at the highest EGR ratio (60%) and injection timings that were heavily advanced from TDC (30 to 40 CA degrees bTDC). This is due to the multiple injection profiles implemented in these low load operating points helping to tamp down high HC and CO emissions along with high pressure rise rates. This allowed for the usage of high levels of EGR and advanced injection timings without performance drops. The optimal EGR and injection timing combinations for the high load operating points fell at the lower EGR levels (30 % to 40%) and injection timings retarded to near TDC (7.5 to 5 CA degrees bTDC) because of limiting factors like high HC emissions, CO emissions, and pressure rise rates. The use of single injection profiles for the high load conditions caused the limiting factors to be much higher and therefore, high EGR levels and advanced injection timings could not be used. These optimal modes fell within 10% performance and provided 70% NO_x improvement over the conventional engine.
3. Of the three methods investigated to reduce pressure rise rates during LTC operation only the multiple injection strategy provided any merit. The high levels of EGR showed some pressure rise rate reduction but this was due to the EGR levels causing

massive combustion inefficiency which led to lower heat release rates and maximum pressure values. The highly cooled EGR showed very little change in the pressure rise rates as the intake temperature was dropped. This was due to offsets caused by the cooler EGR bringing in more air per stroke which caused higher heat release rates and maximum pressures leading to increased pressure rise rates. The multiple injection strategy, however, created a general decrease in combustion noise due to pressure rise rates across a wide range of EGR levels and injection timings. This was caused by the pilot injection drawing out the heat release and decreasing the heat release rate which smoothed out the pressure curve. This allows for higher EGR levels and injection timings to be used which generally have increased performance and emissions values.

6.2 Recommendations

From the development of this model and these parametric studies some recommendations can be made for future work in this area. This work can be conducted through both simulations and experiments in the laboratory.

1. Compare the performance and emissions results from the parametric studies with results from the experimental engine and then calibrate the model to fit the experimental data.
2. Calibrate the HCCI model to more accurately fit the pressure and heat release curves associated with general and LTC experimental results.
3. Include complex CFD flow models and more accurate HC and CO emissions reactions to properly show the emissions amounts during the parametric studies.

REFERENCES

1. Annamalai, K., Puri, I.K., *Combustion Science and Engineering*, First Edition Westview, Boulder, Colorado, 2007.
2. Zheng, M., Tan, Y., Mulenga, M.C., Wang, M., “Thermal Efficiency Analyses of Diesel Low Temperature Combustion Cycles”, SAE Paper 2007-01-4019, 2007.
3. Kumar, R., Zheng, M., “Fuel Efficiency Improvements of Low Temperature Combustion Diesel Engines”, SAE Paper 2008-01-0841, 2008.
4. Bression, G., Soleri, D., Savy, S., Dehoux, S., Azoulay, D., Hamouda, H.B., Doradoux, L., Guerrassi, N., Lawrence, N., “A Study of Methods to Lower HC and CO Emissions in Diesel HCCI”, SAE Paper 2008-01-0034, 2008.
5. Huang, H., Su, W., Pei, Y., “Experimental and Numerical Study of Diesel HCCI Combustion by Multi-Pulse Injection”, SAE Paper 2008-01-0059, 2008.
6. Sun, Y., Reitz, R.D., “Adaptive Injection Strategies (AIS) for Ultra-Low Emissions Diesel Engines”, SAE Paper 2008-01-0058, 2008.
7. Li, T., Okabe, Y., Izumi, H., Shudo, T., Ogawa, H., “Dependence of Ultra-High EGR Low Temperature Diesel Combustion on Fuel Properties”, SAE Paper 2006-01-3387, 2006.
8. Avolio, G., Beatrice, C., Giacomo, N.D., Guido, C., Migliaccio, M., Fraioli, V., “Effects of Highly Cooled EGR on Modern Diesel Engine Performance at Low Temperature Combustion Condition”, SAE Paper 2007-24-0014, 2007.
9. Juttu, S., Thipse, S.S., Marathe, N.V., Gajendrai Babu, M.K., “Diesel HCCI Combustion Control Parameters Study Using n-Heptane Reduced Chemical Kinetic Mechanism”, SAE Paper 2008-28-0036, 2008.

10. Jia, M., Xie, M., Peng, Z., “A Comparative Study of Multi-zone Combustion Models for HCCI Engines”, SAE Paper 2008-01-0064, 2008.
11. Yoshikawa, T., Reitz, R., “Development of an Improved NO_x Reaction Mechanism for Low Temperature Diesel Combustion Modeling”, SAE Paper 2008-01-2413, 2008.
12. Aceves, S.M., Flowers, D.L., “A Detailed Chemical Kinetic Analysis of Low Temperature Non-Sooting Diesel Combustion”, SAE Paper 2005-01-0923, 2005.
13. Zheng, J., “Use of an Engine Cycle Simulation to Study a Biodiesel Fueled Engine”, Master’s Thesis, Texas A&M University, August 2009.
14. GT-Power Users Manual, Version 7.0, Gamma Technologies, Inc, Westmont, Illinois, 2009.
15. Chang, J., Guralp, O., Filipi, Z., Assanis, D., Kuo, T., Najt, P., Rask, R., “New Heat Transfer Correlation for an HCCI Engine Derived from Measurements of Instantaneous Surface Heat Flux”, SAE Paper 2004-01-2996, 2004.
16. Schaberg, P.W., Priede, T., Dutkiewicz, R.K., “Effects of a Rapid Pressure Rise on Engine Vibration and Noise”, SAE Paper 900013, 1990.

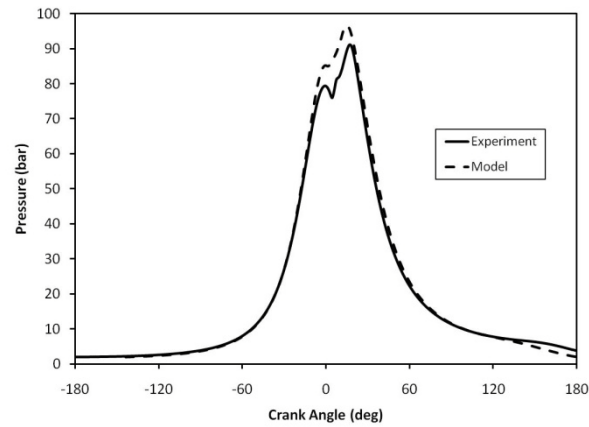
APPENDIX A**VALIDATION DATA FOR THE HIGH LOAD CASES**

Figure A-1 Pressure vs. CA comparison for 1400 rpm and high load

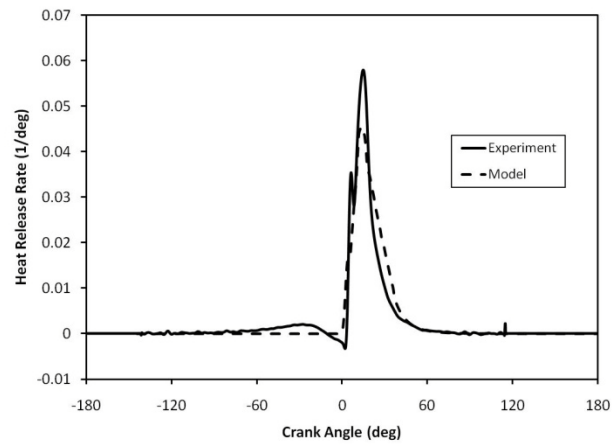


Figure A-2 Heat Release Rate vs. CA comparison for 1400 rpm and high load

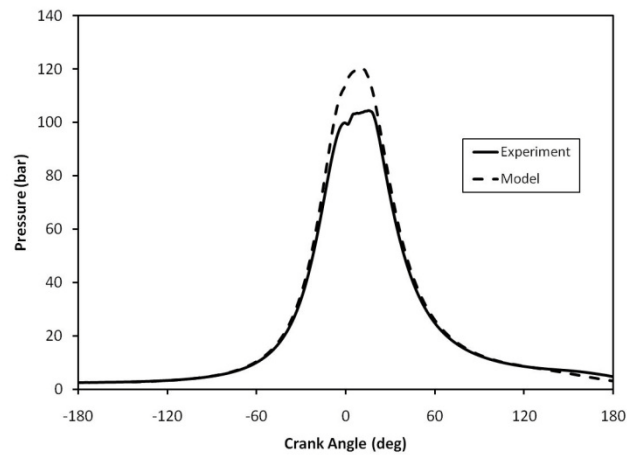


Figure A-3 Pressure vs. CA comparison for 1900 rpm and high load

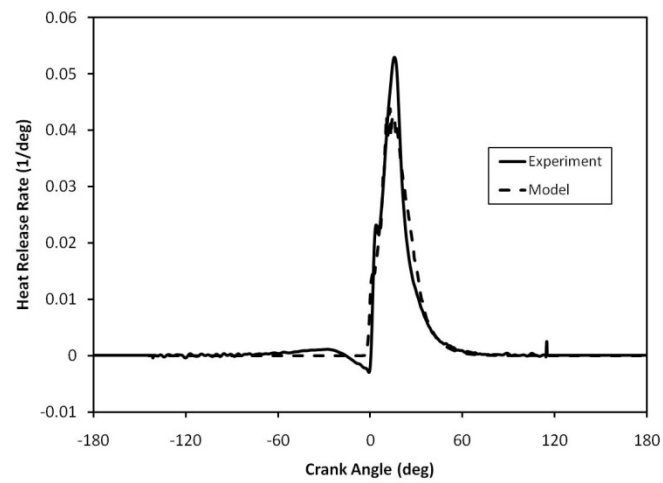


Figure A-4 Heat Release Rate vs. CA comparison for 1900 rpm and high load

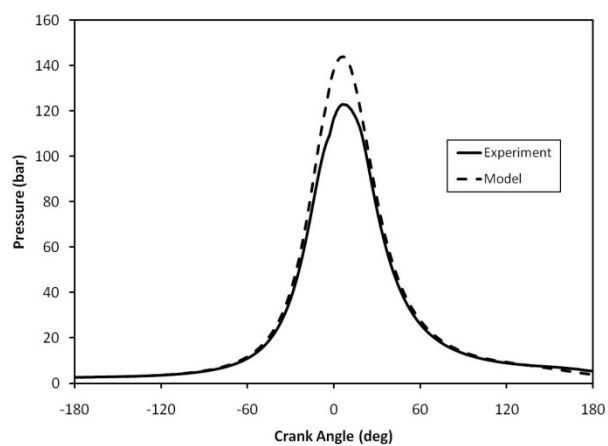


Figure A-5 Pressure vs. CA comparison for 2400 rpm and high load

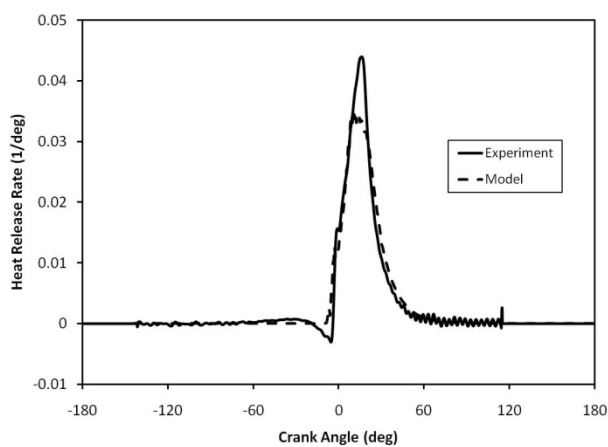


Figure A-6 Heat Release Rate vs. CA comparison for 2400 rpm and high load

APPENDIX B

MULTI-ZONE MODEL RAW DATA

1400 rpm / low load (multi-injection case)

Table B-1 Raw data for multi-injection 1400 rpm / low load 30% EGR case

30% EGR Case															
	Start of Injection (Degrees CA bTDC)														
	40	37.5	35	32.5	30	27.5	25	22.5	20	17.5	15	12.5	10	7.5	5
IMEP (bar)	3.59	3.63	3.66	3.71	3.7	3.67	3.65	3.6	3.51	3.46	3.35	3.15	2.76	2.61	2.43
ISFC (g/kW-h)	214.9	212.8	211.6	210.1	208.7	210.1	211.8	214.4	220	223.9	231.3	248.6	291.8	310.1	331.8
Indicated Efficiency (%)	39	39.4	39.8	39.9	40.1	39.8	39.6	39.1	38.1	37.5	36.3	33.8	28.7	25.3	25.3
Max. Pressure (bar)	95.39	91.82	87.05	84.55	80.4	76.28	73.19	68.64	66.43	65.6	64.63	63.87	63.28	62.54	62.58
dPmax/dCA (bar/degree)	6.367	5.578	4.003	3.877	3.652	3.338	3.053	2.815	2.73	2.171	1.957	1.988	1.955	1.955	1.954
Max. Temperature (K)	1512	1471	1413	1388	1352	1285	1256	1228	1195	1195	1177	1144	1108	1054	1037
NOx (ppm)	541.07	454.71	200.34	128.93	92.93	99.73	109	95.89	92.17	85.84	84.07	83.12	54.06	31.08	48.12
HC (ppm)	0.42	2.14	2.41	4.9	9.33	0.34	2.26	4.35	24.95	9.47	18.39	113.88	405.15	395.68	402.64
CO (ppm)	1.68	1.69	1.71	1.7	1.7	1.7	1.7	1.7	1.71	1.7	1.75	1.67	1.54	1.6	1.91
BSFC (g/kW-h)	501	471.3	446.7	430.1	421.5	415.3	411.6	409.3	423.6	435.1	460.6	524.9	726.9	839.3	1023.1
Volumetric Efficiency (%)	75.3	75.4	75.5	75.5	75.6	75.8	75.8	75.9	76	76.2	76.3	76.3	76.2	76.4	76.6
A/F Ratio	40.77	40.8	40.85	40.87	40.89	41	41.04	41.09	41.06	41.19	41.21	40.81	39.42	39.57	39.64
Brake Efficiency (%)	16.7	17.8	18.7	19.5	19.9	20.2	20.3	20.5	19.8	19.2	18.2	16	11.5	10	8.2

Table B-2 Raw data for multi-injection 1400 rpm / low load 40% EGR case

40% EGR Case															
	Start of Injection (Degrees CA bTDC)														
	40	37.5	35	32.5	30	27.5	25	22.5	20	17.5	15	12.5	10	7.5	5
IMEP (bar)	3.64	3.63	3.66	3.66	3.67	3.64	3.61	3.58	3.48	3.41	3.29	3.11	2.78	2.61	2.35
ISFC (g/kW-h)	211.9	212.2	210.4	210.5	210.4	211.7	213.5	215.6	222.2	226.2	235.5	252.4	293.6	316.3	351.7
Indicated Efficiency (%)	39.5	39.4	39.8	39.8	39.8	39.6	39.2	38.8	37.7	37	35.6	33.2	28.5	26.5	23.8
Max. Pressure (bar)	95.76	91.48	85.89	81.27	78.28	75.14	71.68	67.48	65.82	64.99	64.07	63.28	62.58	61.79	61.89
dPmax/dCA (bar/degree)	10.294	6.881	4.624	4.333	4.016	3.698	3.372	3.078	2.879	2.435	1.933	1.962	1.93	1.927	1.928
Max. Temperature (K)	1529	1478	1398	1337	1308	1264	1233	1213	1172	1172	1153	1122	1088	1041	1024
NOx (ppm)	378.06	269.38	125.18	44.03	30.1	51.44	54.28	56.59	55.81	53.25	51.29	51.97	34.23	14.68	50.96
HC (ppm)	2.03	1.22	2.68	4.89	10.05	0.32	1.81	4.13	21.54	9.89	37.27	124.23	397.74	420.22	509.69
CO (ppm)	2.06	2.1	2.12	2.12	2.12	2.12	2.11	2.11	2.1	2.13	4.3	2.09	2	2.32	3.32
BSFC (g/kW-h)	485.9	470.9	444	430.1	421	418.9	416.3	414.8	431.6	445.3	476.8	539.2	718.2	917.6	1153.7
Volumetric Efficiency (%)	63.5	63.6	63.8	64	64	64.3	64.4	64.5	64.7	64.9	65	65.1	64.5	65	65.2
A/F Ratio	34.34	34.4	34.5	34.6	34.62	34.78	34.85	34.92	34.9	35.05	35.02	34.63	33.2	32.75	32.86
Brake Efficiency (%)	17.2	17.8	18.9	19.5	19.9	20	20.1	20.2	19.4	18.8	17.6	15.5	11.7	9.1	7.3

Table B-3 Raw data for multi-injection 1400 rpm / low load 50% EGR case

50% EGR Case															
	Start of Injection (Degrees CA bTDC)														
	40	37.5	35	32.5	30	27.5	25	22.5	20	17.5	15	12.5	10	7.5	5
IMEP (bar)	3.7	3.71	3.72	3.69	3.65	3.6	3.55	3.51	3.41	3.34	3.22	3.06	2.76	2.64	2.34
ISFC (g/kW-h)	208.9	207.6	207.1	208.9	211.4	214	216.9	220	226.9	231.5	241.4	257.7	299	314.1	359.7
Indicated Efficiency (%)	40.2	40.3	40.4	40.1	39.6	39.1	38.6	38.1	36.9	36.2	34.7	32.5	28	26.7	23.3
Max. Pressure (bar)	93.77	92.41	87.05	82.36	77.63	73.41	70.22	66.57	65.14	64.32	63.38	62.7	61.67	61.09	61.11
dPmax/dCA (bar/degree)	19.478	12.123	8.065	5.053	4.656	4.323	3.713	3.389	3.082	2.67	2.024	1.935	1.8	1.902	1.901
Max. Temperature (K)	1516	1502	1421	1354	1293	1234	1198	1172	1142	1144	1123	1094	1062	1051	1009
NOx (ppm)	136.46	121.44	59.36	19.01	9.54	14.62	18.39	21.25	21.41	19.83	18.86	18.07	18.8	17.69	7.56
HC (ppm)	4.81	2.3	3.12	4.71	10.97	0.76	2.08	4.45	29.74	19.34	53.52	127	401.46	377.9	520.86
CO (ppm)	2.69	2.71	2.73	2.73	2.73	2.73	2.72	2.72	2.7	13.68	11.2	6.66	3.68	30.74	138.95
BSFC (g/kW-h)	458.5	447.9	433.8	427.8	422.8	422.9	425.4	426.9	446.9	462.7	498	560.2	734.8	900.8	1190.7
Volumetric Efficiency (%)	53	53.1	53.4	53.8	54.1	54.5	54.7	54.9	55	55.3	55.5	55.6	55.4	55.7	55.9
A/F Ratio	28.67	28.76	28.89	29.08	29.23	29.48	29.59	29.68	29.64	29.83	29.74	29.46	28.01	27.84	27.73
Brake Efficiency (%)	18.3	18.7	19.3	19.6	19.8	19.8	19.7	19.6	18.7	18.1	16.8	14.9	11.4	9.3	7

Table B-4 Raw data for multi-injection 1400 rpm / low load 60% EGR case

60% EGR Case															
	Start of Injection (Degrees CA bTDC)														
	40	37.5	35	32.5	30	27.5	25	22.5	20	17.5	15	12.5	10	7.5	5
IMEP (bar)	3.84	3.83	3.79	3.77	3.71	3.58	3.49	3.4	3.3	3.16	3.1	2.95	2.68	2.44	2.19
ISFC (g/kW-h)	201	201	203.2	204.8	208.2	215.3	221.3	226.7	234.6	250.3	251.7	268	309.7	359.4	401.7
Indicated Efficiency (%)	41.7	41.6	41.2	40.9	40.2	38.9	37.8	36.9	35.7	33.4	33.3	31.2	27	23.3	20.8
Max. Pressure (bar)	94.86	92.4	88.62	84.81	81.14	74.98	70.76	67	65.75	65.05	64.17	63.3	61.67	61.64	61.69
dPmax/dCA (bar/degree)	26.501	21.194	16.778	9.932	9.976	4.505	3.925	3.797	3.115	2.773	2.014	1.951	1.917	1.915	1.915
Max. Temperature (K)	1522	1484	1434	1381	1335	1237	1183	1146	1118	1096	1081	1051	1028	1006	986
NOx (ppm)	21.53	20.85	11.56	6.5	4.32	3.01	2.98	3.05	2.76	2.46	1.63	1.21	1	0.86	0.6
HC (ppm)	3.8	1.71	2.68	5.37	11.24	1.77	3.14	5.1	32.26	123.05	66.97	126.48	395.86	644.19	702.4
CO (ppm)	3.45	3.5	10.61	3.53	29.25	28.58	30.89	21.05	39.32	57.14	83.8	140.77	225.91	410.23	834.33
BSFC (g/kW-h)	428.6	422	421.2	417	419.5	432.5	442.4	452.2	478.7	535.3	544.6	610.8	790.6	1140.1	1592.8
Volumetric Efficiency (%)	45.8	45.9	46	46.4	46.7	47.4	47.8	48.1	48.3	48.4	48.7	48.9	48.7	48.4	48.8
A/F Ratio	24.75	24.83	24.9	25.11	25.23	25.63	25.84	25.99	25.98	25.56	26.04	25.84	24.45	23.01	23.15
Brake Efficiency (%)	19.5	19.8	19.9	20.1	20	19.4	18.9	18.5	17.5	15.6	15.4	13.7	10.6	7.3	5.3

1400 rpm / low load (single injection case)

Table B-5 Raw data for single injection 1400 rpm / low load 30% EGR case

30% EGR Case															
	Start of Injection (Degrees CA bTDC)														
	40	37.5	35	32.5	30	27.5	25	22.5	20	17.5	15	12.5	10	7.5	5
IMEP (bar)	2.91	2.92	2.92	2.92	2.93	2.96	2.99	3.01	3.02	3.02	3.01	2.99	2.95	2.89	2.8
ISFC (g/kW-h)	265.4	264.2	264.1	264.2	263.1	260.7	258.3	256.1	255.4	255.3	256	258.2	262.2	267.7	276.6
Indicated Efficiency (%)	31.5	31.7	31.7	31.7	31.8	32.1	32.4	32.7	32.8	32.8	32.7	32.4	31.9	31.3	30.3
Max. Pressure (bar)	77.28	76.51	75.9	74.51	73.08	71.31	69.19	66.73	64.46	61.98	59.01	55.94	52.32	48.94	45.18
dPmax/dCA (bar/degree)	24.042	25.602	21.55	23.897	21.608	18.5	14.803	12.886	11.16	7.408	6.71	5.285	4.461	3.51	2.638
Max. Temperature (K)	1837	1819	1805	1776	1740	1702	1659	1615	1565	1521	1475	1433	1391	1360	1324
NOx (ppm)	290.04	392.84	558.84	584.06	469.96	348.85	263.15	193.24	142.05	104.66	73.83	53.17	35.98	26.81	20.96
HC (ppm)	25.93	20.44	27.79	22.34	17.71	13.92	10.31	7.12	10.52	12.07	17.17	25.86	31.43	41.28	56.12
CO (ppm)	15.68	3.73	3.58	3.71	3.78	3.82	18.26	51.67	180.27	221.37	185.25	209.44	234.62	238.38	267.65
BSFC (g/kW-h)	716	695.7	690	684	665.1	640.3	613.2	584.7	569.3	556.1	545.4	539.5	541.5	547.4	566.4
Volumetric Efficiency (%)	46.2	46.1	46.1	46.2	46.3	46.5	46.6	46.8	46.9	47.1	47.2	47.4	47.5	47.5	47.8
A/F Ratio	24.95	24.91	24.89	24.98	25.03	25.16	25.23	25.3	25.35	25.45	25.53	25.61	25.68	25.67	25.76
Brake Efficiency (%)	11.7	12	12.1	12.2	12.6	13.1	13.7	14.3	14.7	15.1	15.4	15.5	15.5	15.3	14.8

Table B-6 Raw data for single injection 1400 rpm / low load 40% EGR case

40% EGR Case															
	Start of Injection (Degrees CA bTDC)														
	40	37.5	35	32.5	30	27.5	25	22.5	20	17.5	15	12.5	10	7.5	5
IMEP (bar)	3.19	3.2	3.18	3.2	3.2	3.22	3.24	3.26	3.28	3.28	3.28	3.25	3.22	3.16	3.07
ISFC (g/kW-h)	241.9	241.5	242.4	241.4	241.4	239.8	238.2	236.4	235.2	234.8	235.6	237.4	240	244.8	251.7
Indicated Efficiency (%)	34.6	34.7	34.5	34.7	34.7	34.9	35.2	35.4	35.6	35.7	35.5	35.3	34.9	34.2	33.3
Max. Pressure (bar)	84.9	83.96	83.38	82.14	81.16	79.52	77.66	75.35	72.95	70.23	67.41	63.87	60.18	56.23	52.24
dPmax/dCA (bar/degree)	26.109	24.932	23.579	26.218	23.11	21.354	18.268	14.627	12.953	9.189	8.684	7.121	5.283	4.141	3.457
Max. Temperature (K)	1725	1713	1704	1679	1659	1629	1597	1558	1519	1484	1448	1404	1370	1334	1299
NOx (ppm)	303.66	290.49	543.48	367.67	479.02	382.99	368.65	281.17	251.97	215.85	196.24	139.71	131.6	122.79	119.09
HC (ppm)	21.56	18.1	12.94	15.25	10.69	13.1	10.59	4.46	6.99	8.02	14.65	15.54	18.43	26.32	37.2
CO (ppm)	3.24	3.37	3.18	3.45	3.31	3.4	3.35	14.8	86.36	133.85	134.35	139.51	133.27	136.87	148.62
BSFC (g/kW-h)	603.1	598.8	600	587.5	581.6	565.3	546.9	527.9	512.2	499.6	492.7	486.1	484.3	489.1	497.9
Volumetric Efficiency (%)	47.3	47.3	47.3	47.5	47.5	47.6	47.7	47.9	48	48.2	48.4	48.6	48.8	48.9	49.1
A/F Ratio	25.54	25.56	25.59	25.66	25.69	25.75	25.82	25.92	25.99	26.08	26.16	26.27	26.36	26.42	26.48
Brake Efficiency (%)	13.9	14	14	14.3	14.4	14.8	15.3	15.9	16.3	16.8	17	17.2	17.3	17.1	16.8

Table B-7 Raw data for single injection 1400 rpm / low load 50% EGR case

50% EGR Case															
	Start of Injection (Degrees CA bTDC)														
	40	37.5	35	32.5	30	27.5	25	22.5	20	17.5	15	12.5	10	7.5	5
IMEP (bar)	3.52	3.51	3.49	3.5	3.49	3.5	3.51	3.52	3.53	3.52	3.51	3.48	3.44	3.4	3.33
ISFC (g/kW-h)	219.7	220.2	221	220.4	221.5	220.5	220	219.2	218.7	219.2	219.9	221.9	224.2	227.2	232.8
Indicated Efficiency (%)	38.1	38	37.9	38	37.8	38	38.1	38.2	38.3	38.2	38.1	37.7	37.3	36.9	36
Max. Pressure (bar)	90.89	90.43	89.74	88.87	87.87	86.44	84.6	82.5	79.88	76.95	73.93	70.25	66.79	63.08	58.46
dPmax/dCA (bar/degree)	29.787	29.381	28.523	24.083	27.4	23.823	22.66	20.342	15.236	13.407	9.756	8.027	6.332	5.828	6.112
Max. Temperature (K)	1651	1646	1636	1622	1607	1583	1555	1523	1488	1455	1421	1384	1357	1333	1301
NOx (ppm)	253.21	358.53	365.87	308.1	398.99	326.54	278.78	227.98	192.9	171.15	165.98	120.62	157.84	218.81	154.09
HC (ppm)	16.85	13.57	12.05	9.49	11.6	10.15	7.87	8.04	5.09	10.72	10.86	14.01	19.41	34.84	
CO (ppm)	3.28	3.21	3.24	3.36	3.29	3.41	3.44	9.89	32.08	91.96	160.69	217.54	165.77	154.96	200.34
BSFC (g/kW-h)	506.3	508.8	507.7	501.4	504	493.9	484	473.6	462.1	454.6	448.3	444.6	443.3	444.7	450.3
Volumetric Efficiency (%)	45.3	45.3	45.4	45.4	45.5	45.6	45.7	45.8	46	46.2	46.4	46.7	46.9	47	47.2
A/F Ratio	24.47	24.49	24.52	24.56	24.57	24.63	24.7	24.79	24.88	24.96	25.08	25.23	25.32	25.39	25.45
Brake Efficiency (%)	16.5	16.5	16.5	16.7	16.6	16.9	17.3	17.7	18.1	18.4	18.7	18.8	18.9	18.8	18.6

Table B-8 Raw data for single injection 1400 rpm / low load 60% EGR case

60% EGR Case															
	Start of Injection (Degrees CA bTDC)														
	40	37.5	35	32.5	30	27.5	25	22.5	20	17.5	15	12.5	10	7.5	5
IMEP (bar)	3.87	3.86	3.84	3.83	3.82	3.8	3.79	3.77	3.75	3.72	3.69	3.66	3.61	3.55	3.48
ISFC (g/kW-h)	199.5	200	200.9	201.6	202.1	202.9	203.9	204.9	206	207.7	209.1	211.4	214.3	218.3	223.5
Indicated Efficiency (%)	42	41.9	41.7	41.5	41.4	41.3	41.1	40.9	40.6	40.3	40	39.6	39.1	38.4	37.5
Max. Pressure (bar)	93	92.45	92.01	91.36	90.33	89.02	87.29	85.49	83.29	80.68	77.69	74.17	70.02	64.9	58.27
dPmax/dCA (bar/degree)	33.825	30.994	28.761	29.904	25.335	23.005	22.031	22.611	22.463	15.981	14.048	13.246	12.09	11.157	8.993
Max. Temperature (K)	1610	1605	1598	1589	1576	1557	1531	1501	1470	1440	1407	1377	1350	1327	1314
NOx (ppm)	5.06	6.79	8.89	11.24	12.36	11.37	9.03	7.46	6.14	4.83	3.88	3.24	2.64	2.06	1.53
HC (ppm)	13.71	12.63	11.4	11.78	8.49	7.61	8.28	7.82	8.42	14.13	12.23	15.76	19.83	29.52	49.36
CO (ppm)	4.3	4.35	4.38	4.42	4.44	5.33	13.12	31.68	39.29	63.73	99.11	110.5	155.43	153.38	104.35
BSFC (g/kW-h)	417.5	418.8	421	422.2	422.6	422.2	420.9	419.3	416.8	415.2	412.6	411	410.3	410.5	413.1
Volumetric Efficiency (%)	40.2	40.2	40.3	40.3	40.4	40.5	40.6	40.8	40.9	41.1	41.4	41.6	41.9	42.1	42.3
A/F Ratio	21.71	21.73	21.76	21.78	21.83	21.88	21.94	22.02	22.12	22.21	22.34	22.46	22.57	22.65	22.71
Brake Efficiency (%)	20.1	20	19.9	19.8	19.8	19.8	19.9	20	20.1	20.2	20.3	20.4	20.4	20.4	20.3

1400 rpm / mid load

Table B-9 Raw data for 1400 rpm / mid load 30% EGR case

30% EGR Case															
	Start of Injection (Degrees CA bTDC)														
	40	37.5	35	32.5	30	27.5	25	22.5	20	17.5	15	12.5	10	7.5	5
IMEP (bar)	6.28	6.29	6.35	6.44	6.54	6.68	6.85	7.09	7.32	7.54	7.71	7.86	7.96	8	7.98
ISFC (g/kW-h)	245.3	245	242.6	239.4	235.6	230.6	224.8	217.2	210.3	204.1	199.7	195.9	193.5	192.5	193
Indicated Efficiency (%)	34.1	34.2	34.5	35	35.5	36.3	37.2	38.5	39.8	41	41.9	42.7	43.3	43.5	43.4
Max. Pressure (bar)	135.46	135.13	134.64	133.76	132.59	131.07	128.5	125.48	122.51	118.55	114.71	109.67	103.92	97.68	90.18
dPmax/dCA (bar/degree)	52.634	66.389	54.953	54.758	47.39	48.931	39.237	30.677	28.767	24.695	20.536	16.935	15.737	11.96	11.291
Max. Temperature (K)	2111	2105	2095	2079	2059	2034	1993	1951	1916	1879	1850	1818	1789	1758	1724
NOx (ppm)	475.67	572.09	619.01	636.67	708.03	749.18	746.57	708.49	649.38	539.83	376.53	329.59	257.37	208.57	163.58
HC (ppm)	15.24	12.75	6.95	5.69	3.85	2.06	0.33	0.31	0.52	0.47	8.04	3.65	0.9	2.53	4.59
CO (ppm)	435.28	494.27	575.22	700.95	859.43	1072.38	1187.11	628.14	525.41	449.68	458.65	484	494.2	517.98	491.72
BSFC (g/kW-h)	409.3	407.9	401.5	391.8	380.5	366.3	349.4	328.8	311	295	283.4	272.9	265.1	260	256.9
Volumetric Efficiency (%)	75.4	75.4	75.4	75.3	75.3	75.4	75.4	75.5	75.6	75.7	75.8	75.9	76	76.2	76.3
A/F Ratio	20.41	20.41	20.41	20.41	20.41	20.42	20.44	20.47	20.48	20.5	20.52	20.55	20.59	20.63	20.67
Brake Efficiency (%)	20.5	20.5	20.5	21.4	22	22.9	24	25.5	26.9	28.4	29.5	30.7	31.6	32.2	32.6

Table B-10 Raw data for 1400 rpm / mid load 40% EGR case

40% EGR Case															
	Start of Injection (Degrees CA bTDC)														
	40	37.5	35	32.5	30	27.5	25	22.5	20	17.5	15	12.5	10	7.5	5
IMEP (bar)	6.63	6.63	6.63	6.68	6.72	6.81	6.93	7.07	7.26	7.47	7.63	7.77	7.85	7.88	7.85
ISFC (g/kW-h)	232.5	232.6	232.2	230.7	229.2	226.2	222.3	217.8	212	206.1	201.8	198.2	196.1	195.5	196.3
Indicated Efficiency (%)	36	36	36	36.3	36.5	37	37.7	38.4	39.5	40.6	41.5	42.2	42.7	42.8	42.6
Max. Pressure (bar)	134.05	133.73	133.17	132.48	131.4	129.93	128.12	125.06	121.3	116.43	112.07	106.42	100.79	94.18	86.99
dPmax/dCA (bar/degree)	59.915	60.391	68.25	62.228	53.638	49.337	43.211	34.075	32.192	26.93	23.689	21.79	17.049	14.574	12.12
Max. Temperature (K)	2095	2089	2078	2064	2044	2019	1991	1946	1900	1850	1814	1772	1736	1703	1670
NOx (ppm)	179.35	221.79	240.26	247.81	280.01	295.8	283.65	248.77	209.59	156.5	121.31	99.02	84.52	74.15	64.82
HC (ppm)	16.47	14.31	8.72	7.85	6.81	5.12	2.51	1.38	1.45	1.14	8.74	4.61	2.42	4.18	5.13
CO (ppm)	1432.2	1525.8	1724.73	1886.71	2091.16	2305.17	2617.82	2860.19	2472.9	1807.9	1606.61	1511.35	1495.93	1454.58	1417.35
BSFC (g/kW-h)	373.3	374	371.9	368	362.2	353.8	343.3	329.9	313.9	297.9	286.3	275.9	268.5	263.8	261.4
Volumetric Efficiency (%)	65.4	65.3	65.3	65.3	65.3	65.4	65.5	65.6	65.8	65.9	66.1	66.3	66.5	66.7	66.9
A/F Ratio	17.69	17.68	17.68	17.68	17.69	17.71	17.73	17.77	17.81	17.87	17.89	17.95	18.01	18.07	18.13
Brake Efficiency (%)	22.4	22.4	22.5	22.7	23.1	23.7	24.4	25.4	26.7	28.1	29.2	30.3	31.2	31.7	32

Table B-11 Raw data for 1400 rpm / mid load 50% EGR case

50% EGR Case															
	Start of Injection (Degrees CA bTDC)														
	40	37.5	35	32.5	30	27.5	25	22.5	20	17.5	15	12.5	10	7.5	5
IMEP (bar)	7.29	7.27	7.24	7.22	7.22	7.2	7.21	7.25	7.3	7.37	7.42	7.48	7.51	7.52	7.47
ISFC (g/kW-h)	211.4	212.3	212.9	213.4	213.5	214.2	213.9	212.7	211.2	209.2	207.9	206.1	205.2	205	206.4
Indicated Efficiency (%)	39.6	39.4	39.3	39.2	39.2	39.1	39.1	39.4	39.6	40	40.3	40.6	40.8	40.8	40.6
Max. Pressure (bar)	131.98	131.56	130.98	130.24	129.35	127.86	126.1	123.57	120.28	116.22	111.81	105.99	99.73	93.54	86.82
dPmax/dCA (bar/degree)	65.351	64.107	62.157	60.004	55.66	62.14	61.662	49.246	40.16	34.207	28.643	29.016	23.972	20.842	17.608
Max. Temperature (K)	2050	2043	2034	2023	2008	1985	1957	1919	1875	1828	1777	1722	1667	1626	1588
NOx (ppm)	6.03	8.5	6.98	7.59	6.18	7.4	6.75	6.37	5.36	3.68	3	2.6	2.28	1.87	1.12
HC (ppm)	19.21	20.33	15.36	15.46	15.6	15.71	15.15	14.87	15.73	12.2	20.71	15.94	12.39	14.86	15.5
CO (ppm)	9774.95	9930.42	10270.4	10614.5	10818.5	10979.5	11057.1	10903.8	10759.9	10742.4	10715.8	10373.7	9787.54	9608.84	9187.66
BSFC (g/kW-h)	322.1	323.5	324.4	324.8	324.5	324.9	322.4	318	312.2	304.9	298.7	291.2	285.2	281	279.7
Volumetric Efficiency (%)	53.2	53.2	53.1	53.1	53.1	53.2	53.3	53.4	53.6	53.9	54.1	54.5	54.9	55.3	55.6
A/F Ratio	14.4	14.38	14.37	14.37	14.37	14.39	14.41	14.45	14.5	14.58	14.64	14.74	14.86	14.95	15.05
Brake Efficiency (%)	26	25.9	25.8	25.8	25.8	25.8	26	26.3	26.8	27.5	28	28.7	29.4	29.8	29.9

1900 rpm / low load

Table B-12 Raw data for 1900 rpm / low load 30% EGR case

30% EGR Case															
	Start of Injection (Degrees CA bTDC)														
	40	37.5	35	32.5	30	27.5	25	22.5	20	17.5	15	12.5	10	7.5	5
IMEP (bar)	4.45	4.38	4.33	4.27	4.14	4.12	3.92	3.78	3.64	3.51	3.2	2.73	2.4	1.95	1.14
ISFC (g/kW-h)	195.7	199	201	204.3	210.8	212	222.9	231.1	240.9	250.6	278.1	336.3	383.5	485.3	908.8
Indicated Efficiency (%)	42.8	42.1	41.6	41	39.7	39.5	37.6	36.2	34.7	33.4	30.1	24.9	21.8	17.2	9.2
Max. Pressure (bar)	88.9	84.25	80.26	76.13	70.82	66.76	65.01	64.38	63.84	63.33	63.03	62.52	62.22	62.18	62.08
dPmax/dCA (bar/degree)	6.123	3.563	3.334	3.156	2.683	2.453	2.259	1.942	1.946	1.952	1.95	1.971	1.944	1.941	1.936
Max. Temperature (K)	1503	1422	1369	1322	1251	1248	1180	1192	1173	1143	1121	1064	986	976	969
NOx (ppm)	339.32	239.79	211.96	172.38	75.42	46.77	47.96	96.92	97.62	100.19	96.58	42.98	94.9	25.04	1.09
HC (ppm)	3.68	7.69	8.61	9.81	14.18	23.85	34.27	46.46	66.67	93.43	212.21	529.29	580.07	819.8	1836.59
CO (ppm)	1.88	1.85	1.88	1.91	1.92	1.93	1.95	1.96	1.98	2.1	2.59	5.2	6.29	4.7	8
BSFC (g/kW-h)	381.1	384.6	384.2	388.8	399.3	407	422	453.9	497.4	542.5	669.1	1051.8	1677.2	10835.7	10835.7
Volumetric Efficiency (%)	76.3	76.3	76.3	76.3	76.4	76.4	76.5	76.5	76.5	76.5	76.5	76.6	76.6	76.7	76.3
A/F Ratio	36.52	36.52	36.53	36.54	36.55	36.51	36.51	36.48	36.42	36.33	35.91	34.82	34.72	33.86	30.67
Brake Efficiency (%)	22	21.8	21.8	21.5	21	20.6	19.8	18.4	16.8	15.4	12.5	8	5	0.8	0.1

Table B-13 Raw data for 1900 rpm / low load 40% EGR case

40% EGR Case															
	Start of Injection (Degrees CA bTDC)														
	40	37.5	35	32.5	30	27.5	25	22.5	20	17.5	15	12.5	10	7.5	5
IMEP (bar)	4.46	4.37	4.4	4.23	4.11	3.95	3.85	3.75	3.56	3.4	3.13	2.72	2.4	2.01	1.35
ISFC (g/kW-h)	195.1	199.2	198.3	206.3	212.1	221	227.1	233.7	246.9	259.3	285.4	342.3	392.1	480.3	790.3
Indicated Efficiency (%)	42.9	42	42.2	40.6	39.5	37.9	36.9	35.8	33.9	32.3	29.3	24.5	21.3	17.4	10.6
Max. Pressure (bar)	90.24	84.84	79.2	75.08	70.71	66.74	65.04	64.33	63.81	63.27	62.94	62.41	62.07	62.04	61.92
dPmax/dCA (bar/degree)	6.448	4.462	3.774	3.505	2.967	2.594	2.38	2.035	1.934	1.946	1.942	1.962	1.935	1.933	1.927
Max. Temperature (K)	1513	1434	1371	1311	1254	1193	1167	1175	1140	1118	1091	1064	986	985	979
NOx (ppm)	315.59	185.91	159.98	91.18	125.2	126.12	125.53	14.8	89.35	132.44	88.01	41.29	59.68	59.97	31.59
HC (ppm)	3.08	7.47	9.02	9.97	14.11	24.87	33.85	42.1	68.2	88.65	208.83	537.79	602.51	779.87	1673.67
CO (ppm)	6.85	2.29	15.72	8.9	2.61	2.36	2.43	2.52	2.62	2.98	8.39	100.41	38.6	6.46	35.99
BSFC (g/kW-h)	389.5	389.1	383.2	392.9	404.6	428.8	449	468.9	522.7	576.5	707.1	1072.4	1727.9	7341.8	7341.8
Volumetric Efficiency (%)	65.4	65.5	65.5	65.6	65.6	65.7	65.8	65.9	65.9	65.9	66	65.9	66	66	65.8
A/F Ratio	31.33	31.34	31.36	31.39	31.4	31.38	31.39	31.38	31.3	31.24	30.77	29.48	29.29	28.61	25.76
Brake Efficiency (%)	21.5	21.5	21.8	21.3	20.7	19.5	18.6	17.9	16	14.5	11.8	7.8	4.8	1.1	0.8

Table B-14 Raw data for 1900 rpm / low load 50% EGR case

50% EGR Case															
	Start of Injection (Degrees CA bTDC)														
	40	37.5	35	32.5	30	27.5	25	22.5	20	17.5	15	12.5	10	7.5	5
IMEP (bar)	4.44	4.4	4.29	4.17	4.03	3.85	3.71	3.6	3.39	3.22	2.96	2.63	2.23	1.87	1.46
ISFC (g/kW-h)	196.1	198.3	203.1	209.1	216.6	227.4	236.4	244.1	260.3	277.8	311.8	361	447.5	539.5	768.6
Indicated Efficiency (%)	42.7	42.2	41.2	40	38.6	36.8	35.4	34.3	32.2	30.1	26.8	23.2	18.7	15.5	10.9
Max. Pressure (bar)	88.79	85.03	80.61	75.62	70.31	66.26	64.68	64.07	63.56	63.06	62.48	61.63	61.55	61.58	61.5
dPmax/dCA (bar/degree)	10.144	7.974	5.802	3.812	3.164	2.679	2.458	1.913	1.914	1.92	1.924	1.943	1.913	1.913	1.909
Max. Temperature (K)	1481	1444	1379	1307	1237	1180	1137	1127	1087	1073	1046	1028	1001	990	983
NOx (ppm)	79.19	90.52	74.6	50.42	66.51	66.18	33.48	67.84	70.45	69.91	25.2	50.49	5.11	71.32	43.2
HC (ppm)	3.53	9.47	10.07	11.51	16.9	26.78	38.35	50.46	85.36	163.46	331.19	569.4	908.14	985.88	1737.41
CO (ppm)	14.82	75.11	55.22	58.07	59.69	36.43	73.06	69.68	118.3	237.27	472.46	508.75	166.43	411.68	3416.4
BSFC (g/kW-h)	384	384.4	395.5	401.7	415.9	446.2	481.2	509.3	582.7	662.4	861.8	1205.6	2581.9	5862.9	6895.2
Volumetric Efficiency (%)	53.6	53.7	53.9	54	54	54.4	54.6	54.7	54.8	54.9	54.8	54.7	54.7	54.9	54.1
A/F Ratio	25.67	25.69	25.77	25.85	25.91	25.96	25.99	26	25.91	25.61	24.83	24.02	22.82	22.69	20.06
Brake Efficiency (%)	21.8	21.8	21.2	20.8	20.1	18.8	17.4	16.4	14.4	12.6	9.7	6.9	3.2	1.5	0.8

Table B-15 Raw data for 1900 rpm / low load 60% EGR case

60% EGR Case															
	Start of Injection (Degrees CA bTDC)														
	40	37.5	35	32.5	30	27.5	25	22.5	20	17.5	15	12.5	10	7.5	5
IMEP (bar)	4.51	4.45	4.39	4.24	4.04	3.81	3.62	3.65	3.24	3.07	2.8	2.52	2.18	1.76	1.51
ISFC (g/kW-h)	193.4	196.1	198.7	205.9	216.1	230	242.4	241.1	273.5	292.8	333.3	381.9	471.4	613.3	777.9
Indicated Efficiency (%)	43.3	42.7	42.1	40.7	38.7	36.4	34.5	34.7	30.6	28.6	25.1	21.9	17.8	13.6	10.8
Max. Pressure (bar)	88.8	85	80.48	77.62	71.14	66.03	64.5	64	63.33	62.54	61.32	61.27	61.22	61.3	61.24
dPmax/dCA (bar/degree)	18.201	14.156	7.352	5.647	3.01	2.678	2.278	1.899	1.9	1.908	1.911	1.931	1.9	1.901	1.898
Max. Temperature (K)	1482	1450	1426	1359	1264	1189	1137	1137	1051	1036	1014	1003	991	987	983
NOx (ppm)	10.35	6.93	4.26	4.04	3.21	2.83	3.43	2.68	5.8	5.69	1.85	5.72	6.15	2.87	8.56
HC (ppm)	10.92	12.32	2.33	14.94	21.38	32.45	46.03	51.51	108.32	187.9	423.21	601.47	998.17	1337.3	1870.46
CO (ppm)	20.74	57.26	154.54	253.46	255.31	282.23	365.54	481.89	691.33	832.81	916.59	662.29	1258.95	6954.45	9247.68
BSFC (g/kW-h)	372.9	37505	381.2	400.4	418.8	456.2	499.1	538.3	649	741.2	950.8	1428.7	3171.6	4258.3	5658.2
Volumetric Efficiency (%)	47.8	47.9	48.1	48.4	48.7	49	49.3	49.5	49.7	49.7	49.6	49.6	49.2	48.8	47.9
A/F Ratio	22.86	22.9	23	23.14	23.24	23.35	23.42	23.46	23.35	23.05	22.2	21.45	19.97	18.84	17.03
Brake Efficiency (%)	22.4	22.3	22	20.9	20	18.4	16.8	15.6	12.9	11.3	8.8	5.9	2.6	1.1	0.2

1900 rpm / mid load

Table B-16 Raw data for 1900 rpm / mid load 30% EGR case

30% EGR Case															
	Start of Injection (Degrees CA bTDC)														
	40	37.5	35	32.5	30	27.5	25	22.5	20	17.5	15	12.5	10	7.5	5
IMEP (bar)	6.91	6.93	6.9	6.92	6.96	7.04	7.13	7.24	7.38	7.57	7.74	7.87	7.98	8.02	8.02
ISFC (g/kW-h)	216.6	216.2	216.9	216.4	215.1	212.8	210.1	206.8	202.7	197.7	193.5	190.1	187.7	186.7	186.7
Indicated Efficiency (%)	38.7	38.7	38.6	38.7	38.9	39.3	39.8	40.5	41.3	42.3	43.3	44	44.6	44.8	44.8
Max. Pressure (bar)	135.33	135.26	134.89	134.38	133.77	132.9	131.7	130.11	127.33	124.18	120.71	116.23	111.54	106.04	99.19
dPmax/dCA (bar/degree)	47.252	51.751	61.967	62.892	54.7	53.796	44.951	42.024	39.38	36.115	33.401	26.499	26.211	23.558	16.977
Max. Temperature (K)	2114	2112	2106	2096	2086	2072	2053	2028	1988	1951	1915	1875	184	1813	1779
NOx (ppm)	328.82	390.8	400.39	359.14	376.83	406.97	416.53	447.31	479.9	491.85	465.28	419.37	362.66	292.17	254.51
HC (ppm)	6.04	5.6	7.62	13.35	11.33	6.54	4.53	3.45	1	0.87	1.25	1.7	1.77	10.04	9.15
CO (ppm)	511.09	529.9	663.32	800.81	916.74	1027.16	1236.22	1511.43	1449.8	976	853.29	778.54	746.47	799.73	823.5
BSFC (g/kW-h)	357.5	357.8	358.6	357.2	352.8	346.1	338	328	315.7	301.5	289.4	279	271.1	265.9	261.9
Volumetric Efficiency (%)	76.6	76.6	76.6	76.5	76.4	76.4	76.3	76.3	76.3	76.3	76.3	76.4	76.4	76.4	76.5
A/F Ratio	21.35	21.35	21.33	21.31	21.29	21.28	21.27	21.26	21.27	21.27	21.27	21.28	21.29	21.29	21.32
Brake Efficiency (%)	23.4	23.4	23.3	23.4	23.7	24.2	24.8	25.5	26.5	27.8	28.9	30	30.9	31.5	32

Table B-17 Raw data for 1900 rpm / mid load 40% EGR case

40% EGR Case															
	Start of Injection (Degrees CA bTDC)														
	40	37.5	35	32.5	30	27.5	25	22.5	20	17.5	15	12.5	10	7.5	5
IMEP (bar)	7.14	7.12	7.11	7.12	7.12	7.16	7.21	7.3	7.38	7.5	7.63	7.75	7.85	7.89	7.88
ISFC (g/kW-h)	209.7	210.3	210.7	210.6	210.4	209.3	207.7	205.3	202.9	199.5	196.1	193.2	190.8	190	190.1
Indicated Efficiency (%)	39.9	39.8	39.7	39.8	39.8	40	40.3	40.8	41.3	42	42.7	43.3	43.9	44.1	44
Max. Pressure (bar)	134.28	134.16	133.8	133.35	132.74	131.99	130.86	129.37	127.26	124.12	120.35	116.24	111.04	105.22	98.61
dPmax/dCA (bar/degree)	53.296	49.84	54.825	69.019	62.751	52.828	54.043	43.589	37.063	39.473	36.282	32.031	24.558	26.145	23.701
Max. Temperature (K)	2107	2105	2098	2089	2078	2065	2046	2022	1992	1950	1908	1867	1828	1793	1761
NOx (ppm)	232.3	302.89	306.4	234.48	228.84	240.18	249.26	204.08	211.67	220.96	213.25	190.53	159.23	131.45	113.14
HC (ppm)	5.75	7.3	7.6	14.56	12.75	8.49	8.07	5.71	3.58	1.93	2.41	3.26	3.21	11.89	11.28
CO (ppm)	1130.41	1214.46	1459.28	1708.83	1939.8	2104.85	2348.95	2729.03	3120.67	3083.79	2850.93	2634.87	2277.3	2204.57	2245.35
BSFC (g/kW-h)	338.4	339.6	339.8	340.4	339.4	335.9	330.7	323.7	316.2	305.9	295.2	286	277.6	272.3	268.7
Volumetric Efficiency (%)	66.9	66.9	66.8	66.7	66.7	66.6	66.6	66.5	66.6	66.6	66.6	66.7	66.8	66.9	67
A/F Ratio	18.64	18.63	18.61	18.58	18.57	18.55	18.54	18.54	18.55	18.56	18.57	18.58	18.6	18.62	18.65
Brake Efficiency (%)	24.7	24.7	24.6	24.6	24.7	24.9	25.3	25.9	26.5	27.4	28.4	29.3	30.2	30.7	31.2

Table B-18 Raw data for 1900 rpm / mid load 50% EGR case

50% EGR Case															
	Start of Injection (Degrees CA bTDC)														
	40	37.5	35	32.5	30	27.5	25	22.5	20	17.5	15	12.5	10	7.5	5
IMEP (bar)	7.63	7.6	7.56	7.55	7.53	7.52	7.5	7.5	7.51	7.54	7.57	7.6	7.64	7.64	7.62
ISFC (g/kW-h)	196.3	197.2	198.2	198.6	199	199.3	199.9	199.9	199.7	198.9	198	197.3	196.1	196.5	197
Indicated Efficiency (%)	42.6	42.5	42.2	42.2	42.1	42	41.9	41.9	41.9	42.1	42.3	42.4	42.7	42.6	42.5
Max. Pressure (bar)	132.23	132.1	131.62	131.51	131.22	130.63	130.21	129.48	128.02	125.71	122.53	118.51	113.42	107.75	100.58
dPmax/dCA (bar/degree)	53.168	52.987	59.501	58.167	45.936	48.39	55.763	53.865	57.802	52.009	42.604	37.326	27.663	28.253	28.926
Max. Temperature (K)	2071	2069	2062	2061	2056	2048	2041	2031	2012	1983	1948	1912	1874	1849	1826
NOx (ppm)	39.89	55.78	31.7	55.83	54.23	48.95	55.07	52.06	50.98	46.59	36.47	29.75	25.81	22.19	18.85
HC (ppm)	8.03	10.1	12.56	19.56	18.87	15.47	16.75	18.05	18.58	16.34	18.01	18.63	16.23	31.55	36.81
CO (ppm)	5515.83	5709.99	6641.35	6469	6852.46	7207.37	7599.93	7938.23	8258.08	8501.06	8788.94	9035.2	9125.39	9037.13	9022.39
BSFC (g/kW-h)	303.9	307	307.5	308.6	310.1	309.7	311.2	310.9	309	305	301.2	296.7	290.6	287.6	283.7
Volumetric Efficiency (%)	55	55	54.9	54.9	54.8	54.7	54.6	54.6	54.7	54.7	54.7	54.8	55	55.2	55.4
A/F Ratio	15.33	15.31	15.29	15.26	15.24	15.22	15.21	15.2	15.21	15.22	15.23	15.26	15.3	15.33	15.38
Brake Efficiency (%)	27.5	27.3	27.2	27.1	27	27	26.9	26.9	27.1	27.4	27.8	28.2	28.8	29.1	29.5

Table B-19 Raw data for 1900 rpm / mid load 60% EGR case

60% EGR Case															
	Start of Injection (Degrees CA bTDC)														
	40	37.5	35	32.5	30	27.5	25	22.5	20	17.5	15	12.5	10	7.5	5
IMEP (bar)	7.58	7.56	7.51	7.49	7.46	7.44	7.41	7.4	7.38	7.37	7.36	7.35	7.35	7.3	7.2
ISFC (g/kW-h)	197.6	198.3	199.7	200.5	201.2	201.8	202.6	202.9	203.6	203.8	204.3	204.6	204.9	206.6	209.6
Indicated Efficiency (%)	42.4	42.2	41.9	41.8	41.6	41.5	41.3	41.3	41.1	41.1	41	40.9	40.9	40.5	39.9
Max. Pressure (bar)	117.89	118.05	117.86	117.56	116.74	116.4	115.57	114.52	112.96	111.44	110.56	106.19	100.34	91.98	81.69
dPmax/dCA (bar/degree)	45.202	44.525	43.166	50.132	40.522	42.189	40.911	40.246	38.166	49.646	42.819	42.688	44.075	36.389	28.938
Max. Temperature (K)	1983	1983	1979	1978	1973	1969	1964	1960	1952	1944	1942	1925	1909	1894	1875
NOx (ppm)	0.67	1.65	1.69	6.09	5.97	1.43	6.6	1.55	5.14	1.48	1.37	1.14	3.87	0.81	0.69
HC (ppm)	8.87	11.07	14.43	23.54	23.88	22.5	25.47	29.37	32.81	33.66	41.06	48.64	53.49	71.38	79.35
CO (ppm)	18842.5	19135.7	19677.4	19444.1	19965.9	20754.8	20738.5	21190.5	20879.9	21134.6	20868.4	20392.6	19340.3	18334.6	16917
BSFC (g/kW-h)	298.7	299.6	301.6	303.6	305.2	306.1	307.4	307.7	307.4	307.6	307.3	304.6	301	298.3	296.9
Volumetric Efficiency (%)	49	49	48.9	48.9	48.8	48.7	48.6	48.6	48.7	48.7	48.8	48.9	49.1	49.4	49.8
A/F Ratio	13.66	13.64	13.62	13.59	13.56	13.53	13.52	13.51	13.52	13.52	13.53	13.56	13.62	13.67	13.78
Brake Efficiency (%)	28	27.9	27.8	27.6	27.4	27.4	27.2	27.2	27.2	27.2	27.2	27.5	27.8	28.1	28.2

2400 rpm / low load

Table B-20 Raw data for 2400 rpm / low load 30% EGR case

30% EGR Case															
	Start of Injection (Degrees CA bTDC)														
	40	37.5	35	32.5	30	27.5	25	22.5	20	17.5	15	12.5	10	7.5	5
IMEP (bar)	5.34	5.33	5.37	5.39	5.39	5.48	5.53	5.53	5.51	5.28	5.45	5.36	5.23	4.95	4.87
ISFC (g/kW-h)	202.9	203.4	196.4	195.8	195.6	192.1	190.6	190.4	191.2	199.5	193.4	196.7	201.9	213.7	217.9
Indicated Efficiency (%)	41.3	41.2	42.6	42.8	42.8	43.6	43.9	44	43.8	42	43.3	42.6	41.5	39.2	38.4
Max. Pressure (bar)	112.98	112.75	111.18	109.49	108.53	105.68	101.3	98.53	93.97	87.27	82.16	75.13	68.36	64.17	62.03
dPmax/dCA (bar/degree)	27.167	37.881	37.219	30.73	24.212	17.064	13.134	12.458	10.229	6.341	4.782	2.319	1.906	1.908	4.249
Max. Temperature (K)	1798	1782	1772	1752	1733	1721	1677	1658	1625	1559	1513	1479	1428	1351	1366
NOx (ppm)	193.6	210.33	336.18	224.04	271.23	373.73	400.61	208.66	354.06	190.43	210.87	120.7	29.82	102.02	48.27
HC (ppm)	28.66	37.59	25.39	24.77	19.54	6.81	9.98	9.37	7.39	30.12	20.33	26.61	50.57	54.41	77.46
CO (ppm)	5.19	237.14	2.14	7.83	38.14	2.14	18.22	15.32	2.24	1334.4	4.21	6.05	228.45	2.34	2.54
BSFC (g/kW-h)	393.8	476.4	390.4	388.5	378.2	363.9	401.9	349.7	344.5	408.2	337.3	336.2	353.3	369	384.1
Volumetric Efficiency (%)	77	76.8	76	75.9	75.8	75.7	75.7	75.6	75.6	75.5	75.6	75.5	75.5	75.5	75.5
A/F Ratio	29.64	29.56	30.03	30	30	30	29.96	29.95	29.95	29.88	29.89	29.86	29.82	29.79	29.72
Brake Efficiency (%)	21.3	17.6	21.4	21.5	22.1	23	20.8	23.9	24.3	20.5	24.8	24.9	23.7	22.7	21.8

Table B-21 Raw data for 2400 rpm / low load 40% EGR case

40% EGR Case															
	Start of Injection (Degrees CA bTDC)														
	40	37.5	35	32.5	30	27.5	25	22.5	20	17.5	15	12.5	10	7.5	5
IMEP (bar)	5.39	5.41	5.43	5.42	5.45	5.46	5.5	5.56	5.44	5.45	5.41	5.31	5.22	4.91	4.87
ISFC (g/kW-h)	204.3	195	194.5	194.9	193.5	192.9	191.5	189.6	193.8	193.4	195.3	198.9	202.6	215.8	218.2
Indicated Efficiency (%)	41	42.9	43	43	43.3	43.4	43.7	44.1	43.2	43.3	42.9	42.1	41.3	38.8	38.4
Max. Pressure (bar)	112.91	111.85	110.64	108.75	107.62	105.03	102.2	99.27	93.27	88.3	82.36	76.59	68.7	63.68	62.06
dPmax/dCA (bar/degree)	30.042	32.877	37.674	30.415	24.18	17.483	14.865	14.493	14.306	7.122	6.034	3.626	4.358	2.232	5.144
Max. Temperature (K)	1789	1780	1773	1753	1734	1715	1693	1672	1606	1564	1513	1476	1427	1331	1333
NOx (ppm)	81.05	97.43	270.32	216.33	82.93	295.92	275.55	199.17	249.54	126.55	63.34	133.89	82.43	20.28	54.76
HC (ppm)	43.15	29.59	24.91	21.79	18.31	8.35	9.1	11.37	18.31	15.32	22.81	26.89	46.63	54.62	79.74
CO (ppm)	935.5	3.59	2.57	2.63	2.93	2.73	5.05	23.96	780.25	41.71	124.68	21.87	83.74	22.95	51.45
BSFC (g/kW-h)	855	387.2	381.7	378.5	374.4	364.7	356.2	350.9	346.1	344.2	349.2	343.5	346.6	374.2	387.6
Volumetric Efficiency (%)	67.6	66.2	66.1	66	66	65.9	65.9	65.8	65.8	65.7	65.7	65.7	65.6	65.6	65.6
A/F Ratio	25.51	26.16	26.14	26.1	26.09	26.09	26.07	26.06	26.04	26.01	25.95	25.93	25.88	25.83	25.72
Brake Efficiency (%)	9.8	21.6	21.9	22.1	22.4	23	23.5	23.9	24.2	24.3	24	24.4	24.2	22.4	21.6

Table B-22 Raw data for 2400 rpm / low load 50% EGR case

50% EGR Case															
	Start of Injection (Degrees CA bTDC)														
	40	37.5	35	32.5	30	27.5	25	22.5	20	17.5	15	12.5	10	7.5	5
IMEP (bar)	5.58	5.56	5.6	5.7	5.57	5.55	5.54	5.56	5.43	5.44	5.32	5.18	4.98	4.84	4.35
ISFC (g/kW-h)	189.3	190.2	188.6	185.6	189.7	190.2	190.6	189.8	194.6	194	198.8	204	213.2	219.8	245.4
Indicated Efficiency (%)	44.2	44	44.4	45.1	44.1	44	43.9	44.1	43	43.2	42.1	41	39.3	38.1	34.1
Max. Pressure (bar)	111.29	110.45	109.38	109.28	106.06	103.52	100.84	97.44	92.95	87.46	82.25	76.27	70.19	64.02	61.59
dPmax/dCA (bar/degree)	37.909	34.456	29.742	29.986	34.071	31.853	23.285	17.424	15.39	10.583	7.784	5.412	3.965	5.348	1.873
Max. Temperature (K)	1790	1781	1771	1766	1735	1711	1687	1663	1628	1590	1533	1464	1389	1370	1202
NOx (ppm)	23.8	72.17	14.17	11.22	49.44	24.06	15.94	19.76	18.87	126.99	8.48	112.43	1.79	1.08	0.53
HC (ppm)	29.45	31.05	26.74	30.34	25.48	23.36	24.24	16.34	31.86	18.84	31.79	34.57	59.24	77.12	113.27
CO (ppm)	3.83	3.95	19.06	59.66	6.03	22.11	38.35	167.42	2275.71	268.88	688.87	422.96	695.9	884.34	1180.72
BSFC (g/kW-h)	361.6	366.5	373.3	367.1	356.4	354.6	351.1	345.6	351.1	343.1	352.8	360.6	374.2	386.9	439.2
Volumetric Efficiency (%)	54.5	54.5	54.3	54.2	54.2	54.2	54.1	54.1	53.8	54	53.9	53.8	53.8	53.8	53.8
A/F Ratio	21.54	21.5	21.45	21.32	21.41	21.39	21.37	21.38	21.2	21.33	21.26	21.24	21.16	21.1	21
Brake Efficiency (%)	23.2	22.8	22.4	22.8	23.5	23.6	23.8	24.2	23.8	24.4	23.7	23.2	22.4	21.6	19.1

Table B-23 Raw data for 2400 rpm / low load 60% EGR case

60% EGR Case															
	Start of Injection (Degrees CA bTDC)														
	40	37.5	35	32.5	30	27.5	25	22.5	20	17.5	15	12.5	10	7.5	5
IMEP (bar)	5.68	6.54	5.67	5.66	6.02	5.62	5.58	6.06	5.5	5.61	5.36	5.38	5.06	4.91	4.51
ISFC (g/kW-h)	188.3	165.9	186.9	187.1	177.9	188.3	189.7	183.2	192.4	192.1	197.9	198.2	210.5	218.5	240.4
Indicated Efficiency (%)	44.5	50.5	44.8	44.8	47.1	44.5	44.1	45.7	43.5	43.6	42.3	42.2	39.8	38.3	34.8
Max. Pressure (bar)	95.25	91.38	98.38	97.45	100.93	95.43	93.92	87.95	88.78	87.68	79.96	71.63	69.67	64.19	60.7
dPmax/dCA (bar/degree)	22.849	28.257	29.637	24.344	26.876	23.929	22.181	16.751	24.813	19.425	16.296	10.697	7.573	3.201	4.679
Max. Temperature (K)	1754	1825	1750	1742	1774	1718	1699	1694	1647	1619	1553	1573	1436	1412	1319
NOx (ppm)	3.55	5.43	0.91	1.14	3.21	1.56	2.61	2.08	1.83	1.25	1.21	1.38	1.11	0.12	0.16
HC (ppm)	39.53	40.2	37.32	34.38	39.15	31.73	34.22	57.18	38.64	53.61	50.43	67.82	68.81	125.04	197.5
CO (ppm)	1330.75	48.61	659.02	168.23	99.88	147.74	92.97	184.85	266.12	1552.68	837.7	941.46	1401.07	3011.57	4150.61
BSFC (g/kW-h)	734.4	306.2	339.2	335.1	329.3	337.5	339.5	361.1	341.7	331.4	343.9	347.7	370.9	390.5	436.8
Volumetric Efficiency (%)	47.7	45.4	46.9	46.8	46.3	46.7	46.6	48.7	46.6	46.5	46.5	46.9	46.5	46.6	46.6
A/F Ratio	18.64	17.17	18.47	18.44	17.89	18.4	18.39	18.1	18.35	18.01	18.31	18.31	18.24	18.12	17.94
Brake Efficiency (%)	11.4	27.3	24.7	25	25.4	24.8	24.7	23.2	24.5	25.3	24.3	24.1	22.6	21.4	19.2

2400 rpm / mid load

Table B-24 Raw data for 2400 rpm / mid load 30% EGR case

30% EGR Case															
	Start of Injection (Degrees CA bTDC)														
	40	37.5	35	32.5	30	27.5	25	22.5	20	17.5	15	12.5	10	7.5	5
IMEP (bar)	8.03	7.84	7.89	7.93	7.99	8.09	8.2	8.3	8.37	8.41	8.4	8.34	8.22	8.05	7.84
ISFC (g/kW-h)	201.1	204.9	203.5	202.5	200.9	198.6	195.7	193.3	191.8	190.9	191.2	192.6	195.4	199.8	205.1
Indicated Efficiency (%)	41.6	40.9	41.1	41.3	41.7	42.2	42.8	43.3	43.7	43.8	43.8	43.5	42.8	41.9	40.8
Max. Pressure (bar)	137.82	134.93	133.56	131.78	129.07	125.23	120.88	115.81	110.55	104.08	97.21	90.3	83.12	75.92	69.11
dPmax/dCA (bar/degree)	66.929	56.181	45.892	42.665	38.61	31.756	28.072	22.131	19.177	15.605	11.754	11.552	8.559	7.814	5.958
Max. Temperature (K)	2161	2130	2111	2087	2047	1995	1945	1892	1846	1797	1751	1713	1675	1636	1608
NOx (ppm)	378.17	420.46	525.64	581.72	564.45	608.74	561.09	475.3	395.86	299.85	231.46	186.71	155.1	97.87	131.61
HC (ppm)	20.87	16.39	7.67	4.49	5.77	3.27	3.39	4.14	6.58	8.03	10.86	14.95	19.58	27.32	37.91
CO (ppm)	2980.43	2240.88	2090.34	2321.7	2558.04	2082.42	1556.12	1282.84	1233.13	1140.19	1101.45	1086.8	1060.76	1137.07	1067.18
BSFC (g/kW-h)	335.8	328.8	324.2	320.3	314.3	305.8	296.3	287.7	281.2	275.8	272.5	271.5	273.1	277.5	283.8
Volumetric Efficiency (%)	74.6	74.7	74.6	74.5	74.4	74.4	74.3	74.3	74.3	74.3	74.3	74.4	74.4	74.5	74.6
A/F Ratio	19.29	19.4	19.39	19.36	19.34	19.33	19.31	19.31	19.3	19.3	19.3	19.31	19.32	19.34	19.35
Brake Efficiency (%)	24.9	25.5	25.8	26.1	26.6	27.4	28.3	29.1	29.8	30.4	30.7	30.8	30.7	30.2	29.5

Table B-25 Raw data for 2400 rpm / mid load 40% EGR case

40% EGR Case															
	Start of Injection (Degrees CA bTDC)														
	40	37.5	35	32.5	30	27.5	25	22.5	20	17.5	15	12.5	10	7.5	5
IMEP (bar)	8.01	7.98	8.01	8.03	8.04	8.05	8.09	8.13	8.15	8.16	8.12	8.04	7.9	7.73	7.51
ISFC (g/kW-h)	200.7	201.5	200.8	200.2	199.8	199.5	198.5	197.7	197	196.9	197.9	200.1	203.6	208.2	214.5
Indicated Efficiency (%)	41.7	41.6	41.7	41.8	41.9	42	42.2	42.4	42.5	42.5	42.3	41.8	41.1	40.2	39
Max. Pressure (bar)	134.82	133.54	132.17	130.35	128.13	125.06	120.59	115.15	109.15	102.36	95.75	89.13	82.37	76.07	69.5
dPmax/dCA (bar/degree)	45.451	60.335	52.519	50.718	42.571	40.11	29.199	24.41	19.716	17.552	14.566	10.935	8.321	6.767	6.161
Max. Temperature (K)	2136	2115	2095	2068	2038	1997	1938	1879	1821	1759	1704	1651	1604	1574	1547
NOx (ppm)	200.07	166.41	175.83	188.59	189.05	172.38	138.99	153.8	183.08	156.81	148.55	135.36	130.96	127.96	128.5
HC (ppm)	27.22	27.59	23.92	19.63	17.35	11.86	11.1	11.19	13.05	15.87	19.88	25.83	31.72	39.21	51.3
CO (ppm)	5176.21	5838.73	5439.79	5475.85	5821.01	6131.6	6181.46	5692.36	4837.48	4473.47	4224.21	4012.84	3882.47	3926.66	4092.57
BSFC (g/kW-h)	318.5	319.6	316.4	313.6	311.2	307.9	302.6	297	292.1	287.8	285.9	286.4	289.5	295	303.1
Volumetric Efficiency (%)	63.2	63	62.9	62.8	62.8	62.7	62.6	62.6	62.6	62.6	62.7	62.7	62.8	62.9	63.1
A/F Ratio	16.38	16.35	16.33	16.31	16.29	16.28	16.27	16.27	16.27	16.27	16.27	16.27	16.29	16.31	16.34
Brake Efficiency (%)	26.3	26.2	26.5	26.7	26.9	27.2	27.7	28.2	28.7	29.1	29.3	29.2	28.9	28.4	27.6

Table B-26 Raw data for 2400 rpm / mid load 50% EGR case

50% EGR Case															
	Start of Injection (Degrees CA bTDC)														
	40	37.5	35	32.5	30	27.5	25	22.5	20	17.5	15	12.5	10	7.5	5
IMEP (bar)	8.04	7.96	8	7.98	7.94	7.92	7.88	7.85	7.77	7.7	7.59	7.45	7.28	7.12	6.97
ISFC (g/kW-h)	200.7	202.7	201.6	202	203.1	203.8	204.7	205.7	207.9	210	213.3	217.8	223.7	229.6	235.9
Indicated Efficiency (%)	41.7	41.3	41.5	41.4	41.2	41.1	40.9	40.7	40.3	39.9	39.2	38.4	37.4	36.5	35.5
Max. Pressure (bar)	125.42	125.26	124.09	122.89	123.46	121.28	118.22	114.23	108.99	103.08	96.22	89.08	80.85	72.49	63.11
dPmax/dCA (bar/degree)	39.959	41.756	34.393	39.687	49.997	43.201	37.277	32.064	26.903	23.291	16.125	14.225	11.919	8.836	7.165
Max. Temperature (K)	2061	2049	2042	2026	2016	1987	1946	1896	1832	1767	1698	1638	1586	1563	1579
NOx (ppm)	19.59	41.47	38.95	43.31	41.41	37.84	36.62	33.61	18.97	23.26	20.15	16.99	10.1	10.11	11.33
HC (ppm)	49.99	52.27	48.17	48.87	55.54	57.46	59.88	63.92	71.28	77.97	100.98	129.86	163.75	215.52	271.22
CO (ppm)	18862.3	18881.8	17242.7	17118.9	17257.9	17422.5	17520.4	17784.5	18818.6	18293.1	18178.8	17989.5	18363.1	17368.7	15733.5
BSFC (g/kW-h)	314.8	318.4	312.9	312.8	315.8	315.7	315.3	314.9	315.3	318.8	318.1	322.3	327.5	334	338
Volumetric Efficiency (%)	52.8	52.7	52.7	52.6	52.5	52.5	52.5	52.5	52.5	52.5	52.5	52.5	52.6	52.7	52.9
A/F Ratio	13.66	13.64	13.63	13.61	13.58	13.58	13.57	13.57	13.55	13.55	13.52	13.51	13.49	13.46	13.44
Brake Efficiency (%)	26.6	26.3	26.8	26.8	26.5	26.5	26.6	26.6	26.6	26.3	26.3	26	25.6	25.1	24.8

Table B-27 Raw data for 2400 rpm / mid load 60% EGR case

60% EGR Case															
	Start of Injection (Degrees CA bTDC)														
	40	37.5	35	32.5	30	27.5	25	22.5	20	17.5	15	12.5	10	7.5	5
IMEP (bar)	8.55	7.97	6.87	6.76	6.78	6.71	6.76	6.65	6.63	6.66	6.41	6.45	6.9	6.06	6.01
ISFC (g/kW-h)	215.6	207.9	235	238.7	238.4	240.9	239.5	243.8	244.9	244.2	254.4	255.2	239.2	273.3	282.6
Indicated Efficiency (%)	38.8	40.3	35.6	35.1	35.1	34.8	34.9	34.3	34.2	34.3	32.9	32.8	35	30.6	29.4
Max. Pressure (bar)	127.52	117.25	80.72	77.9	79.14	76.69	78.42	73.89	72.9	72.47	61.55	60.89	59.16	59.36	60.12
dPmax/dCA (bar/degree)	41.77	35.773	17.584	18.231	18.37	18.221	17.06	16.074	15.51	17.051	10.381	10.965	10.753	3.103	1.843
Max. Temperature (K)	2120	2025	1838	1825	1832	1820	1824	1802	1796	1788	1749	1742	1783	1697	1658
NOx (ppm)	9.31	1.19	0.04	0.01	0.03	0.03	0.04	0.06	0.01	0.03	1.63	0	0.1	0.04	0.03
HC (ppm)	53.86	58.74	50.69	54.61	65.53	73.38	83.91	97.88	118.71	136.96	168.33	192.24	190.31	404.14	621.4
CO (ppm)	34762.1	40551.5	51538	52573.1	52184.6	52282.7	51495	51679.9	50897.8	49592.2	47978.1	46926.4	38926.1	34566.6	32784.2
BSFC (g/kW-h)	289.3	406.7	357.7	360.3	362.6	362.2	364.6	363.2	366.9	371.6	376.3	380	632.4	718.3	756.2
Volumetric Efficiency (%)	51.1	46.5	45.8	45.7	45.7	45.7	45.7	45.7	45.7	45.7	45.9	45.9	46.6	47	47.5
A/F Ratio	11.55	11.5	11.84	11.82	11.79	11.79	11.77	11.77	11.75	11.72	11.72	11.66	11.7	11.78	11.81
Brake Efficiency (%)	28.9	20.6	23.4	23.2	23.1	23.1	23	23.1	22.8	22.5	22.2	22	13.2	11.7	10.9

APPENDIX C

HCCI MODEL RAW DATA

1400 rpm / low load

Table C-1 Raw data for HCCI 1400 rpm / low load case

	EGR Ratio (%)						
	20	25	30	35	40	45	50
IMEP (bar)	7.25	7.22	7.18	7.13	7.07	6.44	5.61
ISFC (g/kW-h)	257.6	257.9	258.3	258.9	259.6	282.3	319.3
Indicated Efficiency (%)	32.4	32.4	32.3	32.2	32.2	29.6	26.1
Max. Pressure (bar)	139.97	139.25	138.47	137.6	136.22	130.94	124.19
dPmax/dCA (bar/degree)	252.036	249.87	247.58	244.914	241.259	218.07	191.331
Max. Temperature (K)	2373	2366	2358	2349	2332	2217	2075
NOx (ppm)	129.49	112.34	94.59	73.69	37	0.1	0
HC (ppm)	0.56	0.56	0.56	0.56	0.56	0.55	0.54
CO (ppm)	8.81	11.72	16.53	26.65	89.06	19711.7	50964
CO2 (ppm)	100854	106820	113172	120557	131773	123960	103215
BSFC (g/kW-h)	402.1	402.4	403.4	405.1	406.3	457.9	550.2
Volumetric Efficiency (%)	87.1	81.2	75.7	69.8	64.3	58.2	52.3
A/F Ratio	19.63	18.36	17.16	15.9	14.72	13.43	12.26
Brake Efficiency (%)	20.8	20.7	20.7	20.6	20.5	18.2	15.2

1400 rpm / mid load

Table C-2 Raw data for HCCI 1400 rpm / mid load case

	EGR Ratio (%)						
	20	25	30	35	40	45	50
IMEP (bar)	8.21	8.17	8.11	8.03	6.84	5.96	5.19
ISFC (g/kW-h)	262.2	262.7	263.4	264.6	307	346.6	390.3
Indicated Efficiency (%)	31.8	31.8	31.7	31.6	27.2	24.1	21.4
Max. Pressure (bar)	149.29	148.46	147.35	146.05	136.79	128.9	121.78
dPmax/dCA (bar/degree)	294.574	292.038	288.662	286.077	241.541	208.498	212.092
Max. Temperature (K)	2553	2544	2531	2523	2287	2124	1983
NOx (ppm)	694.98	552.7	346.2	146.82	0.18	0	0
HC (ppm)	0.65	0.65	0.65	0.65	0.63	0.61	0.59
CO (ppm)	35.12	58.28	146.12	732.93	36506	66184.5	94269.3
CO2 (ppm)	114859	121394	129600	135500	112416	93212	76583
BSFC (g/kW-h)	392.3	392.4	394.6	396.9	481.1	578.7	700.6
Volumetric Efficiency (%)	87.4	81.6	76.2	70.5	63.5	56.7	50.8
A/F Ratio	17.3	16.22	15.19	14.12	12.83	11.62	10.61
Brake Efficiency (%)	21.3	21.3	21.2	21	17.4	14.4	11.9

1900 rpm / low load

Table C-3 Raw data for HCCI 1900 rpm / low load case

	EGR Ratio (%)						
	20	25	30	35	40	45	50
IMEP (bar)	6.94	6.9	6.84	6.77	6.7	6.61	5.63
ISFC (g/kW-h)	237.8	238.4	239.1	239.7	240.6	241.8	279.8
Indicated Efficiency (%)	35.1	35	34.9	34.8	34.7	34.5	29.8
Max. Pressure (bar)	133.23	132.61	131.81	130.68	129.34	127.74	120.32
dPmax/dCA (bar/degree)	171.901	170.175	168.489	166.025	163.144	160.175	136.863
Max. Temperature (K)	2256	2247	2239	2229	2216	2195	2035
NOx (ppm)	26.61	22.52	19.21	15.36	10.39	1.78	0
HC (ppm)	0.5	0.5	0.5	0.5	0.5	0.5	0.49
CO (ppm)	6.47	8.42	10.93	15.56	27.76	356.7	3509.2
CO2 (ppm)	90234.5	97391.2	104196	112327	122742	136705	113788
BSFC (g/kW-h)	395.2	398.2	400.5	402.2	405	407.7	506.3
Volumetric Efficiency (%)	85.8	79.3	73	66.2	59.9	54.1	48.2
A/F Ratio	22.2	20.56	19	17.34	15.8	14.37	12.94
Brake Efficiency (%)	21.1	21	20.8	20.8	20.6	20.5	16.5

1900 rpm / mid load

Table C-4 Raw data for HCCI 1900 rpm / mid load case

	EGR Ratio (%)						
	20	25	30	35	40	45	50
IMEP (bar)	8.25	8.21	8.12	8.01	6.98	5.97	5.14
ISFC (g/kW-h)	241.8	242.3	243.1	244.1	276.6	318.3	362.8
Indicated Efficiency (%)	34.5	34.4	34.3	34.2	30.2	26.2	23
Max. Pressure (bar)	145.04	144.38	143.27	141.76	133.65	125.42	118.22
dPmax/dCA (bar/degree)	212.883	211.097	208.444	205.136	178.808	151.92	129.653
Max. Temperature (K)	2468	2458	2445	2427	2252	2081	1935
NOx (ppm)	294.48	238.57	173.79	91.03	0.11	0	0
HC (ppm)	0.6	0.6	0.6	0.6	0.59	0.57	0.55
CO (ppm)	35.7	54.1	90.05	256.05	27311	60787.3	92497
CO2 (ppm)	108698	115986	123522	132394	118713	96819.6	77948.4
BSFC (g/kW-h)	374.7	376	377.4	380.8	440.1	554.4	707.4
Volumetric Efficiency (%)	85.9	79.5	73.3	66.7	59.7	52.7	46.5
A/F Ratio	18.65	17.3	16.02	14.68	13.26	11.85	10.65
Brake Efficiency (%)	22.3	22.2	22.1	21.9	19	15.1	11.8

2400 rpm / low load

Table C-5 Raw data for HCCI 2400 rpm / low load case

	EGR Ratio (%)						
	20	25	30	35	40	45	50
IMEP (bar)	8.53	8.43	8.39	8.29	6.62	5.56	4.73
ISFC (g/kW-h)	233.4	235.8	236.3	236.7	291.4	338	388.7
Indicated Efficiency (%)	35.8	35.4	35.3	35.3	28.7	24.7	21.5
Max. Pressure (bar)	144.86	144.44	143.59	141.59	128.86	120.5	113.38
dPmax/dCA (bar/degree)	175.107	194.071	202.491	169.077	136.548	114.346	133.226
Max. Temperature (K)	2494	2487	2476	2451	2177	2010	1866
NOx (ppm)	326.28	278.03	200.61	61.32	0.1	0	0
HC (ppm)	0.61	0.61	0.61	0.61	0.59	0.57	0.55
CO (ppm)	62.04	96.23	181.49	967.38	44667.5	80675.2	108957
CO2 (ppm)	109548	117471	125986	135267	107114	84613	68981.8
BSFC (g/kW-h)	372.4	375	374.7	378.4	486.2	644.9	871.7
Volumetric Efficiency (%)	84.7	78.1	71.6	64.5	56.3	49.1	43
A/F Ratio	18.51	17.1	15.74	14.28	12.61	11.21	10.02
Brake Efficiency (%)	22.4	22.3	22.3	22.1	17.2	12.9	9.6

2400 rpm / mid load

Table C-6 Raw data for HCCI 2400 rpm / mid load case

	EGR Ratio (%)						
	20	25	30	35	40	45	50
IMEP (bar)	9.17	9.14	9	7.6	6.38	5.37	4.52
ISFC (g/kW-h)	235.2	236	237.8	277.4	324.1	374.6	434.9
Indicated Efficiency (%)	35.5	35.4	35.1	30.1	25.8	22.3	19.2
Max. Pressure (bar)	150.38	149.81	148.14	138.08	128.17	119.61	111.54
dPmax/dCA (bar/degree)	193.008	191.659	189.069	160.134	133.722	111.237	179.242
Max. Temperature (K)	2589	2579	2564	2333	2133	1966	1807
NOx (ppm)	764.54	546.88	218.22	0.32	0	0	0
HC (ppm)	0.66	0.66	0.66	0.64	0.62	0.6	0.58
CO (ppm)	156.32	312.31	1221.58	35428.8	69768.3	103974	131629
CO2 (ppm)	118242	126694	134405	113074	90885.1	71019	57281.9
BSFC (g/kW-h)	361.3	362.8	366.5	441.1	567.3	751.4	1015.8
Volumetric Efficiency (%)	84.9	78.4	72	63.8	55.8	48.5	42.4
A/F Ratio	17.01	15.74	14.52	12.98	11.51	10.24	9.16
Brake Efficiency (%)	23.1	23	22.8	18.9	14.7	11.1	8.2

APPENDIX D

DIESEL FUEL PROPERTIES

Table D-1 General properties for diesel fuel

State	Property	Value
Vapor	Critical Temperature (K)	569.4
	Critical Pressure (bar)	24.6
	Lower Heating Value (kJ/kg)	43250
	C Atoms per Molecule	13.5
	H Atoms per Molecule	23.6
	O Atoms per Molecule	0
	N Atoms per Molecule	0
	Viscosity (Pa-s)	Table D-2
	Thermal Conductivity (W/m-K)	Table D-2
Liquid	Density (kg/m ³)	830
	Heat of Vaporization (kJ/kg)	250
	Viscosity (Pa-s)	Table D-3
	Thermal Conductivity (W/m-K)	Table D-3

Table D-2 Viscosity and thermal conductivity of diesel vapor

Temperature [K]	Viscosity [Pa-s]	Thermal Conductivity [W/m-K]
303.15	8.02E-06	0.00829904
373.55	6.75E-06	0.00829904
475.35	8.48E-06	0.00829904

Table D-3 Viscosity and thermal conductivity of diesel liquid

Temperature [K]	Viscosity [Pa-s]	Thermal Conductivity [W/m-K]
273.15	2.19E-03	0.116645
290.15	1.71E-03	0.113925
310.15	1.33E-03	0.110725
330.15	1.10E-03	0.107525
350.15	9.60E-04	0.104325
373.15	8.8E-04	0.100645
400.15	8.7E-04	0.096325
450.15	1.12E-03	0.088325

VITA

Name: Jonathan Robert Breen

Address: Texas A&M University, Department of Mechanical Engineering,
3123 TAMU,
College Station, TX 77843

Email Address: jonathan.breen45@gmail.com

Education: B.S., Mechanical Engineering, Texas A&M University, 2008
M.S., Mechanical Engineering, Texas A&M University, 2010